University of Alberta

Regulation of Calcium and Exocytosis in Rat β cells

by

Catherine Elizabeth Hughes

A thesis submitted to the Faculty of Graduate Studies and Research in partial fulfillment of the

requirements for the degree of Master of Science

Department of Pharmacology

Edmonton, Alberta
Fall 2004

Your file Votre référence
ISBN: 0-612-95770-5
Our file Notre référence
ISBN: 0-612-95770-5

Dedication

In memory of my Grandpa Ron and Aunt Kathleen who passed away during the course of this work.

Acknowledgments

I would like to thank past and present members of the Tse lab for their comments, suggestions, and help including Dr. Andy Lee, Cecilia Shiu, Kim San Tang, Dr. Jianhua Xu, and Fenglian Xu. Thank-you to my committee members Drs. Connie Chik and Peter Light for their suggestions and comments. I also wish to thank my supervisor Dr. Amy Tse for her suggestions and support and Dr. Fred Tse for his comments and suggestions.

Table of Contents

List of tables

List of figures

List of abbreviations and symbols

ACh: acetylcholine

ADP: adenosine 5'-diphosphate

ATP: adenosine 5'-triphosphate

ATP/ADP: ATP to ADP ratio

2-APB: 2-aminoethoxydiphenyl borate

AU: arbitrary units

BHQ: 2,5-di-(t-butyl)-1,4-hydroquinone

$[Ca^{2+}]_i$: cytosolic free calcium concentration

$[Ca^{2+}]_m$: mitochondrial calcium concentration

cAMP: cyclic adenosine 3´,5´-monophosphate

cADPR: cyclic ADP-ribose

CCCP: carbonyl cyanide m-chlorophenylhydrazone

CCE: capacitative calcium entry

CCK: cholecystokinin

CICR: calcium induced calcium release

ΔC_m: change in membrane capacitance

C_m: membrane capacitance

CPA: cyclopiazonic acid

DNAse: deoxyribonuclease

EPAC: exchange protein activated by cAMP

F405: indo-1 fluorescence measured at 405nm, the shortwave fluorescence

FBS: fetal bovine serum

fF: femtofarad

GLP-1: glucagon-like-peptide 1

GRP: gastrin releasing peptide

GTP: guanosine 5'-triphosphate

HBSS: Hanks Buffered Saline Solution

Hepes: 4-(2-hydroxyethyl) 1-piperazineethanesulfonic acid

I_{Ca}: calcium current

I_{Na}: sodium current

IP_3: inositol 1,4,5-trisphosphate

K_{ATP} channel: ATP sensitive potassium channel

mV: millivolt

NAADPH: nicotinic acid adenine dinucleotide phosphate

NCX: sodium calcium exchanger

pF: picofarad

pC: pico coulomb

PMCA: plasma membrane calcium ATPase

RRP: readily releasable pool (of vesicles)

SEA0400: 2-[4-[(2,5-difluorophenyl)methoxy]phenoxy]-5-ethoxyaniline

SERCA: sarcoplasmic endoplasmic reticulum Ca^{2+}-ATPases

τ: time constant

TPCK: L-1-tosylamide-2-phenylethyl chloromethyl ketone

VGCC: voltage gated calcium channels

V_m: membrane potential

Chapter 1: Introduction

I. Introduction to glucose and insulin

Regulation of insulin secretion from the β cells of the pancreas is a critical process as insulin is the most important hormone involved in decreasing blood glucose levels and β cells are the only cells capable of synthesizing and secreting insulin. Both excessive insulin (e.g. persistent hyperinsulinemic hypoglycemia of infancy (PHHI)) and insufficient insulin (e.g. diabetes) can result in serious clinical conditions. This results in the need to tightly regulate insulin secretion, which can occur on several levels.

β cells, which make up approximately 60-80 % of islet cells, release insulin in response to increases in blood glucose. In addition, amino acids, acetylcholine (ACh), and other hormones including glucagon and glucagon-like-peptide 1 (GLP-1) also stimulate insulin release. Somatostain, leptin, and noradrenaline inhibit insulin secretion. Insulin acts to decrease blood glucose levels through several actions including increasing the uptake of glucose into adipose tissue and peripheral muscle, decreasing the production of glucose by the liver, and increasing glycogen synthesis by the liver. Because of the importance of glucose regulation of insulin secretion, it will be discussed in further depth in the next section.

II. Glucose regulation of insulin secretion

The major regulator of the membrane potential (V_m) of β cells is the ATP sensitive potassium channel (K_{ATP} channel). The K_{ATP} channel is an ATP sensitive inwardly rectifying potassium channel that is composed of two subunits: the regulatory

sulfonylurea receptor (SUR) and the pore subunit Kir 6.2 (Ashcroft, 2000; Light, 2002). Under resting conditions these channels are opened, allowing the outflow of K^+ from the cell which keeps the cell at a negative resting membrane potential (~ -60 to -70 mV) (Ashcroft, 2000; Rorsman, 1997). Following increases in blood glucose levels, there is an increase in glucose transport into β cells, mediated by glut-2 transporters, resulting in increases in cytosolic glucose concentrations. This increases glucose metabolism through glycolysis and the Krebs cycle with the result being an increase in the ATP concentration and a corresponding decrease in ADP concentration. The increase in the ATP to ADP ratio (ATP/ADP) closes the K_{ATP} channel causing a decrease in K^+ efflux and depolarization of the cell (Rorsman, 1997; Light, 2002). Depolarization in turn activates voltage gated calcium channels (VGCC). In β cells it is believed that the majority of the VGCC are L-type. The presence of other types of VGCC (e.g. T-type and N-type) have been reported, but whether they have any significant role in insulin secretion is still contentious (Satin, 2000). The activation of the VGCC allows Ca^{2+} to enter the cell, and the resulting increase in the intracellular Ca^{2+} concentration ($[Ca^{2+}]_i$) stimulates the exocytosis of insulin containing vesicles. This is summarized in Figure 1.1

A second parallel mechanism, by which glucose stimulates insulin secretion, is the K_{ATP} independent pathway or amplifying pathway. In this pathway increases in cytosolic glucose levels and glucose metabolism result in the production of a mediator. This mediator then amplifies or enhances Ca^{2+}-stimulated insulin secretion (Henquin, 2000; Aizawa *et al.*, 1998; Maechler, 2003; Henquin *et al.*, 2003) (Figure 1.1). The identity of the mediator is presently a matter of some debate. Mediators that have been

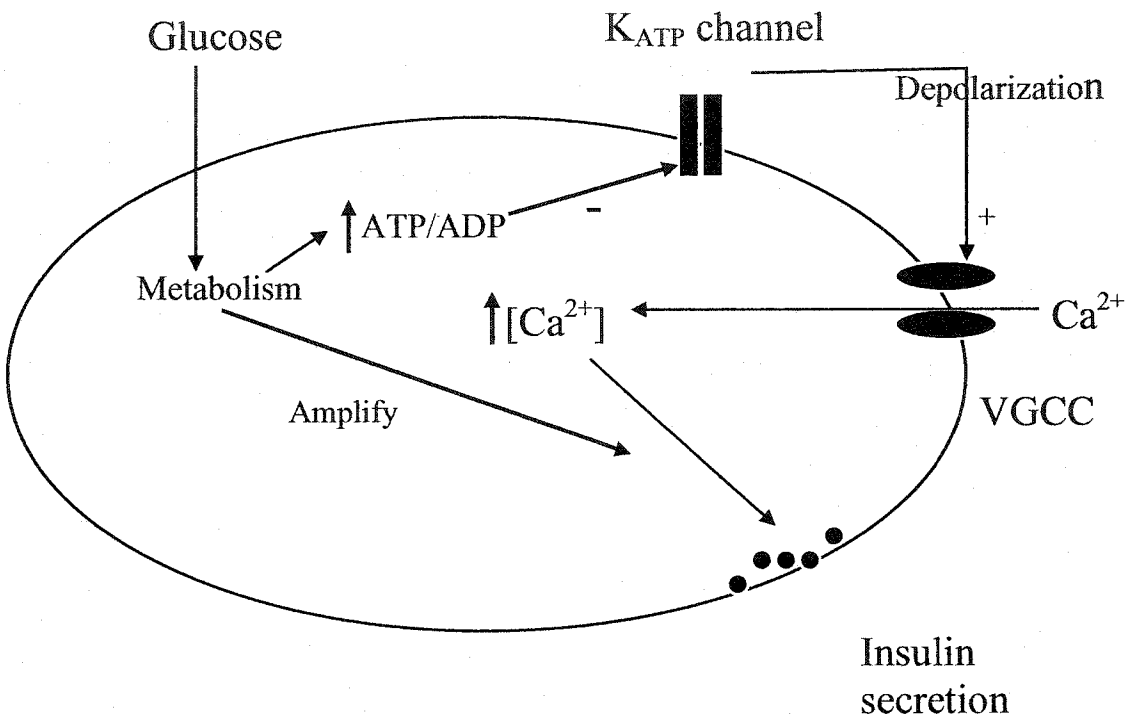

Figure 1.1: The K_{ATP} independent and dependent pathways of glucose stimulated insulin secretion.

suggested in the literature include glutamate, ATP/ADP, acyl CoAs, and various protein kinases; but contradictory findings on the actions of many of these mediators have been reported (Maechler, 2003; Henquin, 2000; Henquin *et al.*, 2003; Straub & Sharp, 2002). Presently, the two most widely accepted potential mediators are the ATP/ADP and glutamate, which have been both hypothesized to work through similar mechanisms (Barg *et al.*, 2001a). Glutamate has been proposed to prime vesicles for release by being transported into vesicles resulting in vesicular acidification (Hoy *et al.*, 2002; Maechler, 2003). ATP has been proposed to enhance acidification of vesicles by increasing Cl^- uptake into vesicles, which allows for increased H^+ transport, while ADP decreases Cl^- transport (Rorsman & Renstrom, 2003; Barg *et al.*, 2001a). Both the ATP/ADP and glutamate hypotheses involve vesicular acidification, which may be a step necessarily for vesicles to be primed for release (Rorsman & Renstrom, 2003). By increasing the number of primed vesicles and enhancing vesicle replenishment, glutamate and/or ATP would enhance insulin secretion. However, the role of both glutamate (Bertrand *et al.*, 2002; Straub & Sharp, 2002) and ATP (Straub & Sharp, 2002) has been questioned.

In addition to stimulating Ca^{2+} influx into β cells, glucose may also stimulate Ca^{2+} release from intracellular stores. However, this is a controversial subject. There is evidence that indicates that glucose, through a mediator, causes Ca^{2+} release (Ammäla *et al.*, 1991b; Takasawa *et al.*, 1993); however, there is also evidence glucose causes Ca^{2+} release via modulation of Ca^{2+} pumps (Arredouani *et al.*, 2002b; Gilon *et al.*, 1999); while other evidence indicates glucose has absolutely no effect on intracellular Ca^{2+} stores (Liu *et al.*, 1995). Some of these discrepancies may be due to differences in cell type (e.g. cell lines vs. primary cell cultures) (Okamoto *et al.*, 1997) or cell preparation

(e.g. single cell vs. whole islets) in the various studies. Adding to the confusion, there have been different reports as to what this mediator is. For example, there have been reports that suggest that glucose mediated cell depolarization stimulates IP_3 production (Ammäla *et al.*, 1991a; Gromada *et al.*, 1996; Roe *et al.*, 1993). In contrast, other work indicates that glucose does not stimulate IP_3 production, but stimulates cyclic ADP-ribose (cADPR) production leading to Ca^{2+} release (Takasawa *et al.*, 1993; Okamoto *et al.*, 1997). However, the role of cADPR in β cells is also controversial (Islam & Berggren, 1997). NAADP has also been suggested to be the mediator (Patel, 2003; Yamasaki *et al.*, 2004). It has also been hypothesized that glucose's role in stimulating Ca^{2+} release from intracellular stores is more passive. The increase in ATP and $[Ca^{2+}]_i$ following glucose stimulation enhances Ca^{2+} uptake into intracellular stores by sarcoplasmic endoplasmic reticulum Ca^{2+}-ATPases (SERCA) pumps (Gilon *et al.*, 1999). When Ca^{2+} entry through VGCC decreases, Ca^{2+} passively leaks out of the Ca^{2+} stores (Gilon *et al.*, 1999; Arredouani *et al.*, 2002b). In this model, the stores help to limit increases in $[Ca^{2+}]_i$ during a depolarization and help to keep $[Ca^{2+}]_i$ above basal levels in-between Ca^{2+} oscillations (Gilon *et al.*, 1999; Arredouani *et al.*, 2002b). Despite of this confusion, the majority of the work on this subject suggest that intracellular Ca^{2+} stores play a role in glucose mediated $[Ca^{2+}]_i$ increase.

III. Other regulators of Ca^{2+} stores

In addition to glucose, other physiological agonists can stimulate intracellular Ca^{2+} release. ACh stimulates the release of Ca^{2+} from intracellular Ca^{2+} stores (Gilon & Henquin, 2001). This release is most likely mediated by a G_q coupled muscarinic M_3

receptor (Gilon & Henquin, 2001). In addition to the well-known effect of ACh, other agonists may also trigger Ca^{2+} release from stores. For example, GLP-1, which is released from the L-cells of the intestine in response to increases in blood glucose, stimulates insulin secretion in a mechanism involving closure of K_{ATP} channels (Light *et al.*, 2002; Gromada *et al.*, 1998), enhancement of I_{Ca} (Gromada *et al.*, 1998), and exocytosis (Gromada *et al.*, 1998). In addition, GLP-1 releases Ca^{2+} from intracellular Ca^{2+} stores (Gromada *et al.*, 1998; Holz *et al.*, 1999). The underlying mechanism appears to be an increase in intracellular cAMP levels, following GLP-1 stimulation, sensitizes ryanodine receptors (Holz *et al.*, 1999). This then allows the Ca^{2+} entering the cell through VGCC to stimulate Ca^{2+}-induced Ca^{2+} release (CICR) from ryanodine-sensitive Ca^{2+} stores (Gromada *et al.*, 1998; Holz *et al.*, 1999). However, the existence of ryanodine sensitive stores in β cells has been questioned (Tengholm *et al.*, 1998). Other agonists that stimulate intracellular Ca^{2+} release from IP_3 stores include gastrin releasing peptide (GRP) and cholecystokinin (CCK) (Ahren, 2000). Finally, ATP, which is postulated to be released from neurons (Hellman *et al.*, 2004), stimulates the release of Ca^{2+} from IP_3 stores (Li *et al.*, 1991; Hellman *et al.*, 2004; Theler *et al.*, 1992).

IV. Differences in rat and mouse response to glucose

The information presented above is a general overview of β cell physiology that is applicable to both rat and mouse β cells. However, rat and mouse β cells differ in several respects. The major difference is in the pattern of glucose induced insulin secretion. In rat, there is a clear biphasic increase in insulin release in response to glucose. There is a large first phase that lasts ~10 minutes followed by a second phase

that initially starts small, but increases in amplitude with time (Ma *et al.*, 1995; Zawalich *et al.*, 2001; Maechler *et al.*, 2002). In mouse there are also two phases of insulin secretion, but the first phase is smaller than in rat and the second phase is considerably smaller than the first phase and does not increase in size with time (Ma *et al.*, 1995; Zawalich *et al.*, 2001; Maechler *et al.*, 2002). When normalized to body size (but not islet number or pancreas weight) the first phase of insulin secretion is similar in mouse and rat (Ma *et al.*, 1995; Zawalich *et al.*, 2001). However, the second phase of secretion is considerably smaller in mouse (Ma *et al.*, 1995; Maechler *et al.*, 2002; Zawalich *et al.*, 2001). The reason for these differences is not well understood. It has been suggested that the glucose amplifying pathway may not work as efficiently in mouse β cells (Maechler *et al.*, 2002) and rat β cells may have a greater ability to generate glutamate (Maechler *et al.*, 2002; Hoy *et al.*, 2002), cAMP (Ma *et al.*, 1995), or inositol phosphates (Zawalich *et al.*, 2001) in response to glucose.

In addition to differences in insulin secretion, there are differences between rat and mouse β cells in their electrophysiological and Ca^{2+} response to glucose. In rat β cells, glucose mediated K_{ATP} channel closure causes a sustained depolarization (Antunes *et al.*, 2000; Theler *et al.*, 1992), in contrast to mouse where the depolarization is oscillatory (Antunes *et al.*, 2000; Speier & Rupnik, 2003). Glucose consistently causes Ca^{2+} oscillations in mouse β cells (Antunes *et al.*, 2000; Miura *et al.*, 1997; Liu *et al.*, 1995). In rat β cells, however, the Ca^{2+} response is more variable; glucose typically causes a sustained increases in $[Ca^{2+}]_i$ with only some cells showing slow Ca^{2+} oscillations (Antunes *et al.*, 2000; Theler *et al.*, 1992). These differences have been suggested to be related to a larger increase in the ATP/ADP in rats than in mouse when

stimulated by glucose (Antunes *et al.*, 2000). However, it has also been suggested that the difference in $[Ca^{2+}]_i$ in response to glucose is due to a higher expression of the Na^+/Ca^{2+} exchanger (NCX) in rat (Herchuelz *et al.*, 2002) and the reverse mode of the NCX is thought to mediate the sustained $[Ca^{2+}]_i$ increase (Herchuelz *et al.*, 2002).

The review above indicates that there are clear differences between mouse and rat β cells. However, it is not clear which one represents a better model of human β cells. It has been reported in both human subjects and isolated human islets that glucose produces a clear biphasic increase in insulin secretion (Misler *et al.*, 1992a; Misler *et al.*, 1992b; Luzi & DeFronzo, 1989; Ricordi *et al.*, 1988). Although, $[Ca^{2+}]_i$ in human islets can oscillate in response to glucose, there is a greater heterogeneity of responses than in mouse (Martin & Soria, 1996; Misler *et al.*, 1992b). Therefore, the $[Ca^{2+}]_i$ response of human islets shares traits with both rat and mouse islets, while the insulin response is clearly rat-like. This supports that the human β cell is more rat like and rat is a better model for studying β cell physiology (Maechler *et al.*, 2002). However, most studies looking at β cell physiology use mouse. The differences between mouse and rat islets and the relevance of rat as a model for human suggests rat β cells should be further studied. Two important aspects of rat β cell physiology that are especially understudied are the regulation of exocytosis by Ca^{2+} and Ca^{2+} homeostasis.

V. Regulation of exocytosis by $[Ca^{2+}]_i$

Like other endocrine cells, $[Ca^{2+}]_i$ elevation In β cells is the major trigger of exocytosis (Wollheim & Sharp, 1981; Satin, 2000). The relationship between $[Ca^{2+}]_i$ and exocytosis has been extensively studied in mouse β cells (for example see (Renstrom *et*

al., 1996; Renstrom *et al.*, 1997; Barg *et al.*, 2001b; Takahashi *et al.*, 1999), but very little has been studied in rats.

In mouse β cells, it has been shown that exocytosis can occur at $[Ca^{2+}]_i$ as low as 0.2 μM (Rorsman & Renstrom, 2003), and is very temperature dependent with almost no exocytosis occurring at room temperature (Renstrom *et al.*, 1996). ATP and ADP concentrations regulate exocytosis at several steps. This includes vesicle transport (Burgoyne & Morgan, 2003) and priming (Eliasson *et al.*, 1997). ATP reportedly enhances priming by acidifying vesicles while ADP inhibits this process (Barg *et al.*, 2001a). However, it is not clear if ATP has any action post vesicle priming (Renstrom *et al.*, 1997; Takahashi *et al.*, 1999). Protein kinases including protein kinase A (PKA; Ammäla *et al.,* 1993a; Eliasson *et al.*, 2003; Renstrom *et al.*, 1997) protein kinase C (PKC; Ammäla *et al.*, 1994a), calmodulin-dependent kinase II (CaM kinase II; Gromada *et al.*, 1999) and phosphatidylinositol 4-kinase (PI 4-kinase; Olsen *et al.*, 2003) enhance exocytosis. This enhancement may involve enhancement of the replenishment of the readily releasable pool (RRP) of vesicles (Renstrom *et al.*, 1997; Ammäla *et al.*, 1993a; Ammäla *et al.*, 1994b; Olsen *et al.*, 2003; Gromada *et al.*, 1999). However, it is not clear if this enhancement is an increase in the rate of mobilization (i.e. vesicle movement and docking) or priming (i.e.: vesicle modification) or a post-priming process. In addition, cAMP acts independently of PKA, possibly through the exchange protein activated by cAMP (EPAC) (Holz, 2004), to enhance vesicle priming or vesicle release probability by promoting granular acidification (Renstrom *et al.*, 1997; Eliasson *et al.*, 2003). In addition to closing K_{ATP} channels, it has also been proposed that sulfonylureas enhance exocytosis by enhancing vesicle acidification (Barg *et al.*, 1999; Renstrom *et al.*, 2002).

However, there have been doubts expressed on whether sulfonylurea indeed affects exocytosis (Garcia-Barrado *et al.*, 1996; Mariot *et al.*, 1998) and whether this action is clinically relevant (Henquin *et al.*, 2003).

It has been shown that L-type VGCC channels are closely coupled to vesicles through exocytotic proteins on the vesicles interacting with a portion of the L-type VGCC (Satin, 2000; Barg *et al.*, 2002a; Barg *et al.*, 2001b; Bokvist *et al.*, 1995). This interaction results in fast exocytosis following depolarization and results in very high $[Ca^{2+}]_i$ near the secretary granules (Barg *et al.*, 2001b; Satin, 2000). The half-maximum rate of exocytosis occurs between 17-23 μM Ca^{2+} with the maximum rate happening at ≥30 μM Ca^{2+} (Barg *et al.*, 2001b; Takahashi *et al.*, 1999). In contrast to earlier reports (Eliasson *et al.*, 1996), these values of Ca^{2+} dependence are similar to those reported in other endocrine and neuroendocrine cells (reviewed by (Burgoyne & Morgan, 2003). Physiologically, the average $[Ca^{2+}]_i$ never reaches such high concentrations. However, due to the local Ca^{2+} gradient this large $[Ca^{2+}]_i$ rise may occur locally near the VGCC to trigger exocytosis.

In contrast to the large body of information on exocytosis in mouse β cells very little is known about exocytosis in rat β cells. In rat β cells, it is known that Ca^{2+} entry stimulates exocytosis (Kim *et al.*, 1998; Gillis & Misler, 1992; Barnett & Misler, 1995), cAMP enhances exocytosis (Gillis & Misler, 1993), and exocytosis in response to a depolarization is quite variable in magnitude and tends to run down (Kim *et al.*, 1998; Gillis & Misler, 1992). Exocytosis is also temperature dependent with exocytosis occurring less frequently in response to a depolarization at room temperature (Gillis &

Misler, 1992). Studying exocytosis in rat β cells may help to understand the differences in glucose stimulated insulin secretion between rat and mouse.

VI. Regulation of $[Ca^{2+}]_i$ homeostasis in β cells

As $[Ca^{2+}]_i$ is the ultimate trigger of insulin secretion it is important that it is regulated to ensure proper regulation of insulin release. As in other cells, there are multiple mechanisms of Ca^{2+} removal including extrusion out of the cell, transport of Ca^{2+} into intracellular organelles including the endoplasmic reticulum (ER), mitochondria, and vesicles (Berridge *et al.*, 2003). Extrusion mechanisms include plasma-membrane Ca-ATPases (PMCA) and the Na^+/Ca^{2+} exchanger (NCX). These are summarized in Figure 1.2

Previous studies in mouse β cells indicates that the most important Ca^{2+} removal mechanism is the pumping of Ca^{2+} into intracellular stores by SERCA pumps (Chen *et al.*, 2003). The SERCA pumps contribute to the removal of approximately 50 to 70 % of cytoplasmic Ca^{2+} (Chen *et al.*, 2003; Gall *et al.*, 1999). The SERCA mediated Ca^{2+} uptake is mediated by two isoforms: SERCA 2b and 3 (Arredouani *et al.*, 2002a). A study with SERCA 3 knock-out mice suggests that SERCA 3 acts to limit $[Ca^{2+}]_i$ increase following a stimulus while SERCA 2b regulates basal $[Ca^{2+}]_i$ (Arredouani *et al.*, 2002a). Extrusion via the NCX contributes to 20-30 % of Ca^{2+} removal when $[Ca^{2+}]_i$ is above 1μM and the PMCA contributes 21-27 % of removal at sub-micromolar $[Ca^{2+}]$ (Chen *et al.*, 2003; Gall *et al.*, 1999). Other removal mechanisms, including mitochondrial Ca^{2+} uptake, only contribute to the removal of 3 to 11 % of Ca^{2+} (Chen *et al.*, 2003).

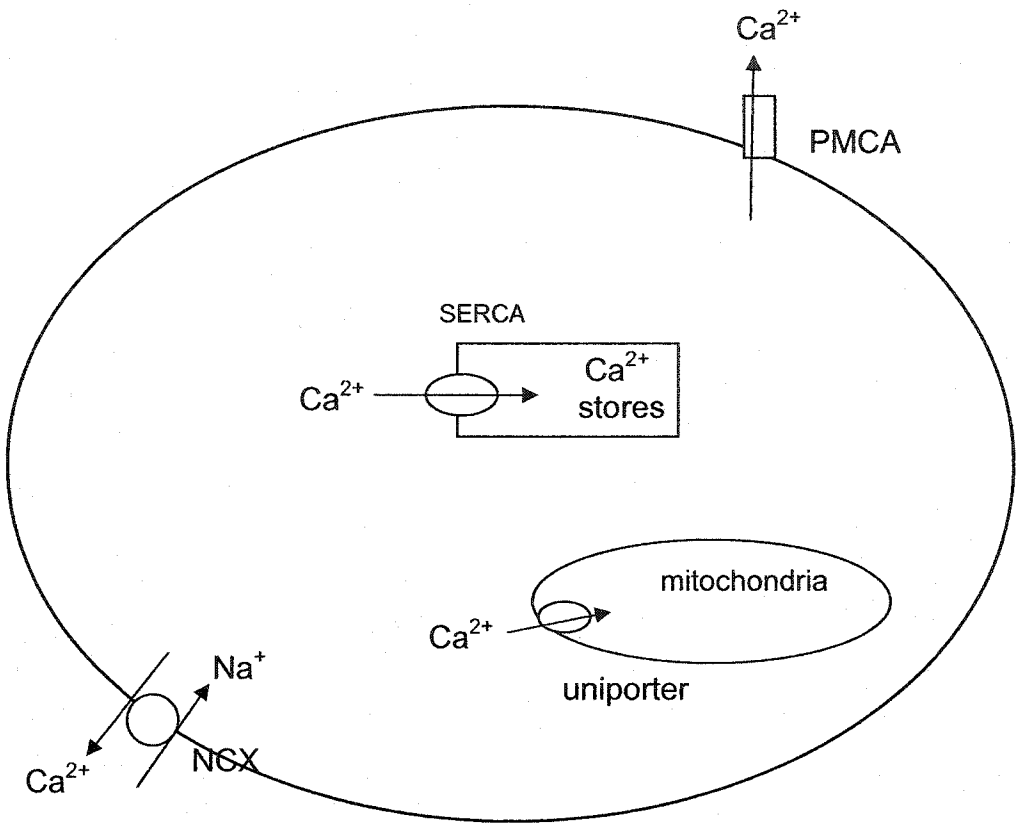

Figure 1.2: Summary of the Ca^{2+} removal mechanisms in rat β cells. See text for details and abbreviations.

Less work has been done to characterize Ca^{2+} removal mechanisms in rat β cells. Work by Van Eylen *et al.* (Van Eylen *et al.*, 1998) suggests that NCX contributes to the removal of 70 % of Ca^{2+} in rat β cells. However, in this study, they did not examine any other mechanisms of Ca^{2+} removal, and the protocol used to determine this effect is not without flaws. It is important to understand the mechanisms of Ca^{2+} removal in rat β cells as it has been suggested that differences in Ca^{2+} handling may underlie some of the differences in glucose mediated $[Ca^{2+}]_i$ increase between rat and mouse (Herchuelz *et al.*, 2002).

VII. Goals and objectives

The purpose of the work presented in this thesis is to examine two aspects of rat β cell physiology: 1) the relationship between $[Ca^{2+}]_i$ and exocytosis; 2) the roles of the different Ca^{2+} removal mechanisms in Ca^{2+} homeostasis. This will provide some insight into the differences between rat and mouse β cells. As well, because the rat may be a better model for human β cell physiology, knowledge of rat β cells may provide some understanding of human β cells.

Chapter 2: Methods and Materials

I. Chemicals

Dulbecco's Modified Eagle Media (DMEM), fetal bovine serum (FBS), Hanks Buffered Saline Solution (HBSS), penicillin V, RPMI 1640, and streptomycin were all purchased from Gibco (Burlington, ON). 2-aminoethoxydiphenyl borate (2-APB), 2,5-di-(t-butyl)-1,4-hydroquinone (BHQ), and carbonyl cyanide m-chlorophenylhydrazone (CCCP) were purchased from Calbiochem (San Diego, CA). Indo-1 K^+ salt and indo-1-AM were purchased from Teflabs (Austin, TX). Bovine serum albumin (BSA) (fraction V), collagenase, deoxyribonuclease (DNAse), ficoll (type 400DL), oligomycin, poly-l-lysine, and trypsin were purchased from Sigma (Oakville, ON). 2-[4-[(2,5-difluorophenyl)methoxy]phenoxy]-5-ethoxyaniline (SEA0400) was a gift of Taisho Pharmaceutical Co. The Ca^{2+} and Mg^{2+} free Earle's Hepes buffer contains (in mM): 124 NaCl, 5.4 KCl, 1 NaH_2PO_4, 14.3 $NaHCO_3$, 2.8 glucose,10 Hepes, and 0.2 % BSA (pH = 7.2 with NaOH) (Josefsen *et al.*, 1996). HBSS contains (in mM): 136.9 NaCl, 5.4 KCl, 5.6 glucose, 4.2 $NaHCO_3$, 1.3 $CaCl_2$, 0.8 $MgSO_4$, 0.4 KH_2PO_4, and 0.44 Na_2HPO_4.

II. Islet isolation and β cell culture

The rat islets were isolated using methods modified from previous work by Lacy and Kostianovsky (Lacy & Kostianovsky, 1967) and Shapiro *et al.* (Shapiro *et al.*, 1996). Male (150-175 g) Sprague Dawley rats (Biosciences, Edmonton, AB or Charles River, Montreal, QC) that were fed *ad libitum* were euthanized with an overdose of halothane in accordance with the standards of the Canadian Council on Animal Care. The pancreas

was distended by injecting, with a 27-gauge needle, 10 ml of ice cold HBSS into the common bile duct. After removal, the isolated pancreas is minced into small pieces, with scissors, while suspended in HBSS. Following removal of the floating fat tissue, the tissue solution was centrifuged at 2000 rpm for 20 s and the pellet was resuspended in HBSS containing collagenase (type V, 1.2 mg ml^{-1}) and DNAse (type II, 5 μg ml^{-1}) and was constantly shaken by hand for 12 minutes while immersed in a 37°C water bath. The tissue was then centrifuged (2000 rpm for 20 s) and the pellet was resuspended in HBSS and filtered through a 500 μm stainless steel wire mesh to separate the islets from other tissue such as lymph nodes. To separate further the islets from the acinar (exocrine) tissue, the filtrate was resuspended in the bottom layer of a discontinuous ficoll gradient with layers of 25 %, 23 %, 21.5 %, and 11.5 %. Following a 10 minute centrifugation at 2000 rpm, the islets were removed from the gradient at the interface of the 21.5 % and 11.5 % layers.

The islets were then washed twice in HBSS. To further ensure the purity of the islets, the islets were handpicked under a dissecting microscope using a lightly fire polished glass pipette. The islets were then incubated, for a minimum of 2 hrs, in RPMI/10 % FBS media supplemented with 50units ml^{-1} penicillin G and 50 μg ml^{-1} streptomycin at 37 °C.

Following the incubation the islets were again handpicked and then spun down. The pellet was resuspended in the Earle's buffer supplemented with 0.3 % BSA, 3 mM EDTA, and 7.5 μg ml^{-1} DNAse (Josefsen *et al.*, 1996). After centrifugation, the pellet, containing the islets, was suspended in the Earle's buffer containing either trypsin type X (0.02 mg ml^{-1}) or TPCK treated trypsin (0.0025 mg ml^{-1}). The islets were incubated in

the trypsin solution in a 37 °C water bath for 4-10 minutes (depending on enzyme type). Following the incubation, the islets were gently triturated with a fire polished glass pipette to ensure dissociation of the islets into single cells. The enzyme reaction is stopped by the addition of DMEM/BSA (containing 50 units ml^{-1} penicillin G and 50 μg ml^{-1} streptomycin). Following 2 further washes in DMEM/BSA, the single cells were then diluted with DMEM/BSA, and plated onto poly-l-lysine (0.1mg ml^{-1}) coated glass coverslips (Fisher Scientific Ottawa, ON). The cells were incubated at 37 °C, 5 % CO_2 and 80 % humidity for 30 to 45 minutes to allow the cells to adhere to the coverslip before being flooded with RPMI/FBS media. Cells were kept in culture for up to 4 days at 37 °C, 5 % CO_2, and 80 % humidity.

III. Electrophysiology

Single β cells were voltage clamped at -70 mV (corrected for 10 mV junction potential through out) using an EPC-7 patch-clamp amplifier (List-Electronic, Darmstadt-Eberstadt Germany) with the whole-cell gigaseal method (Hamill *et al.*, 1981). The recording pipettes, made with hemacrite glass (VWR Scientific, Mississauga, ON), were pulled using a vertical puller (ALA scientific instruments Westbury NY). The tip was coated with Sylgard-182 (Dow Corning) and lightly fire polished before use. The pipettes had a seal resistance of approximately 2.5 to 4 MΩ when filled with the recording solution. β cell identification was based on cell size with the large cells being selected. The average size of the cells used was 5.90 ± 0.15 pF. The coverslips with attached cells were mounted in a chamber (ALA Scientific Instruments, Westbury NY) that held a volume of ~500 μl. External solution was perfused, by gravity, at 1-2 ml

min^{-1}. The experiments were done at either room temperature (22-25 °C) or the more physiological temperature of ~30 °C by perfusing with pre-warmed external solution.

To measure changes in membrane capacitance (ΔC_m), which reflects the incorporation of membranes of vesicles onto the cell's plasma membrane during exocytosis (Neher, 1998), a software based phase-sensitive detector, Pulse Control 4.7, (Herrington J. *et al.*, 1995) was used. A 50 mV (peak to peak) sinusoid wave with a frequency of 810 Hz was superimposed over the holding potential. The resulting sinusoidal current is phase shifted from the original sinusoid. This output sinusoidal current is separated into two independent (orthogonal) sinusoidal components. The component that is in phase with the original sinusoid is proportional to the conductance (G), while, the out of phase component is proportional to the cell membrane capacitance. A ΔC_m results in a linear change in this sinusoid component. The ΔC_m is calibrated by electrically adding 0.2 pF to the cell's capacitance and measuring the resulting changes in the output sinusoidal current. This has been described in detail by Gillis (Gillis, 1995). Pulse Control was also used to control membrane potential and voltage depolarizations.

In some experiments, the time integral of the Ca^{2+} current (I_{Ca}) was analyzed to estimate Ca^{2+} entry. To eliminate contamination from the I_{Na} that exists in some rat β cells, the time integral I_{Ca} was calculated by determining the area under the curve of the inward current from 8 ms after the onset of depolarization to the end of the depolarization step (150 ms). An example of an I_{Ca} showing the estimation of the tine integral of I_{Ca} is in Figure 2.1.

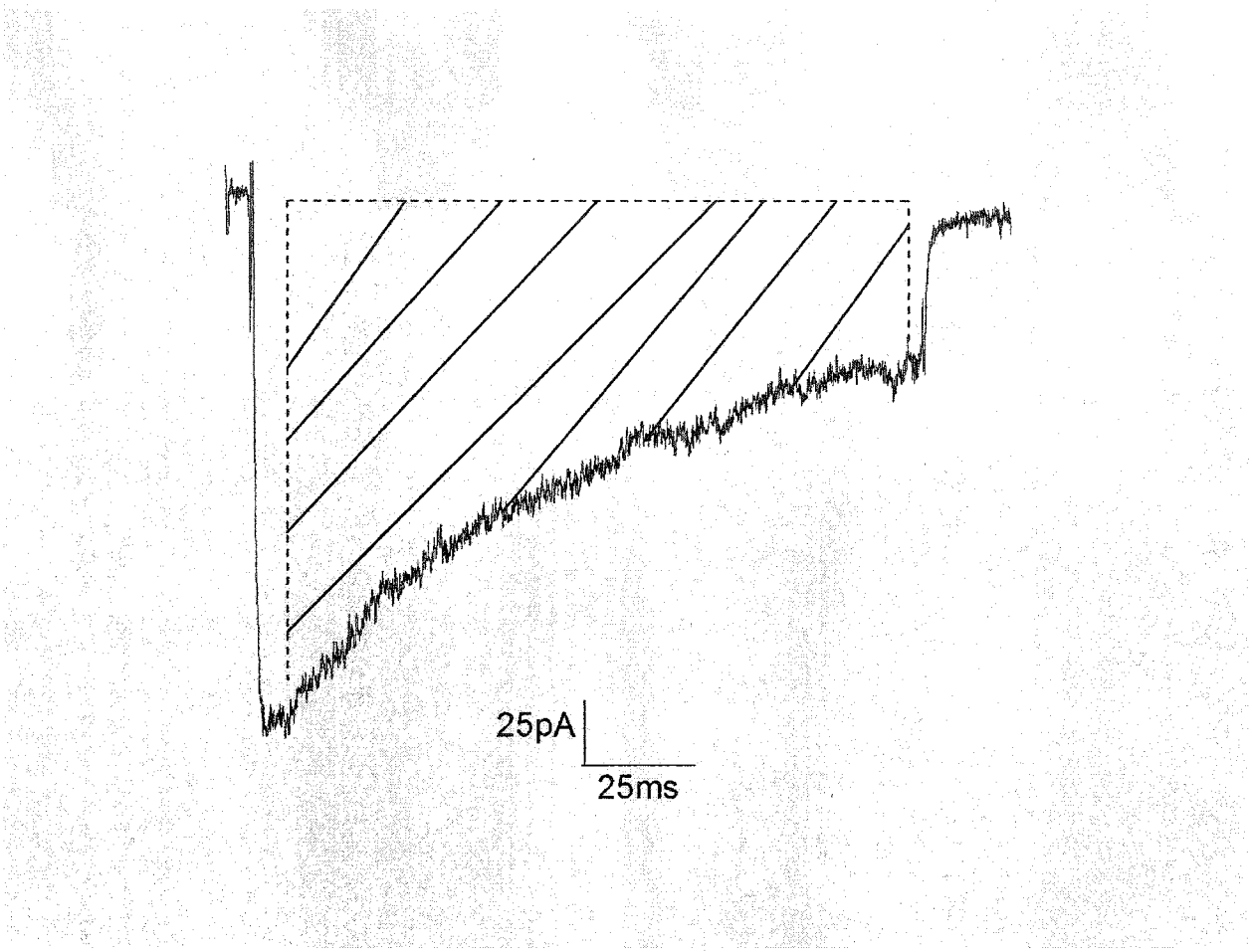

Figure 2.1: An example of time integral of I_{Ca} recorded from a rat β cell.
An example of an I_{Ca} recorded from a β cells elicited by a depolarization from -70 mV to +10 mV. The shaded area was the time integral of the I_{Ca}.

IV. Calcium measurements

Microfluorometry was used to measure $[Ca^{2+}]_i$ using either 0.1 mM indo-1 K^+ salt (for combined electrophysiology and $[Ca^{2+}]_i$ measurements) or indo-1-AM (for manganese quench experiments). The indo-1 salt was included in the pipette solution and was dialyzed into the cell through the recording pipette. For quenching experiments, the cells were incubated with 5 μM indo-1-AM in the standard extracellular solution for 15-20 minutes at 37 °C followed by 5 minute incubation in the dye-free extracellular solution at 37 °C to allow cellular esterases to cleave off the AM portion of the dye.

Cells were placed on the stage of an inverted microscope (Nikon) equipped with a fluorescent 40X oil immersion objective lens (Nikon). The dye was excited at 360 nm using a 100W mercury lamp and fluorescence signals were collected at 405 nm and 500 nm using two photomultiplier tubes. The ratio of the fluorescence (405/500) was used to calculate the $[Ca^{2+}]_i$ using the following equation (Grynkiewicz *et al.*, 1985),

$$[Ca^{2+}]_i = K^* (R-R_{min})/(R_{max}-R) \quad \text{(equation 1)}$$

where R was the measured 405/500 ratio. R_{max} and Rmin, were values of R measured by dialyzing cells with a pipette solutions containing (in mM):136 K-aspartate, 50 Hepes, and 15 $CaCl_2$ (pH = 7.4) for R_{max}; 53 K-aspartate, 50 Hepes, 50 EGTA, and 10 KCl (pH = 7.4) for R_{min}. K^* was calculated by dialyzing a pipette solution containing (in mM): 60 K-aspartate, 50 Hepes, 20 EGTA, and 15 $CaCl_2$ (pH = 7.4) which had a calculated $[Ca^{2+}]_i$ of 212 nM.

Background subtraction was done either by subtracting the fluorescence of the pipette and cell during cell attached patch configuration (electrophysiology) or an area containing no cells or debris (manganese quench).

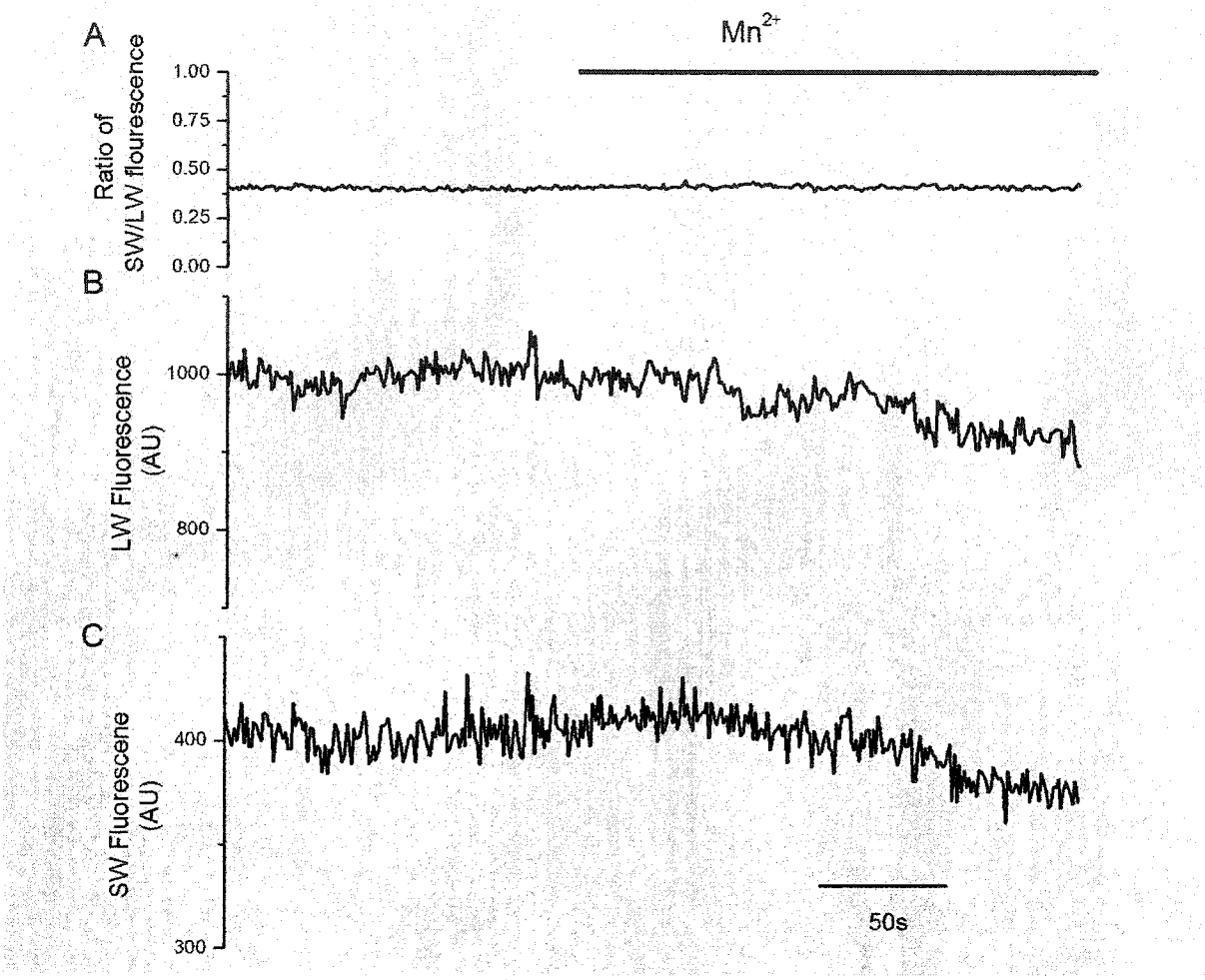

Figure 2.2: Manganese application decreased fluorescence without affecting the ratio of SW/LW.
Following 0.2 mM Mn^{2+} application indo-1 fluorescence was quenched resulting in a decrease in (B) long wave (LW) and (C) short wave (SW) fluorescence decrease without affecting the ratio of the SW/LW fluorescence (A).

V. Manganese quench

To measure the influx of Ca^{2+} into cells, Mn^{2+} quench experiments were performed on un-patched indo-1-AM loaded cells. The cells were exposed to 0.2mM $MnCl_2$ in the external solution. Mn^{2+} entered the cell through Ca^{2+} permeable pathways. Once inside the cell, Mn^{2+} bound to the indo-1 with high affinity causing the fluorescence to decrease at all wavelengths (Grynkiewicz *et al.*, 1985). In my experiments, the short wavelength (SW) (405 nm) fluorescence was not sensitive to changes in $[Ca^{2+}]_i$, but the long wavelength (LW) (500 nm) fluorescence decreased in response to $[Ca^{2+}]_i$ rise. Because of this property, a decrease in SW fluorescence following Mn^{2+} application was due to Mn^{2+} quenching indo-1 fluorescence indicating Ca^{2+} influx. This allowed the SW fluorescence to be used to monitor changes in fluorescence due to Mn^{2+} quench. Thus, an increase in the rate of SW fluorescence decrease reflected an increase in the rate of Ca^{2+} influx. Although Mn^{2+} also quenched the LW fluorescence, the ratio of SW/LW fluorescence was not affected by Mn^{2+} application (Figure 2.1). Therefore, the ratio of SW/LW fluorescence could still be used to calculate $[Ca^{2+}]_i$.

VI. Experimental solutions

The extracellular normal ringer solution (NMR) contained (in mM): 150 NaCl, 2.5 KCl, 10 Hepes, 3 glucose, 1 $MgCl_2$, and either 5 or 10 (exocytosis experiments) $CaCl_2$ (pH = 7.4 with NaOH). In experiments examining the role of PMCA's in Ca^{2+} removal, PMCA's were inhibited using a pH 8.8 extracellular solution (Xu *et al.*, 2000). It was identical to NMR, but had a pH of 8.8. To look at the role of the NCX in Ca^{2+}

removal, NCX was inhibited using a Na^+-free solution where NaCl was replaced with 150 mM N-methyl-glucamine (NMG). For zero Ca^{2+} experiments, $CaCl_2$ was omitted from the NMR and 1 mM EGTA and 2 mM $MgCl_2$ was added. The pipette solution contained (in mM): 120 cesium aspartate, 20 tetraethylammonium chloride, 20 HEPES, 0.1 Na-GTP, 0.1 indo-1 and either 1 $MgCl_2$ and 2 Na_2-ATP or 2.5 $MgCl_2$ and 5 Na_2-ATP (for calcium homeostasis experiments) (pH = 7.4 with CsOH). All drugs were diluted to their final concentration using the external solution.

VII. Statistics

All values presented are of means ± SEM. To determine statistical significance Student's t test was performed for two independent populations when data was compared between two populations of cells, while Student's t test for paired populations was used to compare data within a single cell (e.g. before and after application of a drug). For examining changes (e.g. change in $[Ca^{2+}]_i$) a one population t-test was preformed with the tested mean being zero. A p-value of less then 0.05 was considered significant.

Chapter 3: Calcium Regulation of Exocytosis in Rat β Cells

The importance of insulin to organisms has resulted in insulin secretion being tightly regulated. The final trigger of insulin secretion is $[Ca^{2+}]_i$ with increases in $[Ca^{2+}]_i$ resulting in increases in insulin secretion. Therefore, it is important to understand the relationship between $[Ca^{2+}]_i$ and exocytosis in β cells. In this chapter, I will attempt to describe the relationship between $[Ca^{2+}]_i$ and exocytosis in rat β cells and how this relationship changes with temperature.

I. Experimental protocol

Individual, cultured rat β cell was voltage clamped and held at -70 mV. $[Ca^{2+}]_i$ was monitored simultaneously with exocytosis (monitored as changes in membrane capacitance (ΔC_m)). A train of 15 depolarizations (150 ms) to +10 mV was applied to the cell at a frequency of 2.5 Hz. This train of depolarizations activated VGCC causing an influx of Ca^{2+} into the cell and thus creating a transient increase in $[Ca^{2+}]_i$. This increase in $[Ca^{2+}]_i$ stimulated the exocytosis of insulin containing vesicles resulting in an increased C_m. An example of this experiment at 22 °C (room temperature) is shown in Figure 3.1A.

In order to ensure a fair comparison between cells the following criteria were employed to select cells for analysis and inclusion in the data presented here. First, only cells that exocytosed during the $[Ca^{2+}]_i$ increase were included. Secondly, only cells with resting $[Ca^{2+}]_i$ below ~0.35 μM were included.

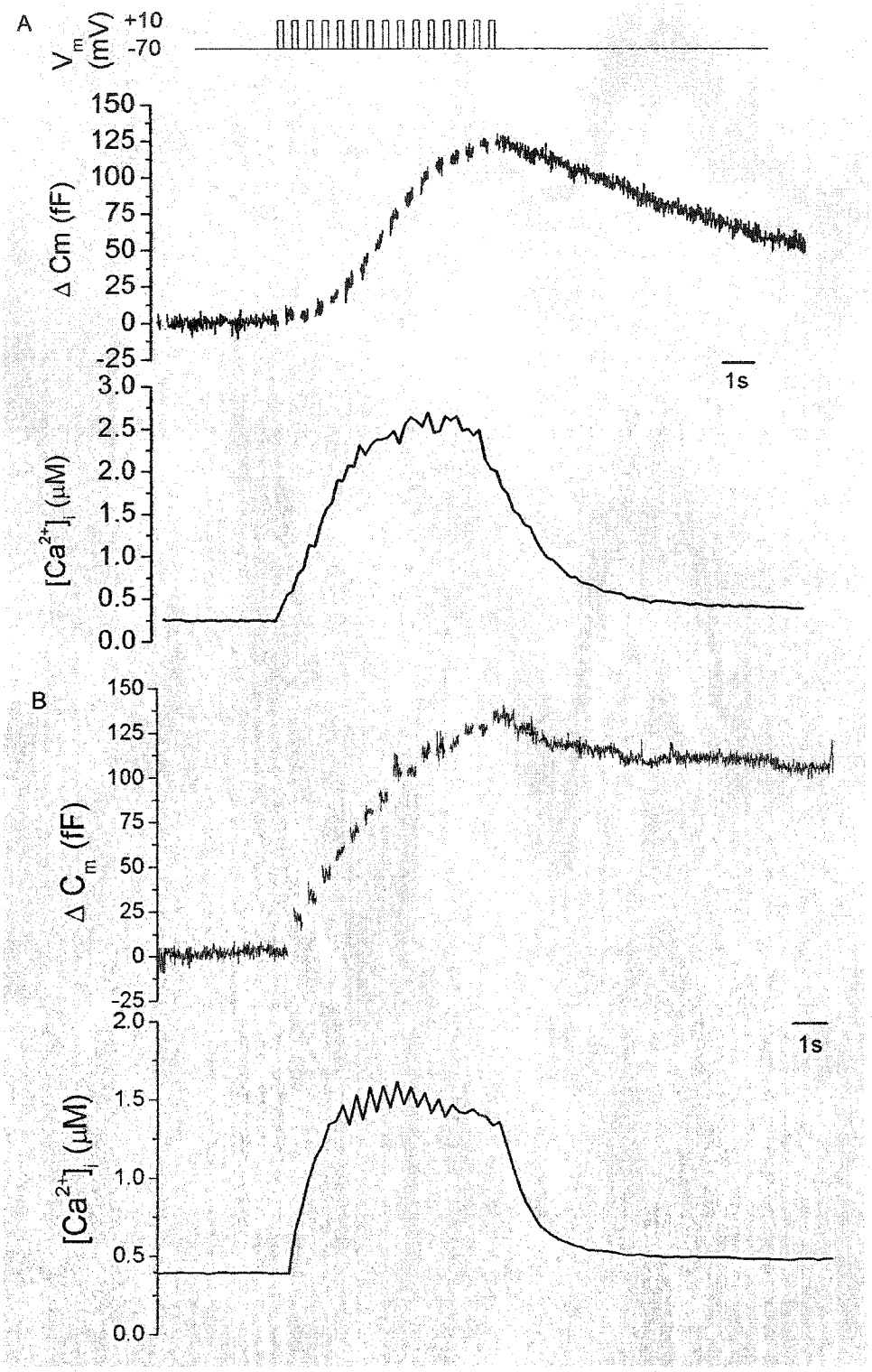

Figure 3.1: Changes in C_m in response to a depolarization triggered increase in $[Ca^{2+}]_i$. Applying a train of depolarizations from -70 mV to +10 mV caused an increase in $[Ca^{2+}]_i$ which was accompanied by an increase in C_m at both (A) room temperature ~22 °C and (B) elevated temperatures ~30 °C.

II. Pattern of exocytosis during the stimulation

A typical example of ΔC_m and change in $[Ca^{2+}]_i$ at 22 °C during a train of depolarizations is shown in Figure 3.1A. In this cell, after 3 depolarizations $[Ca^{2+}]_i$ rose to ~1μM, but caused barely detectable ΔC_m. It was not until after the 4th depolarization, when $[Ca^{2+}]_i$ rose to ~2 μM, that exocytosis was clearly triggered. Exocytosis continued to occur at a sustained rate for the following 7 steps. At this point, capacitance increase slowed down, likely, due to depletion of releasable vesicles. On the other hand, endocytosis could also be occurring and might mask additional C_m increases due to exocytosis. This pattern was typical of cells recorded at 22 °C. In this cell, the total C_m increase was 125 fF and the peak $[Ca^{2+}]_i$ rise was 2.6 μM. Using the estimate of 1.7 fF/vesicle (Ammäla *et al.*, 1993c), approximately 74 vesicles were released during this train of depolarization.

In contrast to the slowly developing exocytosis for cells recorded at 22 °C, for cells recorded at 30 °C the first depolarization typically triggered C_m increase. An example of this is shown in Figure 3.1B. In this cell, the first depolarization raised $[Ca^{2+}]_i$ to ~0.6 μM and resulted in a large jump in ΔC_m. In this example and in most cells recorded at 30 °C the first depolarization triggered C_m increase was often the largest increase throughout the whole train of depolarization. During subsequent depolarizations, the cell continued to exocytose, but at a rate that was typically slower (Figure 3.1B). In the cell shown in Figure 3.1B $[Ca^{2+}]_i$ reached 1.6 μM total increase in C_m was 135 fF, equivalent to the release of approximately 79 vesicles.

Figure 3.1 clearly shows that the pattern of exocytosis was different at the two temperatures. This suggests that the relationship between exocytosis and $[Ca^{2+}]_i$, may

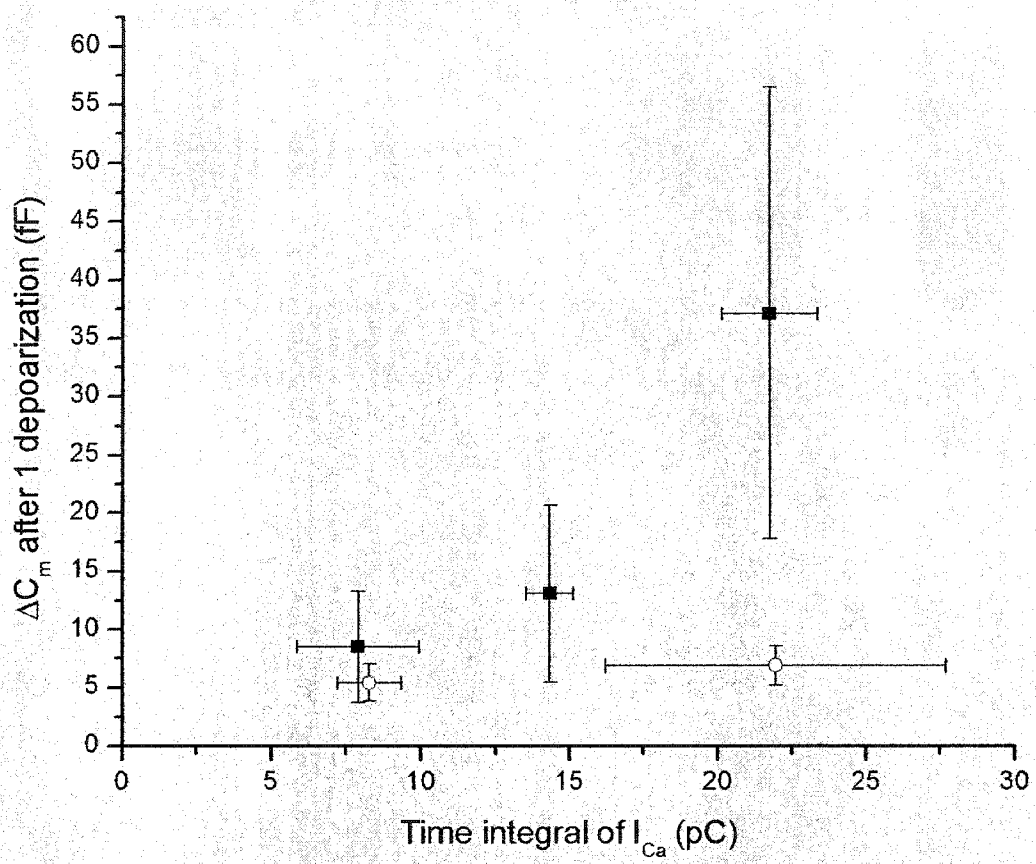

Figure 3.2: The amount of exocytosis triggered by a single depolarization was dependent on temperature and the amount of Ca^{2+} entry.
The ΔC_m after 1 depolarization was graphed against the integrated I_{Ca} of the same depolarization. (22 °C: hollow circle, 30 °C solid square) (n = 3-5)

change with temperature. In the remaining portion of this chapter I shall document the relationship between $[Ca^{2+}]_i$ and exocytosis in the two temperatures and speculate on possible mechanisms underlying the temperature dependence.

III. Exocytosis triggered by a single depolarization

One clear difference between the cells recorded at the two temperatures was the ability of the cell to exocytose following only a single 150 ms depolarization at 30 °C. In contrast, at 22 °C, one depolarization caused barely any detectable C_m increase. To further examine this, the ΔC_m after one depolarization was determined from a number of cells recorded at 22 °C and 30 °C and graphed as a function of the time integral of I_{Ca} (Figure 3.2). The integral of the I_{Ca} was used here instead of $[Ca^{2+}]_i$ because exocytosis occurred during the depolarization. The integral of I_{Ca}, was a measure of the amount of Ca^{2+} entry and thus more accurately reflected the actual $[Ca^{2+}]_i$ near the plasma membrane where vesicles were located. In contrast, my measured $[Ca^{2+}]_i$ was the average $[Ca^{2+}]_i$ over the entire cell and this underestimated the $[Ca^{2+}]$ near the cell membrane.

Figure 3.2 shows that at 22 °C, the average ΔC_m after one depolarization was ~6 fF and this value was not affected by increases in Ca^{2+} entry. At 30 °C, when the amount of Ca^{2+} entry was low the C_m increase was similar to that at 22 °C. However, at 30 oC when the amount of Ca^{2+} entry increased there was an increase in the ΔC_m. The amount of ΔC_m increased 1.6 fold when the time integral of I_{Ca} increased from 8 pC to 14 pC. There was a further 2.8 fold increase in exocytosis when the integrated I_{Ca} increased to 21 pC (Figure 3.2). Thus, when the amount of Ca^{2+} entry was low the amount of exocytosis at both temperatures was similar, but at 30 °C, the amount of exocytosis

increased with the amount of Ca^{2+} entry (Figure.3.2). These results suggest that when compared at similar Ca^{2+} entry more exocytosis was triggered at higher temperatures.

IV. Exocytosis triggered during the first five depolarizations

To further characterize the Ca^{2+} sensitivity of exocytosis and how it may change with temperature the rate and amount of exocytosis triggered by the first 5 depolarizations were examined. The first 5 steps of depolarization was analyzed here because it is unlikely that the cell would be depleted of vesicles and there may be less contamination of the C_m increases by endocytosis. The rate of exocytosis was calculated by fitting a linear line on the C_m trace during the first 5 steps of depolarization. The slope of the line represented the average rate of exocytosis. This rate was compared to both the average $[Ca^{2+}]_i$ over the 5 depolarizations and the cumulative integral of I_{Ca} from the 5 depolarizations. This was done because in some cells exocytosis occurred during the voltage steps (where I_{Ca} integral was more accurate), while in other cells exocytosis occurred both during the voltage step and between depolarizations (where $[Ca^{2+}]_i$ was more accurate). By using both estimates of $[Ca^{2+}]$, one can see if they show a similar relationship to exocytosis and if these relationships change with temperature.

Figure 3.3A shows that at 22 °C increases in the I_{Ca} integral were accompanied by a small increase in the rate of exocytosis. The rate of exocytosis when Ca^{2+} entry was ~20 pC was 1.3 fF s^{-1} and a ~5 fold increase in the I_{Ca} integral (~90 pC) increased the rate of exocytosis to 9.6 fF s^{-1}. However, at 30 °C a similar change in I_{Ca} integral increased the rate of exocytosis from 6.8 fF s^{-1} to 54.6 fF s^{-1} (Figure 3.3A). These results showed that at both temperatures the rate of exocytosis increased with the amount of Ca^{2+} entry.

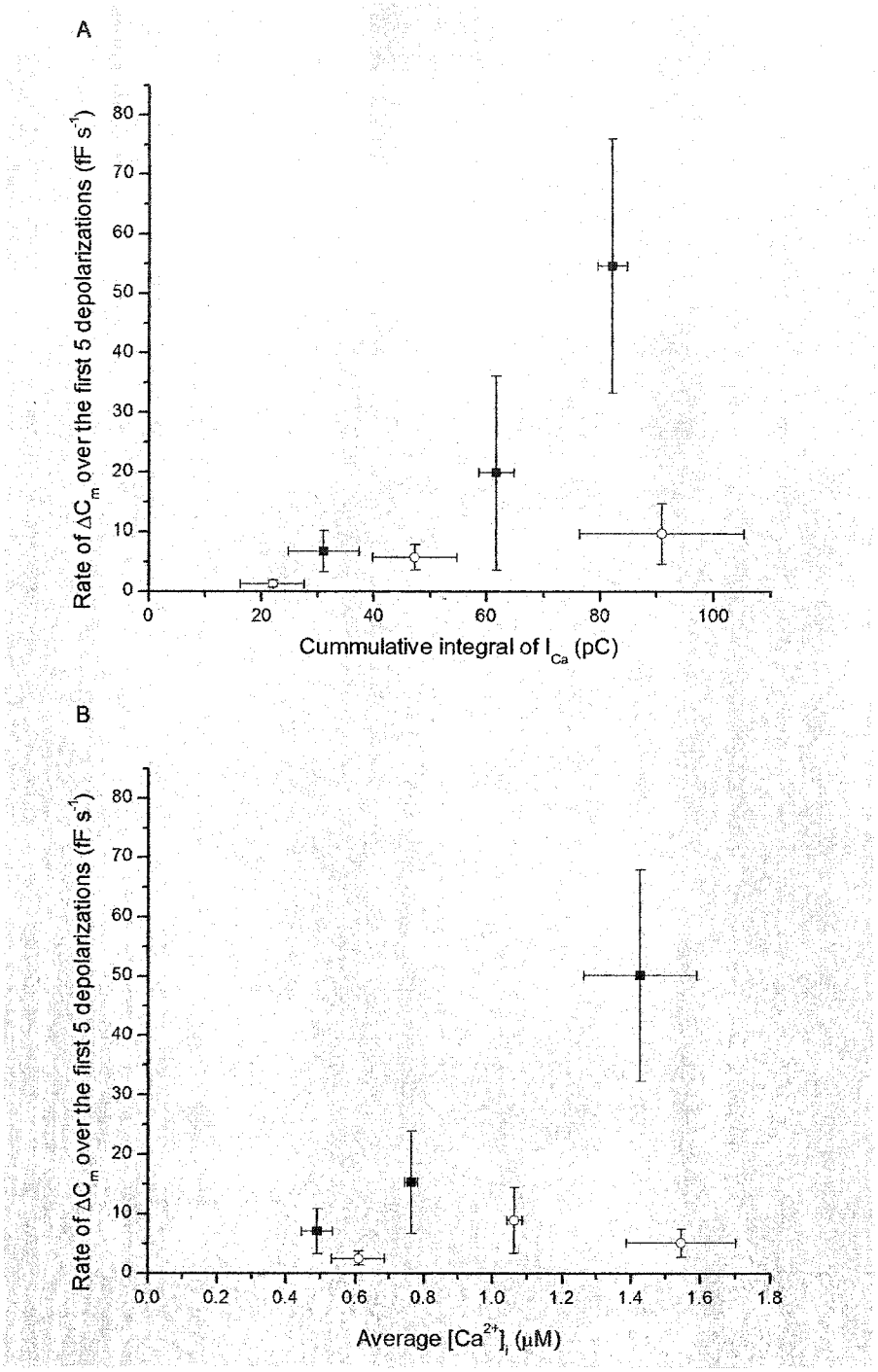

Figure 3.3: The rate of exocytosis during the first five depolarizations was dependent on temperature and Ca^{2+}.

The rate of ΔC_m over the first five depolarizations was plotted against (A) the cumulative integrated I_{Ca} of the five steps or (B) the average $[Ca^{2+}]_i$ over the five steps. (22 °C: hollow circle, 30 °C solid square) (n = 3-5)

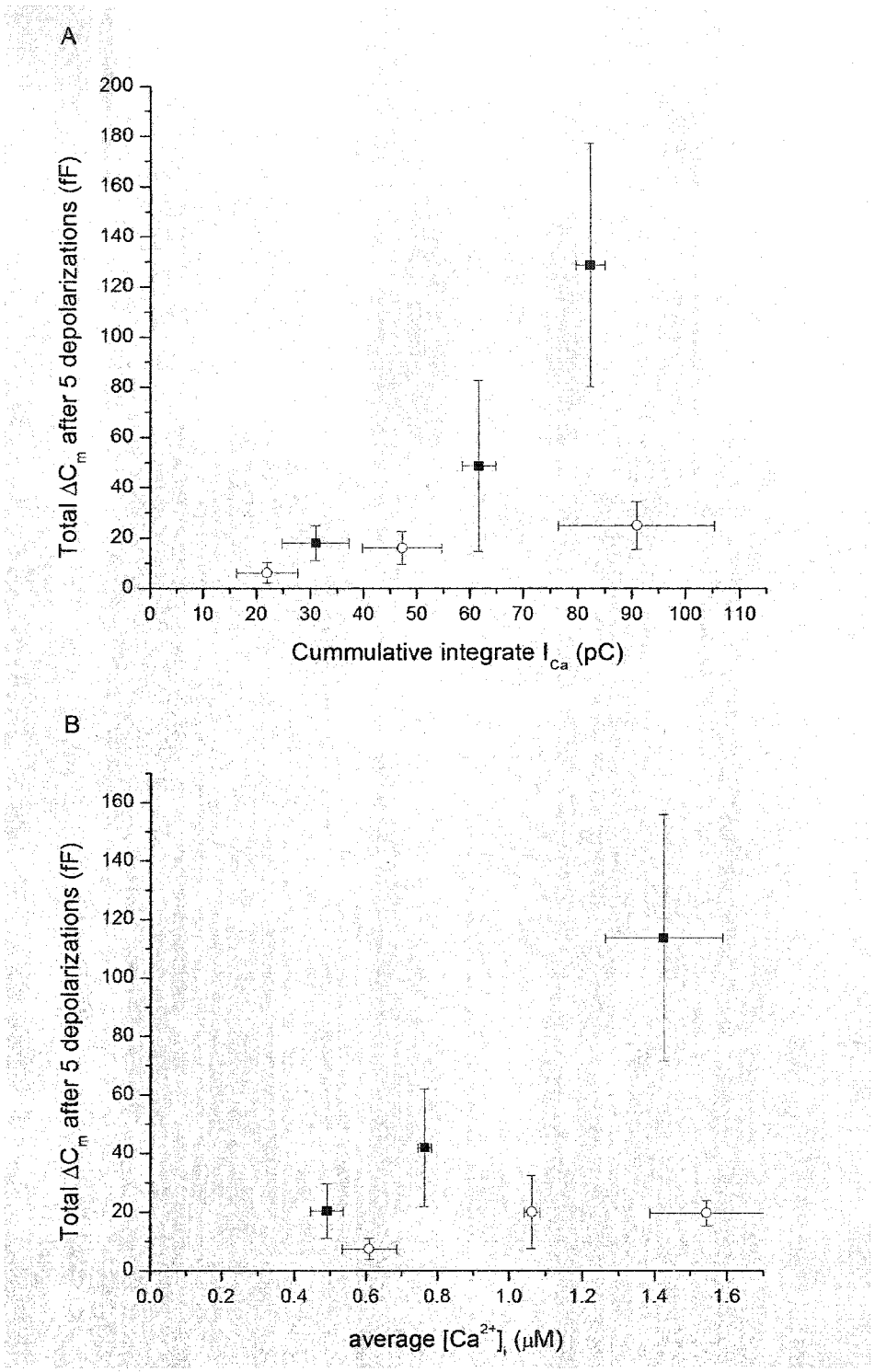

Figure 3.4: The amount of exocytosis triggered by five depolarizations was dependent on temperature and Ca^{2+}.

The total ΔC_m after the first five depolarizations was plotted against (A) the cumulative integrated I_{Ca} of the five steps or (B) the average $[Ca^{2+}]_i$ over the five steps. (22 °C: hollow circle, 30 °C solid square) (n = 3-5)

However, this relationship was a lot more pronounced at higher temperatures.

When the relationship between the rate of exocytosis and the average $[Ca^{2+}]_i$ over this same period was compared in the same cells a similar picture emerged. At 22 °C, the rate of exocytosis only increased slightly at higher $[Ca^{2+}]_i$ (Figure3.3B). When $[Ca^{2+}]_i$ increased from 0.6 μM to 1.6 μM there was a ~2 fold increase (from 2.5 fF/s to 5 fF/s) in the rate of exocytosis (Figure 3.3B). At 30 °C, the rate of ΔC_m increased ~7 fold (from 7 fF/s to 50 fF/s) when $[Ca^{2+}]_i$ increased from 0.4 μM to1.4 μM (Figure 3.3B). At low (~0.6 μM) $[Ca^{2+}]_i$ the rate of exocytosis at both temperatures was similar, however as $[Ca^{2+}]_i$ increased there was a clear difference with 30 °C having a 10 fold faster rate of exocytosis (Figure 3.3B).

A similar pattern was evident when examining the total C_m increase after 5 depolarizations (Figure 3.4A). At 22 °C when the time integral of I_{Ca} increased from 22 pC to 90 pC there was a 3 fold increase in the total C_m increase (7 fF to 24 fF) (Figure 3.4A). While at 30 °C, similar increases in Ca^{2+} entry cause a ~5.5 fold increase in C_m (20 fF to 114 fF) (Figure 3.4A). When compared at similar Ca^{2+} entry (~80 to 90 pC) there was ~5 times more cumulative exocytosis at 30 °C. A similar result was found when examining the relationship between the average $[Ca^{2+}]_i$ and the total C_m increase (Figure 3.4B). When $[Ca^{2+}]_i$ increased from 0.6 μM to 1.5 μM at 22 °C the total ΔC_m increased by ~3 fold. At 30 °C when $[Ca^{2+}]_i$ increased from 0.5 μM to 1.4 μM there was a ~6 times increase in cumulative exocytosis (Figure 3.4B). When compared, at similar $[Ca^{2+}]_i$ (1.4 to 1.5 μM) there was ~6 times more exocytosis at 30 °C than at 22 °C (Figure3.4B).

V. Total amount of exocytosis triggered by a train of depolarizations

The previous results suggest that, during the initial five depolarizations, there was more exocytosis and a faster rate of exocytosis at higher temperatures. Assuming that the readily releasable pool (RRP) of vesicles was not completely depleted by the train of 15 depolarizations, the faster rate of exocytosis at 30 °C should result in a larger total C_m increase at the end of the train of depolarizations. On the other hand, if the train of depolarizations could exhaust the RRP then the total ΔC_m should be similar at both temperatures, but at 30 °C, it would occur over a shorter period of time. However, the rate of the replenishment of the RRP is Ca^{2+} and temperature dependent so it is possible that more exocytosis may occur at higher temperatures because of mobilization of vesicles. Figure 3.5 is a plot of the total $\Delta C_{m,}$ (measured as the amplitude of the ΔC_m at than end of the train of depolarizations) versus the peak $[Ca^{2+}]_i$ elicited by the train of depolarizations. The I_{Ca} integral cannot be used here because during the later depolarizations of the train the I_{Ca} was contaminated with a gradual development of an outward current. At both 22 °C and 30 °C, increases in $[Ca^{2+}]_i$ was accompanied by an increase in the total ΔC_m (Figure 3.5). When compared at a $[Ca^{2+}]_i$ of approximately 1.4 μM the ΔC_m at 22 °C was an average of approximately 70 fF which was ~4 fold smaller than the C_m increase at 30 °C (285 fF) (Figure 3.5). At approximately 3.25 μM $[Ca^{2+}]_i$ the total C_m increase at 22 °C increased to 195 fF, but was still ~1.8 fold smaller then the C_m increase (360fF) at 30 °C (Figure 3.5). These results indicate that the total amount of exocytosis was greater at higher temperatures.

All of the data presented in this chapter indicate that the amount of Ca^{2+} entering the cell (measured either by I_{Ca} integral or by $[Ca^{2+}]_i$) regulates the rate of exocytosis

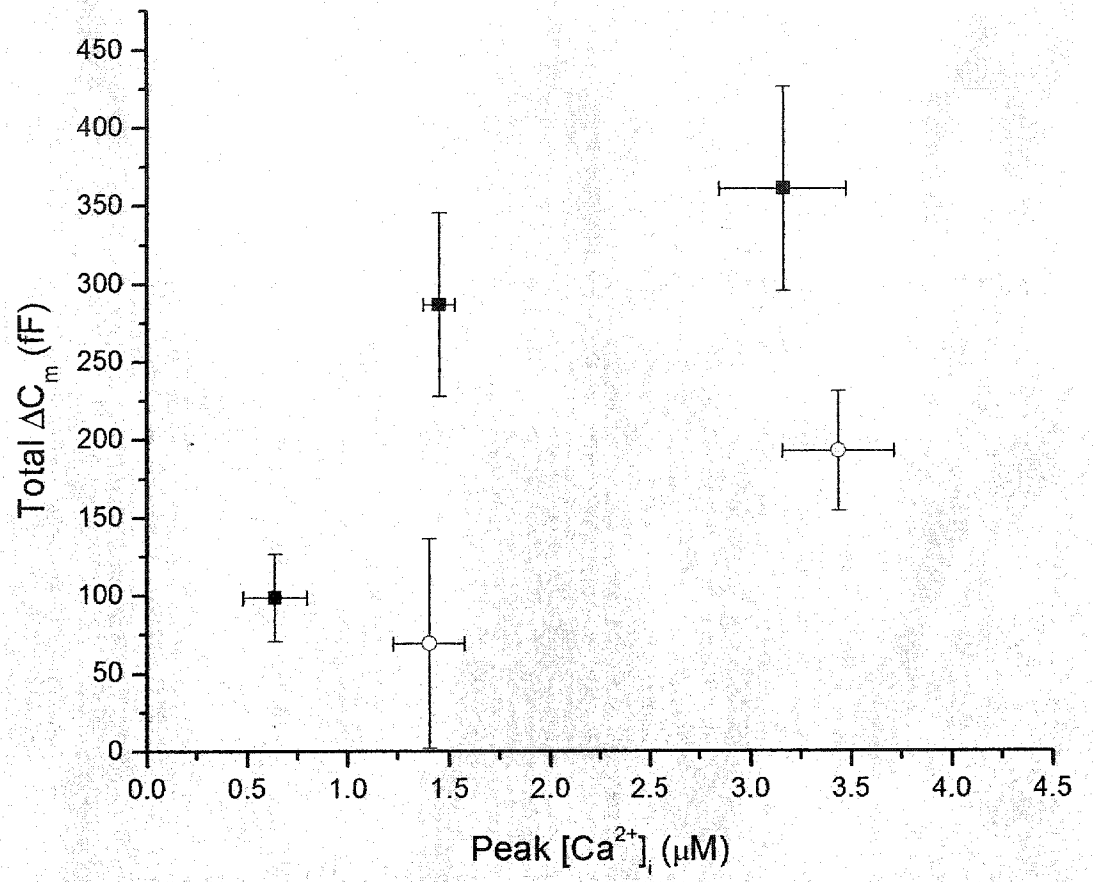

Figure 3.5: The total amount of exocytosis triggered by a train of depolarizations was dependent on temperature and $[Ca^{2+}]_i$.
Plot of the total ΔC_m (measured at the end of the train of depolarizations) versus the peak $[Ca^{2+}]_i$. (22 °C: hollow circle, 30 °C solid square) (n = 2-6)

and/or the amount of exocytosis. This data also indicates that exocytosis is highly temperature dependent such that more exocytosis is triggered at elevated temperatures. An indicator of temperature sensitivity is a Q_{10} value. This value is the factor of the increase caused by raising the temperature 10 °C. Although a Q_{10} can not be calculated here a Q_8 can be for the ΔC_m after 1 and 5 depolarizations as well as the rate of ΔC_m. These Q_8s are ~5-5.5. In Chapter 5 (the discussion), potential causes for the temperature differences will be discussed.

Chapter 4: Regulation of Calcium Homeostasis in Rat β Cells

Ca^{2+} regulates many process in cells including secretion, gene transcription, and apoptosis (Berridge *et al.*, 2000). In β cells, increases in $[Ca^{2+}]_i$ trigger insulin secretion. As shown in Chapter 3, depolarization triggered $[Ca^{2+}]_i$ rise in turn stimulated exocytosis. The amplitude of the $[Ca^{2+}]_i$ rise was a determining factor in the amount of exocytosis. Following the $[Ca^{2+}]_i$ rise, $[Ca^{2+}]_i$ quickly returned to basal levels (for an example see Figure 3.1). This is important as sustained $[Ca^{2+}]_i$ rise would result in depletion of vesicles as well as toxicity to the cell. This observation leads to the question: what mediates this fast restoration of basal $[Ca^{2+}]_i$ in rat β cell? This chapter tries to address this question. In addition, what regulates basal $[Ca^{2+}]_i$ and what limits $[Ca^{2+}]_i$ increases following a stimulus will also be examined.

I. Experimental procedure

Individual β cells were voltage clamped at -70 mV. A train of 150 ms depolarizations to +10 mV was applied (2.5 Hz) to the cell to activate VGCC and cause a transient increase in $[Ca^{2+}]_i$. The number of steps applied was constant within a single cell, but could vary between cells depending on the I_{Ca} of the cell to ensure a similar $[Ca^{2+}]_i$ rise in all cells. The number of steps ranged from 2 to 10, but typically was 5 to 7. The number of steps applied to the cell was determined by applying a single depolarization to the cell and observing both the I_{Ca} and change in $[Ca^{2+}]_i$ induced by the depolarization. The time constant (τ) of Ca^{2+} removal was calculated by fitting the

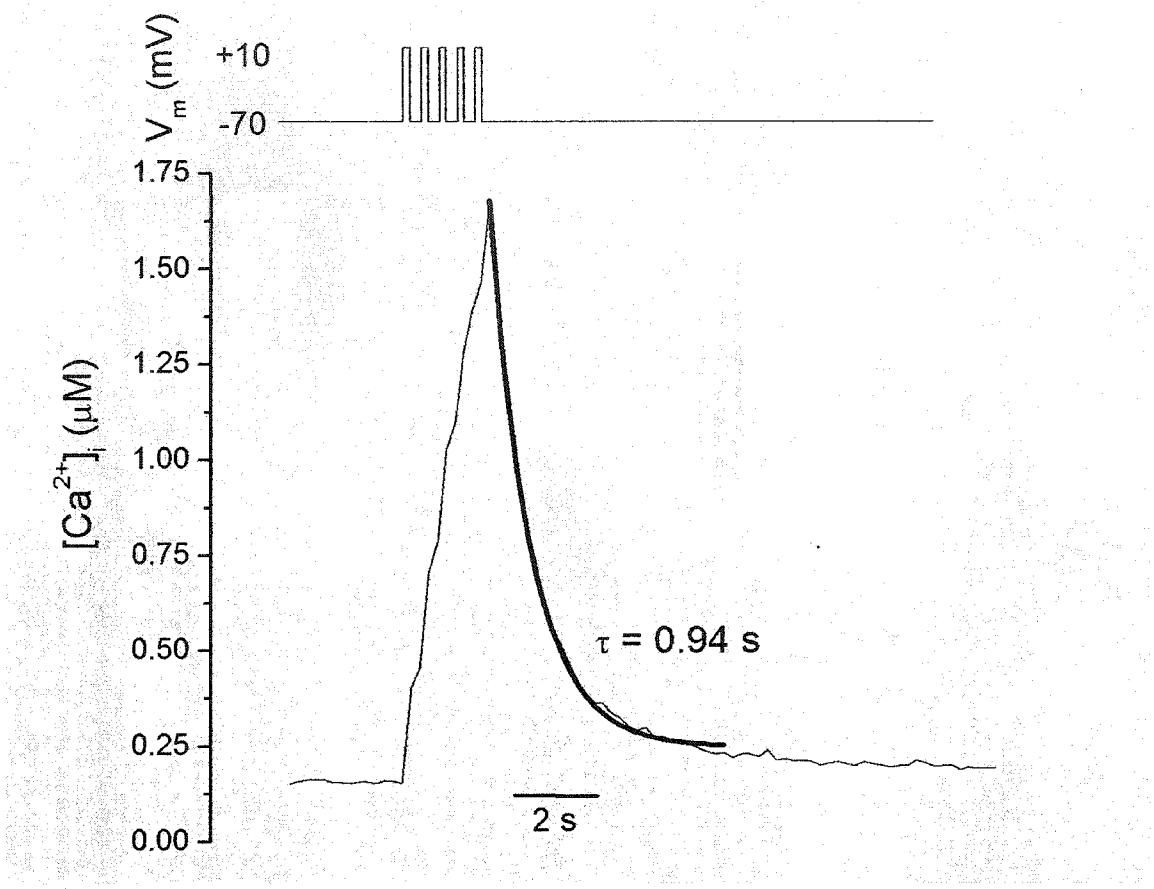

Figure 4.1: An example of the procedure for determining the τ of Ca^{2+} removal. The cell was voltage clamped at -70 mV and five depolarizations to +10 mV were applied to induce a transient Ca^{2+}increase. To calculate τ, the decrease in $[Ca^{2+}]_i$ was fitted with a single exponential (dark line). In this cell, the τ was 0.94 s.

decrease in $[Ca^{2+}]_i$ with a single exponential. An example of this procedure is shown in Figure 4.1. In this cell, five depolarizations raised the $[Ca^{2+}]_i$ to 1.65 μM and the τ of Ca^{2+} removal was 0.94 s. The τ of $[Ca^{2+}]_i$ decrease was determined under control conditions and after the application of an inhibitor that blocks a single Ca^{2+} removal mechanism. The two values were compared to see what effect, if any, inhibiting one removal mechanism had on Ca^{2+} removal.

The τ of Ca^{2+} removal averaged 1.51 ± 0.06 s (n = 68) under control conditions. In order to determine the effect of inhibiting a Ca^{2+} removal mechanism, it was necessary to know how much τ changed with time after whole-cell, as some cytosolic contents might be lost during dialysis. Under control condition τ increased from 1.49 ± 0.14 s (n = 5) at time 0 (approximately 3 minutes after whole-cell) to 1.83 ± 0.10 s (n=5) 4 minutes later (a time similar to when an inhibitor was tested) (Figure 4.2A). This ~22 % increase was not statistically significant ($p < 0.056$), but did indicate that there was a gradually slowing of Ca^{2+} removal with time. Any effects of inhibiting a Ca^{2+} removal mechanism on τ must exceed this basal increase if the removal mechanism plays a role in Ca^{2+} removal. Note that between 4 and 7 minutes of whole-cell, the τ appears to be stable (Figure 4.2A).

Two other parameters that can be examined to determine if a particular Ca^{2+} removal mechanism has a role in Ca^{2+} homeostasis are basal $[Ca^{2+}]_i$ and the amplitude of the depolarization-triggered Ca^{2+} transient (peak $[Ca^{2+}]_i$ minus pre-depolarization $[Ca^{2+}]_i$). The effect of whole-cell on these parameters was also examined in the control

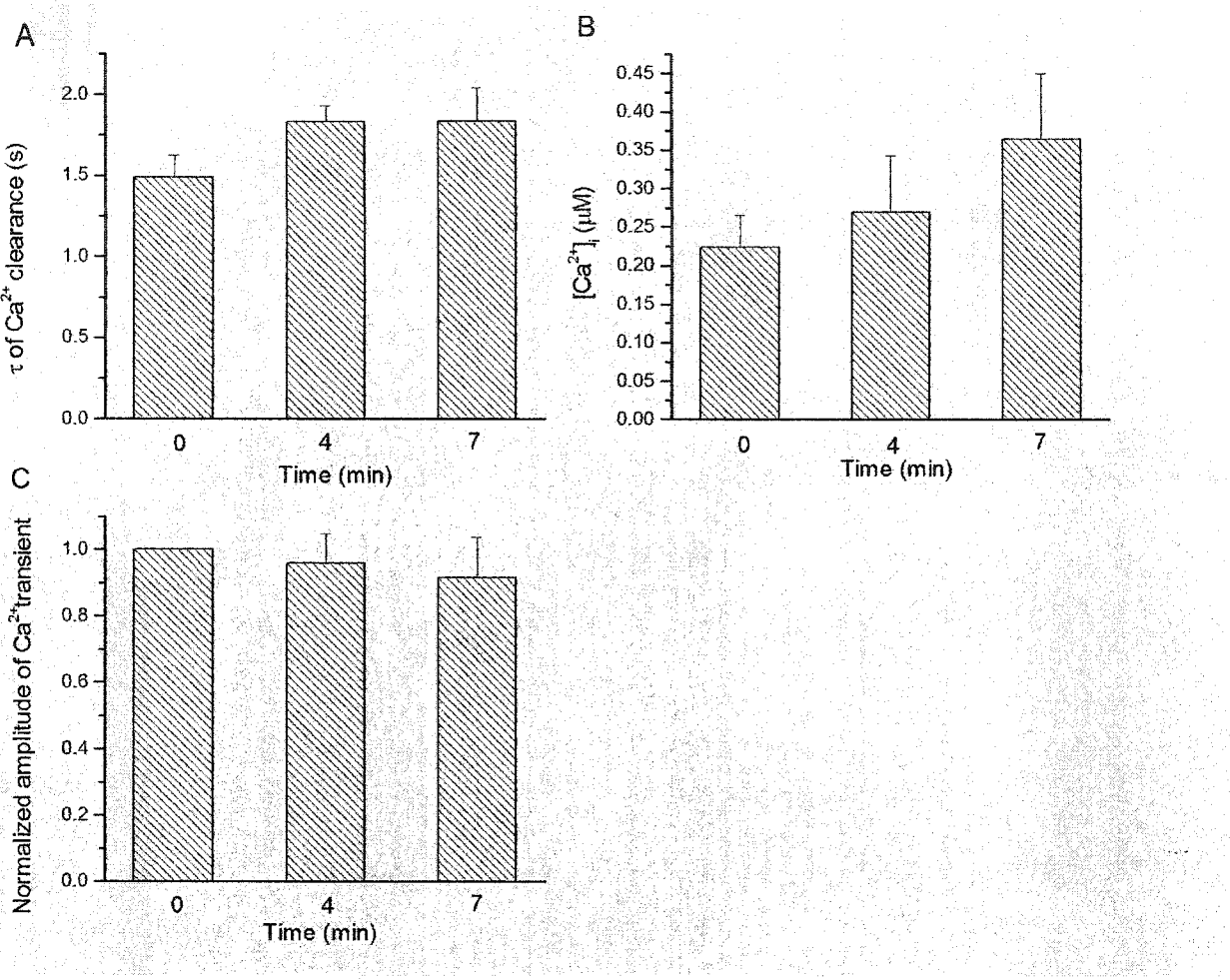

Figure 4.2: Time dependent changes in Ca^{2+} homeostasis under control conditions. Time dependent changes in (A) τ, (B) basal $[Ca^{2+}]_i$, and (C) normalized amplitude of the depolarization triggered Ca^{2+} transient (peak $[Ca^{2+}]_i$ minus basal $[Ca^{2+}]_i$) under control conditions (n = 5). Time 0 was approximately 3 minutes after whole-cell and was the approximate time when control values were determined. Note that none of these changes was statistically significant.

cells (Figure 4.2C). No statistically significant change occurred in either parameter in the first 7 minutes of whole-cell. However, the trend was for the amplitude of the Ca^{2+} transient to get smaller (Figure 4.2C), and the basal $[Ca^{2+}]_i$ (Figure 4.2B) to increase with time.

II. Role of mitochondria in Ca^{2+} removal

The large electrochemical gradient for Ca^{2+} influx into the mitochondria exists because the V_m of the mitochondria is approximately -180 mV due to the large H^+ gradient created by the electron transport chain (Bernardi, 1999; Rizzuto *et al.*, 2000). Ca^{2+} handling by the mitochondria can be disrupted in several ways that result in a decrease in the Ca^{2+} gradient. One method is to inhibit the electron transport chain with cyanide, which results in a decrease in the extrusion of H^+ from the mitochondria. However, in an attempt to preserve the H^+ gradient, the F_0F_1 ATPase may begin to pump H^+ out of the mitochondria by consuming ATP. To prevent this, the ATPase was inhibited with oligomycin. The combination of cyanide and oligomycin should result in disruption of Ca^{2+} uptake into the mitochondria. A second way of disrupting the H^+ gradient and Ca^{2+} uptake into the mitochondria is to apply the protonophore CCCP. CCCP transports H^+ into the mitochondria resulting in the disruption of the H^+ gradient and inhibition of Ca^{2+} uptake (Kadenbach, 2003; Rizzuto *et al.*, 2000).

In my study, cyanide (5 mM) alone was initially bath applied. This was followed by bath application of both cyanide and oligomycin (5 μM). In the example in Figure 4.3, cyanide alone increased τ of Ca^{2+} removal s from 1.41 s to 1.59 s, an increase that was smaller than the average basal increase. Following oligomycin application, the τ of Ca^{2+}

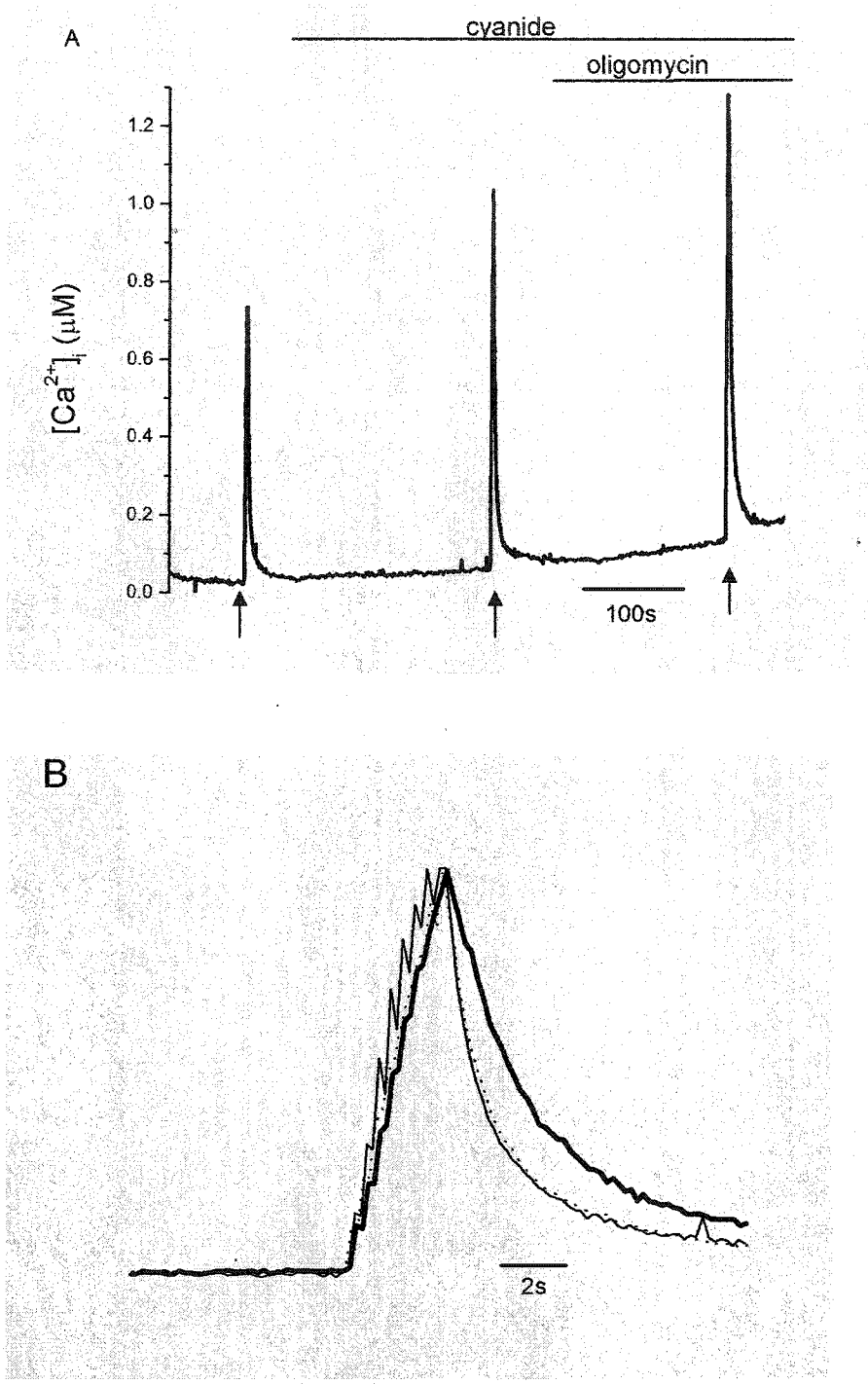

Figure 4.3: Mitochondrial inhibitors had a small effect on basal $[Ca^{2+}]_i$, and Ca^{2+} clearance.
A. Application of cyanide (5 mM) caused a slight increase in $[Ca^{2+}]_i$ and a slight slowing of Ca^{2+} removal. When oligomcyin (5 μM) was co-applied, a larger effect on both parameters was seen. Each arrow represents a train of depolarizations being applied to the cell. B. An expanded, scaled trace of the Ca^{2+} decay (control thin black line, cyanide dotted line, CN and oligomcyin thick black line).

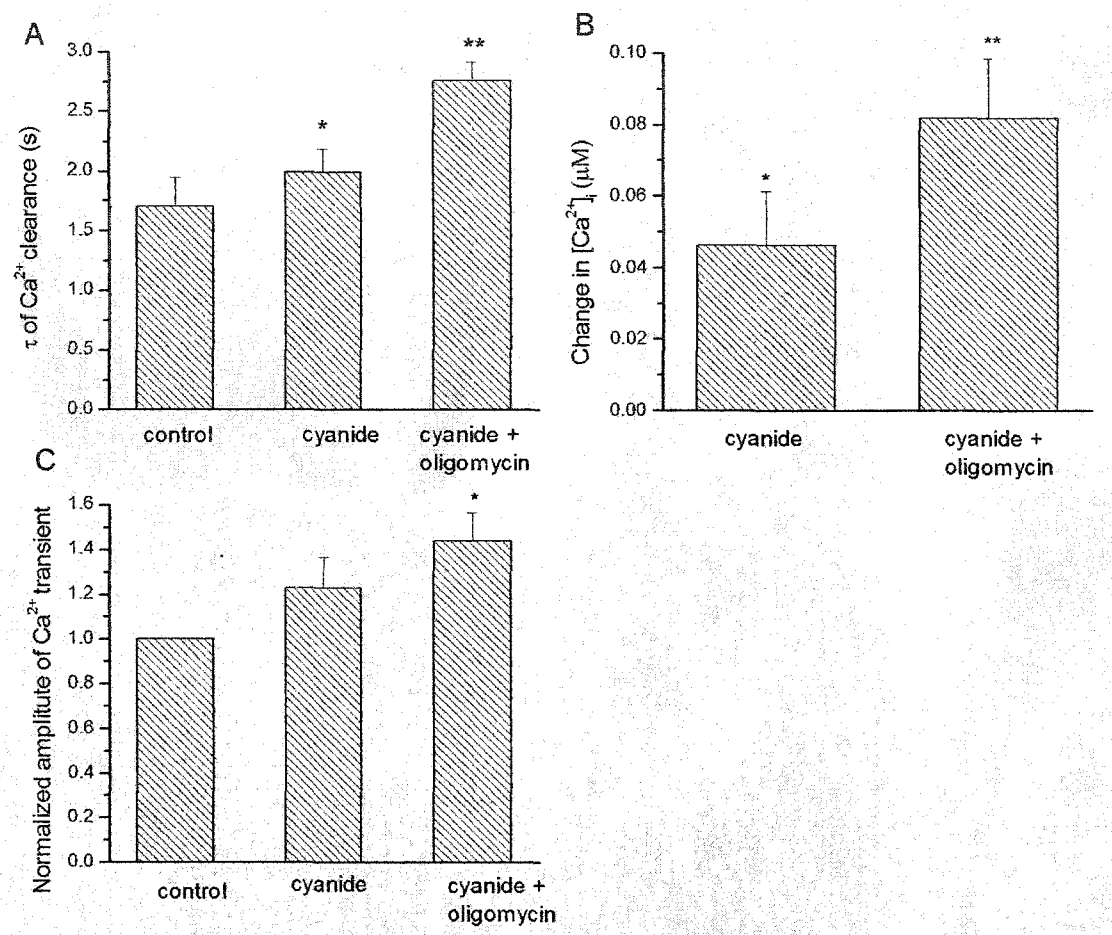

Figure 4.4: Inhibition of mitochondrial Ca^{2+} uptake with cyanide and oligomycin influenced Ca^{2+} homeostasis.

The changes in (A) τ, (B) basal $[Ca^{2+}]_i$, and (C) normalized amplitude of the depolarization triggered Ca^{2+} transient after inhibition of mitochondrial Ca^{2+} uptake with cyanide and oligomcyin. (n = 8) *$p < 0.05$, **$p < 0.005$

removal increased to 2.79 s (Figure 4.3B). In 7 of 8 cells where both cyanide alone and cyanide in combination with oligomcyin were tested, a similar pattern of increase in τ by cyanide and cyanide with oligomycin was observed. On average, τ increased from 1.70 ± 0.24 s under control conditions to 1.99 ± 0.19 s with cyanide and 2.76 ± 0.16 s with cyanide plus oligomycin ($p < 0.005$; $n = 8$) (Figure 4.4A). Although the effect of cyanide on τ was statistically significant ($p < 0.05$) it was a smaller change (17 %) than the change seen due to basal slowing of Ca^{2+} removal (22 %) (Figure 4.2A). Therefore, cyanide alone was not sufficient to disrupt mitochondrial Ca^{2+} uptake. However, the increase in τ (60 %) by the combination of cyanide and oligomycin was more than the expected basal increase.

In addition to slowing Ca^{2+} removal, inhibition of the mitochondria also increased the resting $[Ca^{2+}]_i$ (Figure 4.3A). When cyanide was applied there was a small increase in resting $[Ca^{2+}]_i$ (0.02 μM) and after oligomycin application the resting $[Ca^{2+}]_i$ increased further by 0.06 μM (Figure 4.3A). In 2 of 8 cells tested, the increase in basal $[Ca^{2+}]_i$ following cyanide was under 0.01 μM. In the remaining 6 cells, the increase in basal $[Ca^{2+}]_i$ ranged from 0.02 μM to 0.11 μM. The average increase in all 8 cells was 0.05 ± 0.02 μM ($p < 0.05$) (Figure 4.4B). Following application of oligomcyin, all 8 cells had further increases in $[Ca^{2+}]_i$ ranging from 0.03 μM to 0.15 μM with the average increase being 0.08 ± 0.02 μM ($p < 0.005$) (Figure 4.4B). When the amplitude of the Ca^{2+} transient was compared, there was no change following cyanide application, but the amplitude of the Ca^{2+} transient increased by 1.44 fold ($p < 0.05$) following cyanide plus oligomcyin (Figure 4.4C).

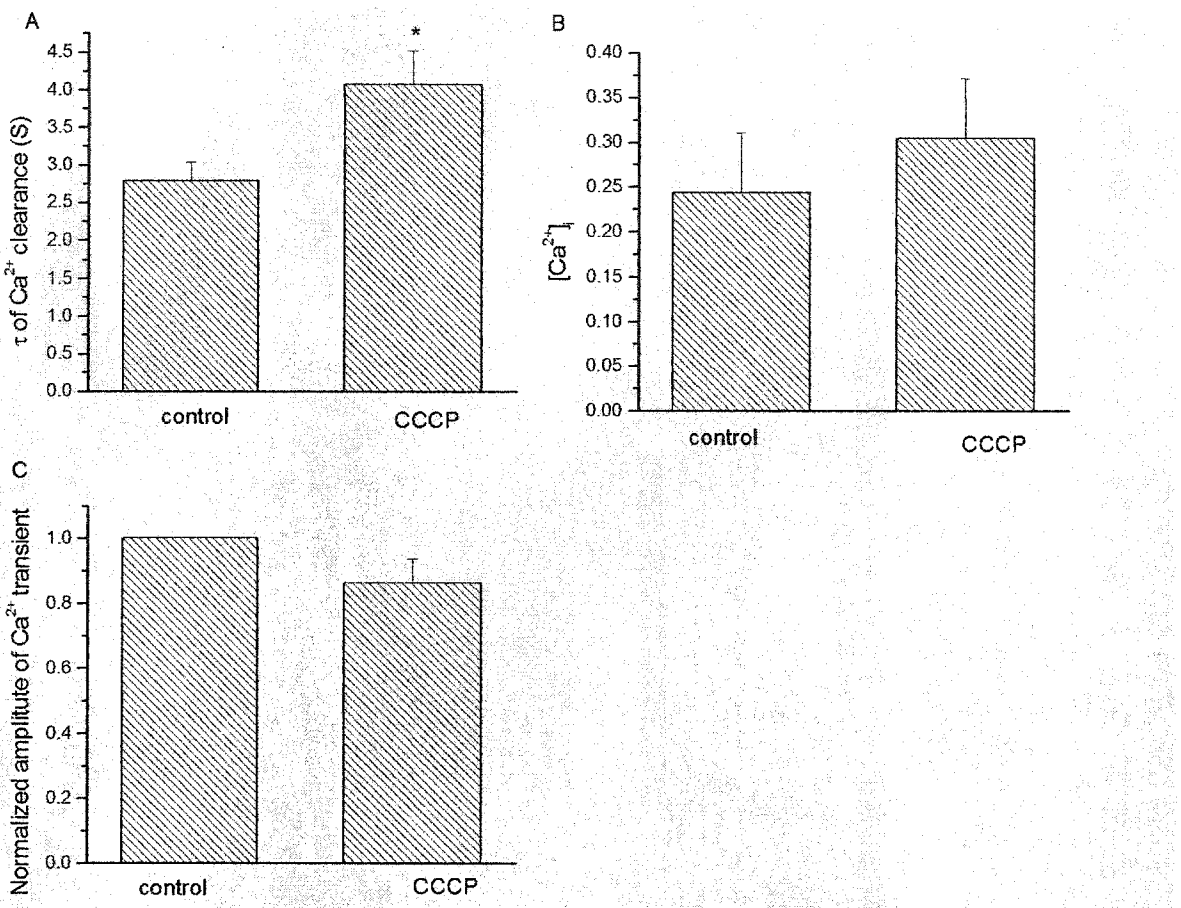

Figure 4.5: Inhibition of mitochondrial Ca^{2+} uptake with CCCP influenced Ca^{2+} homeostasis.

The changes in (A) τ, (B) basal $[Ca^{2+}]_i$, and (C) normalized amplitude of the depolarization triggered Ca^{2+} transient after inhibition of mitochondrial Ca^{2+} uptake with CCCP (2 μM). (n = 5) *$p < 0.05$

To examine whether the combination of cyanide and oligomycin could indeed fully dissipate the H^+ gradient, and disrupt mitochondrial function, the more potent CCCP (2 μM) was also tested. CCCP increased the τ of Ca^{2+} removal from 2.79 ± 0.25 s to 4.06 ± 0.44 s ($p < 0.05$; $n = 5$) an increase of 45 % (Figure 4.5A). In terms of basal $[Ca^{2+}]_i$ change in the five cells one had a decrease (0.1 μM) in resting $[Ca^{2+}]_i$ following CCCP, one had a small increase in basal $[Ca^{2+}]_i$ (0.02 μM), and 3 had increases in basal $[Ca^{2+}]_i$ of over 0.10 μM. On average the $[Ca^{2+}]_i$ went from 0.24 ± 0.07 μM to 0.30 ± 0.07 μM ($p < 0.27$) and the average increase in $[Ca^{2+}]_i$ was 0.06 ± 0.05 μM (Figure 4.5B). The effect of CCCP on the Ca^{2+} transient amplitude was also examined, but no difference was found (Figure 4.5C). This might be due to a weak inhibitory effect of CCCP on I_{Ca} (Park *et al.*, 1996). Nevertheless, the increase in τ and basal $[Ca^{2+}]_i$ with CCCP were similar to those of cyanide and oligomycin indicating that maximum inhibition of the mitochondria had only small effects on Ca^{2+} homeostasis.

These results suggest that inhibition of mitochondrial Ca^{2+} uptake has a small effect on the amplitude of the Ca^{2+} transient, basal $[Ca^{2+}]_i$, and the time course of Ca^{2+} removal indicating the mitochondria does play a role in Ca^{2+} homeostasis in rat β cells. However, the mitochondria's role may be small, as its inhibition has no dramatic effect on Ca^{2+} regulation.

III. Role of the plasma membrane calcium$^+$ATPase in Ca^{2+} removal

The PMCA functions by pumping $[Ca^{2+}]_i$ out of the cell with extracellular H^+ acting as a counter ion. Therefore, decreasing extracellular H^+ by increasing the pH of the

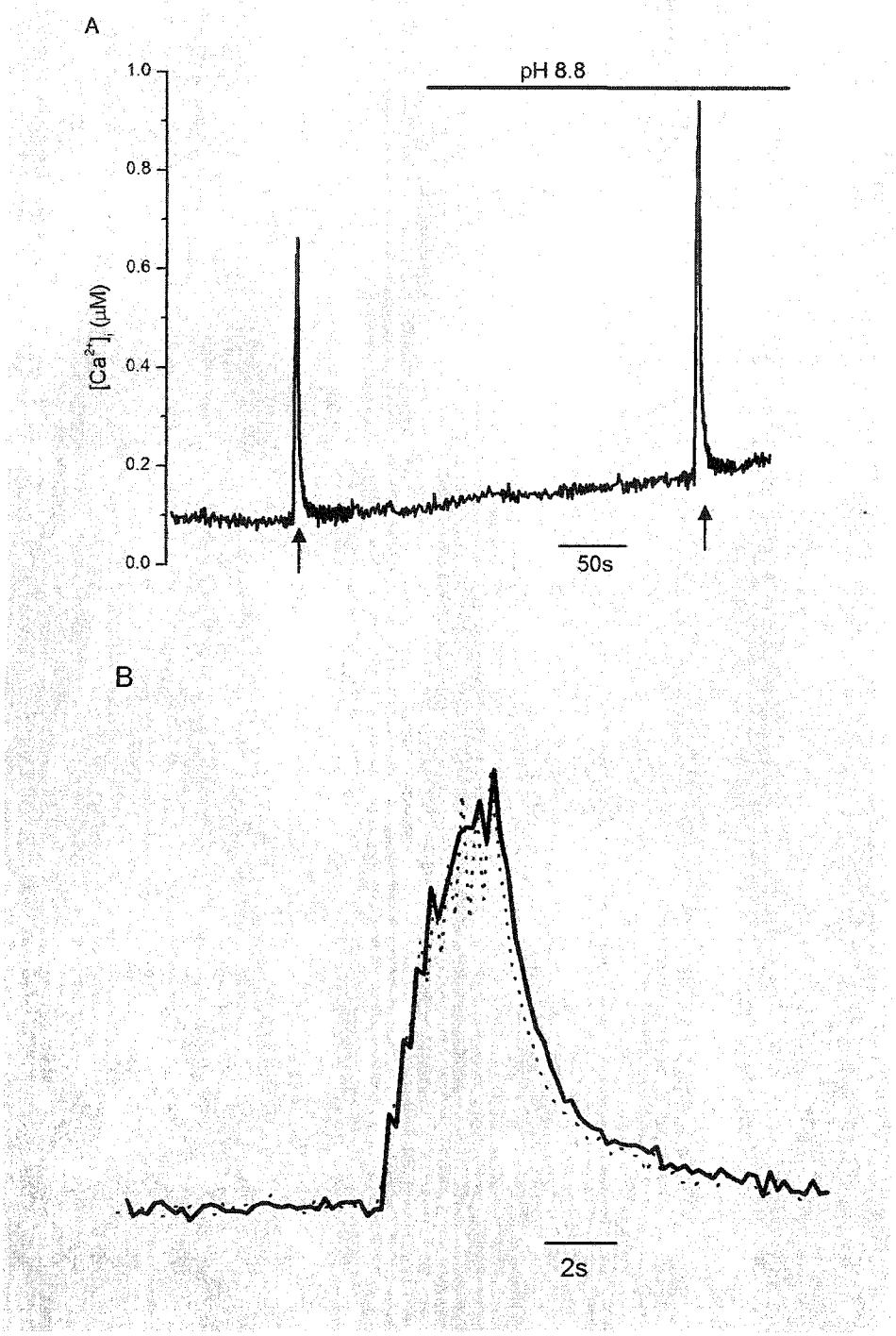

Figure 4.6: Inhibition of the PMCA with a pH 8.8 solution had a small effect on $[Ca^{2+}]_i$ and Ca^{2+} clearance.
A. Application of a pH 8.8 external solution caused a small increase in basal $[Ca^{2+}]_i$ and slightly slows the τ of Ca^{2+} removal. Each arrow represents a train of depolarizations being applied to the cell. B. An expanded scaled trace of the Ca^{2+} decay (control: dotted black line, pH 8.8: thick black line).

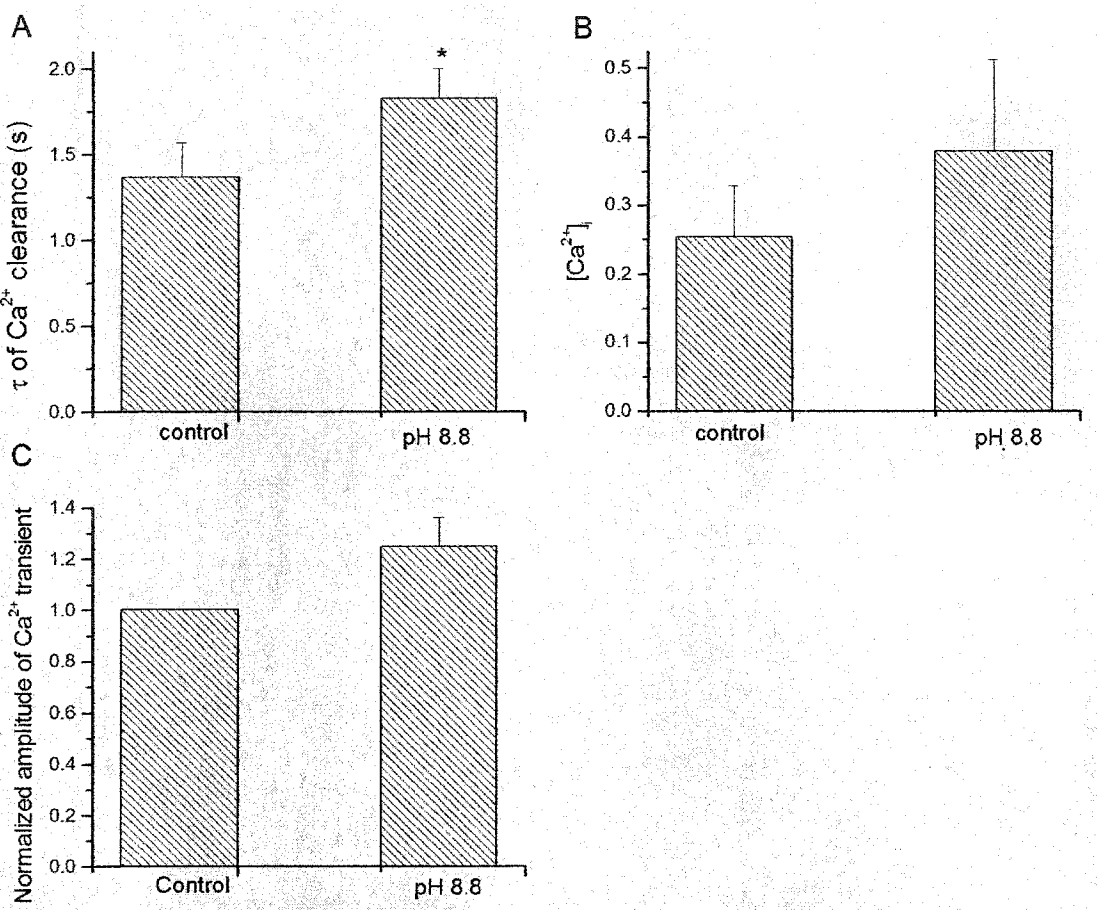

Figure 4.7 Inhibition of the PMCA with a pH 8.8 external solution influenced Ca^{2+} homeostasis.

The changes in (A) τ, (B) basal $[Ca^{2+}]_i$, and (C) normalized amplitude of the depolarization triggered Ca^{2+} transient after inhibition of PMCA with a pH 8.8 external solution. (n = 6) *p < 0.05

extracellular solution will reduce the activity of the PMCA (Xu *et al.*, 2000). In order to test the role of the PMCA in Ca^{2+} removal, a pH 8.8 extracellular solution was applied to cells (Figure 4.6A). In the cell shown in Figure 4.6, the application of the pH 8.8 solution increased the τ of Ca^{2+} removal from 1.1 s to 1.3 s. In the 6 cells tested, 5 cells showed small increases in τ following application of the pH 8.8 solution. In the remaining cell, a pH 8.8 extracellular solution had no effect on τ. On average, the τ of Ca^{2+} removal increased from 1.36 ± 0.20 s to 1.83 ± 0.17 s ($p< 0.05$ n = 6) (Figure 4.7A). This increase of approximately 35 % was more than the expected basal increase in τ. The change in resting $[Ca^{2+}]_i$ following pH 8.8 application was also examined. All 6 cells had increases in $[Ca^{2+}]_i$ ranging from 0.04 μM to 0.45 μM. However, the average increase (from 0.25 ± 0.08 μM to 0.38 ± 0.13 μM) was not statistically significant ($p < 0.11$) (Figure 4.7B). The amplitude of the Ca^{2+} transient was also examined. The normalized amplitude of the Ca^{2+} transient was not significantly different following pH 8.8 application ($p < 0.08$; n = 6) (Figure 4.7C). These results suggest that the PMCA has only a minor role in the removal of Ca^{2+} from the cytosol, the regulation of basal $[Ca^{2+}]_i$, and the amplitude of a Ca^{2+} transient.

IV. Role of the Na^+/Ca^{2+} exchanger in Ca^{2+} removal.

The NCX exchanges Na^+ for Ca^{2+} across the plasma membrane. The exact direction of this exchange depends on $[Na^+]$ and $[Ca^{2+}]$ (intracellular and extracellular), and the membrane potential of the cell. Because of the lack of specific pharmacological inhibitors the NCX traditionally has been inhibited by exchanging extracellular Na^+ for Li^+ or impermeant ions such as choline, sucrose or NMG.

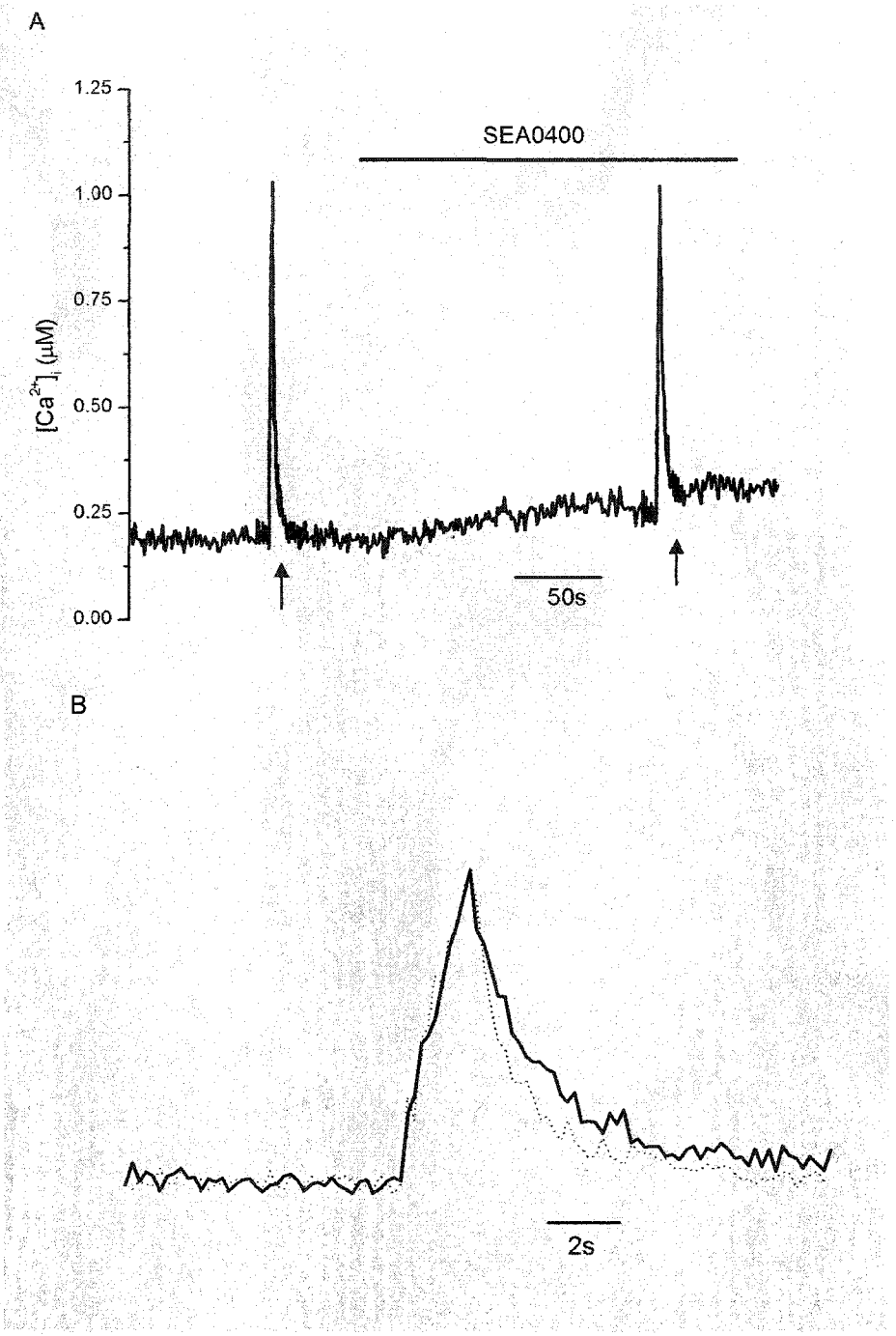

Figure 4.8: Inhibition of NCX with SEA0400 had a small effect on $[Ca^{2+}]_i$, and Ca^{2+} clearance.
A. Application of SEA0400 (1 μM) had no effect on $[Ca^{2+}]_i$ and slightly slowed the τ of Ca^{2+} removal. Each arrow represents a train of depolarizations being applied to the cell.
B. An expanded scaled trace of the Ca^{2+} decay (control: dotted line, SEA0400: thick black line).

However, in the last few years, more specific NCX inhibitors including KB-R7943 and SEA0400 have been developed (Tanaka *et al.*, 2002; Matsuda *et al.*, 2001). To test the effects of the NCX in Ca^{2+} removal in rat β cells both the traditional method of replacing Na^+ with NMG and the newer NCX inhibitor SEA0400 were tested.

In the cell in Figure 4.8 the application of SEA0400 (1 μM) increased the τ of Ca^{2+} removal from 1.20 s to 1.84 s. In the 14 cells tested with SEA0400 τ increased in 12 of them. In the remaining 2 cells, τ was unchanged. The average τ increased from 1.20 ± 0.10 s to 1.62 ± 0.14 s ($p < 0.001$; $n = 14$) reflecting an increase of approximately 35 % (Figure 4.9A). The effects of SEA0400 on basal $[Ca^{2+}]_i$ was also examined. In the cell shown in Figure 4.8 basal $[Ca^{2+}]_i$ increased by ~0.09 μM after SEA0400 application. In the 14 cells, 4 had basal $[Ca^{2+}]_i$ that either decreased, did not change, or increased by less than 0.02μM . The other 10 cells had increases ranging from 0.03 μM to 0.11 μM. On average, the resting $[Ca^{2+}]_i$ went from 0.24 ± 0.04 μM to 0.29 ± 0.04 μM (Figure 4.9B). Although the average change was only 0.05 ± 0.01μM it was statistically significant ($p < 0.001$; $n = 14$). The effect of SEA0400 on the amplitude of the Ca^{2+} transient was also examined and no change was found (Figure 4.9C).

To examine whether the increase in τ with SEA0400 was indeed due to the inhibition of the NCX, the effect of replacing extracellular Na^+ with NMG on $[Ca^{2+}]_i$ was also tested. In the four cells tested, the average τ increased from 2.0 ± 0.15 s to 2.41 ± 0.22 s ($p < 0.05$; $n = 4$) (Figure 4.9D). This 20 % changes was statistically significant, but, it was similar to the increase that occurred basally (Figure 4.2A) indicating the removal external Na^+ and had very little effect on Ca^+ removal. In addition, the Na^+ removal had no statistically significant effect on either basal $[Ca^{2+}]_i$ or

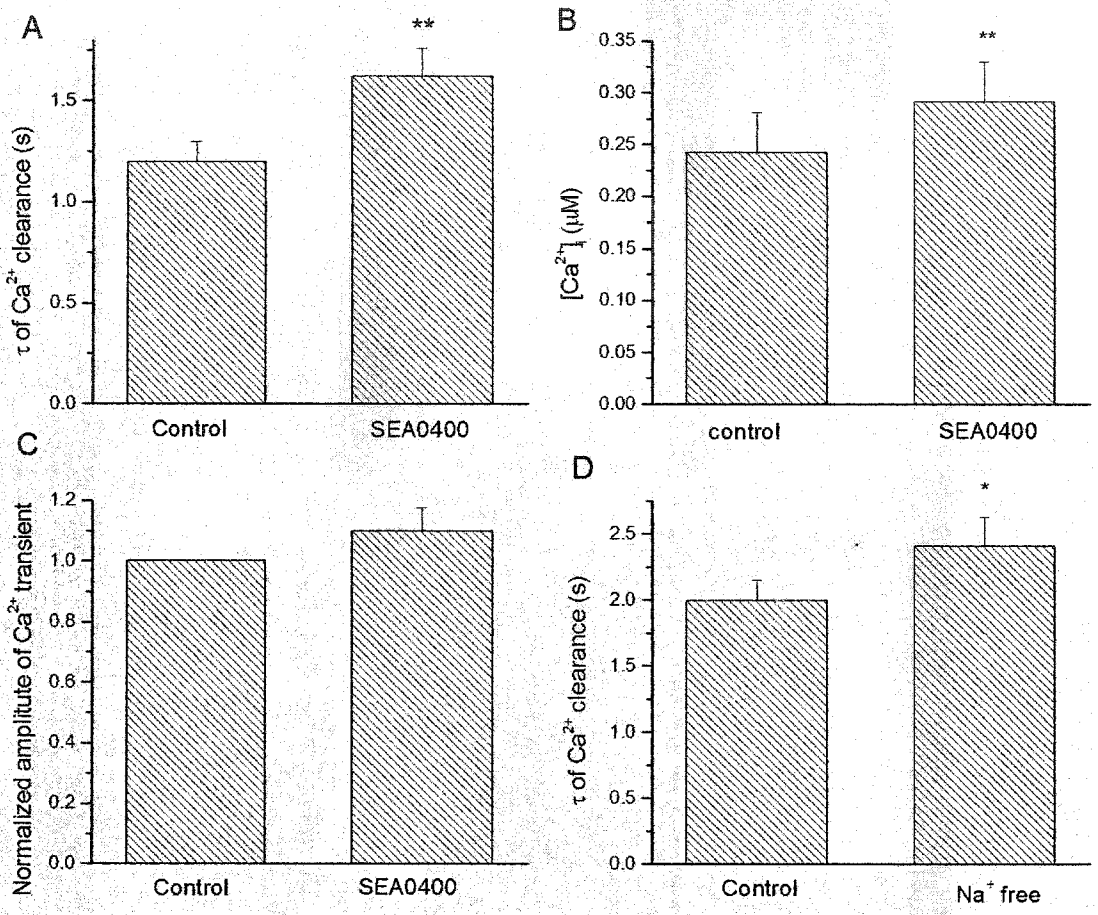

Figure 4.9: Inhibition of NCX by SEA0400 or by removal of extracellular Na^+ had a small effect on Ca^{2+} homeostasis.

The effects of inhibition of NCX with SEA0400 on (A) τ, (B) basal $[Ca^{2+}]_i$, and (C) normalized amplitude of the depolarization triggered Ca^{2+} transient (n = 14). D. Removal of external Na^+ had almost no effect on τ (n = 4). *$p < 0.05$ **$p < 0.001$

the amplitude of Ca^{2+} transient (data not shown). These results indicate that the NCX exchanger plays a minor role in the removal of Ca^{2+} from the cytosol in rat β cells.

V. Role of the sarcoplasmic endoplasmic reticulum Ca^{2+}-ATPases pumps in Ca^{2+} removal

SERCA pumps transport Ca^{2+} into intracellular Ca^{2+} stores in a multi-step process requiring ATP hydrolysis and changes in conformation of the SERCA pump (Pozzan *et al.*, 1994). BHQ reversibly inhibits SERCA pumps by blocking the pump in a conformation that cannot bind Ca^{2+} (Pozzan *et al.*, 1994).

When BHQ (10 μM) was bath applied to a β cell a few phenomena were apparent. In the cell in figure 4.10 in the presence of BHQ the basal $[Ca^{2+}]_i$ rose by more than 0.40 μM, Ca^{2+} removal clearly slowed down, and the amplitude of the Ca^{2+} transient appeared to increase. In this example, τ increased from 0.98 s to 10.40 s an increase of more than 10 fold. In 20 cells, all exhibited an increase in τ following BHQ exposure. The average τ increased from 1.59 ± 0.11 s to 6.72 ± 0.83 s ($p < 0.0001$; $n = 20$) an increase of over 400 % (Figure 4.11A). This increase was clearly more than either the control or any other of the inhibitors tested.

Of those 20 cells, the amplitude of the Ca^{2+} transient was examined in 19 of them. In the remaining cell the basal $[Ca^{2+}]_i$ was too unstable to accurately estimate the amplitude of the Ca^{2+} transient. Of the 19 cells, 17 showed an increase in the size of the Ca^{2+} transient following BHQ application. This increase ranged from 0.09 μM to 1.57 μM. In the remaining 2 cells the amplitude decreased by 0.10 μM and 0.16 μM. If the size of the Ca^{2+} transient was normalized to its control, the average amplitude of the Ca^{2+}

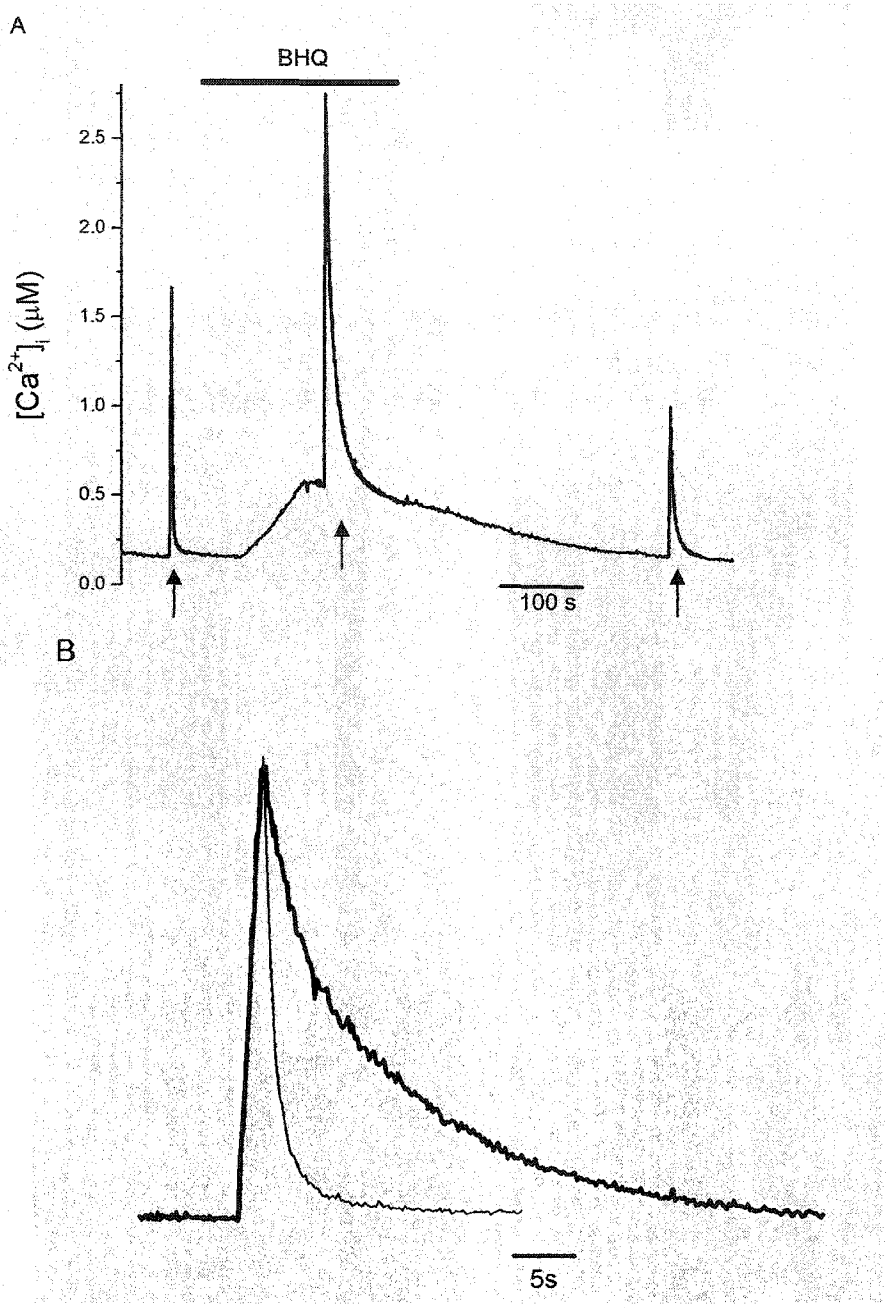

Figure 4.10: Inhibition of SERCA pumps with BHQ had a dramatic effect on Ca^{2+} homeostasis.
A. Application of BHQ (10 μM) slowed Ca^{2+} removal, increased $[Ca^{2+}]_i$, and increased the amplitude of the Ca^{2+} transient. Each arrow represents a train of depolarizations being applied to the cell. B. An expanded scaled trace of the Ca^{2+} decay (control: thin black line, BHQ: thick black line).

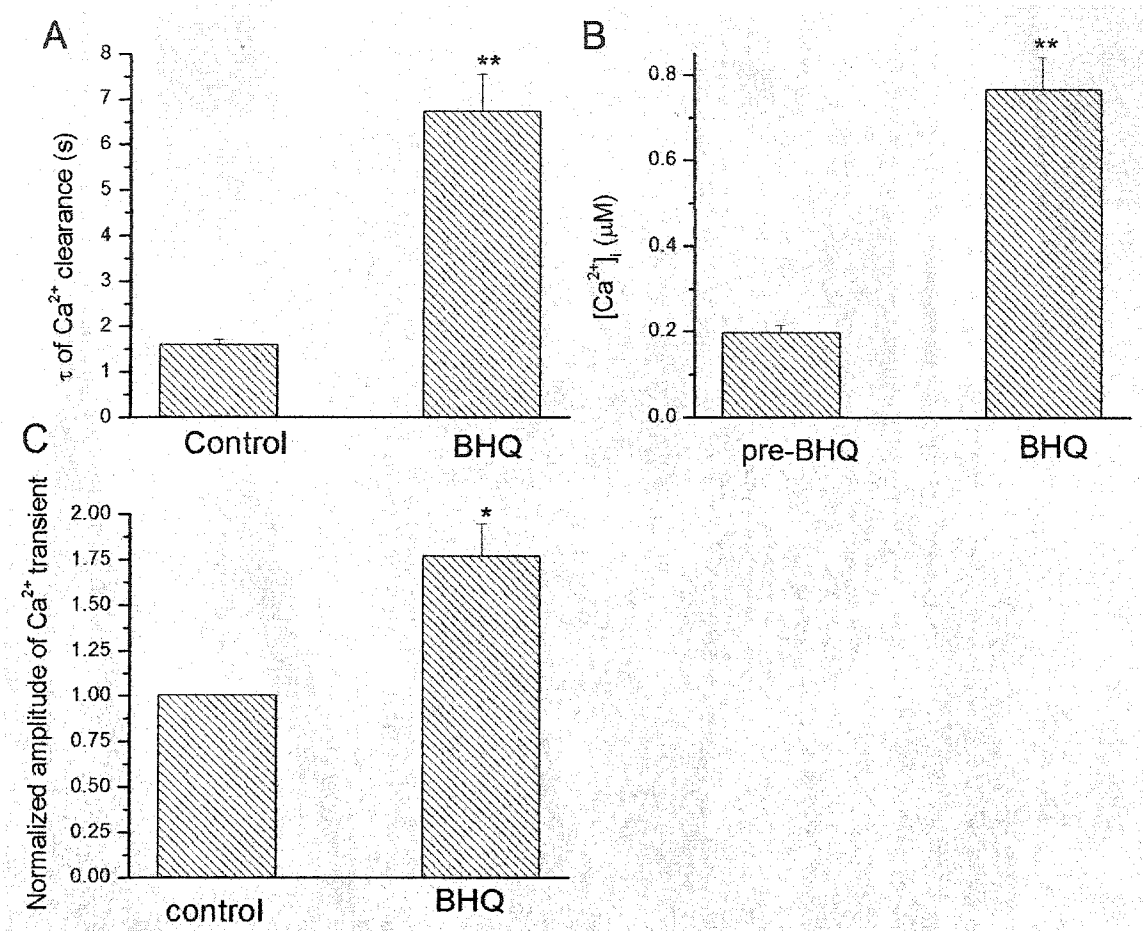

Figure 4.11: Inhibition of SERCA pumps with BHQ had a large influence on Ca^{2+} homeostasis.

The effects of inhibition of SERCA with BHQ on (A) τ, (n = 20) (B) basal $[Ca^{2+}]_i$, (n = 33) and (C) normalized amplitude of the depolarization triggered Ca^{2+} transient (n = 19). *p < 0.001 **p < 0.0001)

transient with BHQ was 1.77 times the control ($p < 0.001$; $n = 19$) (Figure 4.11C).

The effect of BHQ on resting $[Ca^{2+}]_i$ was examined in 33 cells. Of the 33 cells, one cell had a decrease in $[Ca^{2+}]_i$ of 0.22 μM, two had increases of <0.05 μM, while the remaining 30 cells had increases in $[Ca^{2+}]_i$ ranging from 0.14 μM to 1.44 μM. Following BHQ application, the average basal $[Ca^{2+}]_i$ increased from 0.20 ± 0.02 μM to 0.76 ± 0.08 μM (an average increase of 0.57 ± 0.07 μM) ($p < 0.0001$; $n = 33$) (Figure 4.11B).

These results clearly demonstrate the SERCA pumps play a major role in determining the time course of Ca^{2+} removal, basal $[Ca^{2+}]_i$, and the amplitude of the depolarization induced Ca^{2+} transient. The SERCA pumps appear to be the major regulator of Ca^{2+} homeostasis in rat β cells.

VI. Mechanism of the BHQ induced increase in basal $[Ca^{2+}]$

The dramatic effect of BHQ on basal $[Ca^{2+}]_i$ prompted the question as to where all of the Ca^{2+} was coming from? There are two potential sources for this Ca^{2+}: intracellular and extracellular. One potential source of Ca^{2+} is the leak from intracellular Ca^{2+} stores (Camello *et al.*, 2002). Normally the leak of Ca^{2+} from the stores is balanced by Ca^{2+} uptake into intracellular stores by SERCA pumps. When the cell is exposed to BHQ the SERCA pumps are inhibited, but Ca^{2+} continues to leak out of the stores and results in an increase in $[Ca^{2+}]_i$ (Figure 4.12A) (Camello *et al.*, 2002). A second potential mechanism is that the inhibition of SERCA by BHQ results in the intracellular Ca^{2+} stores being emptied. This emptying then activates a Capactitative Calcium Entry (CCE) channel which allows Ca^{2+} to enter the cell resulting in an increase in $[Ca^{2+}]_i$ (Figure 4.12B) (Berridge *et al.*, 2003; Parekh, 2003; Putney, Jr. & McKay, 1999). What separates

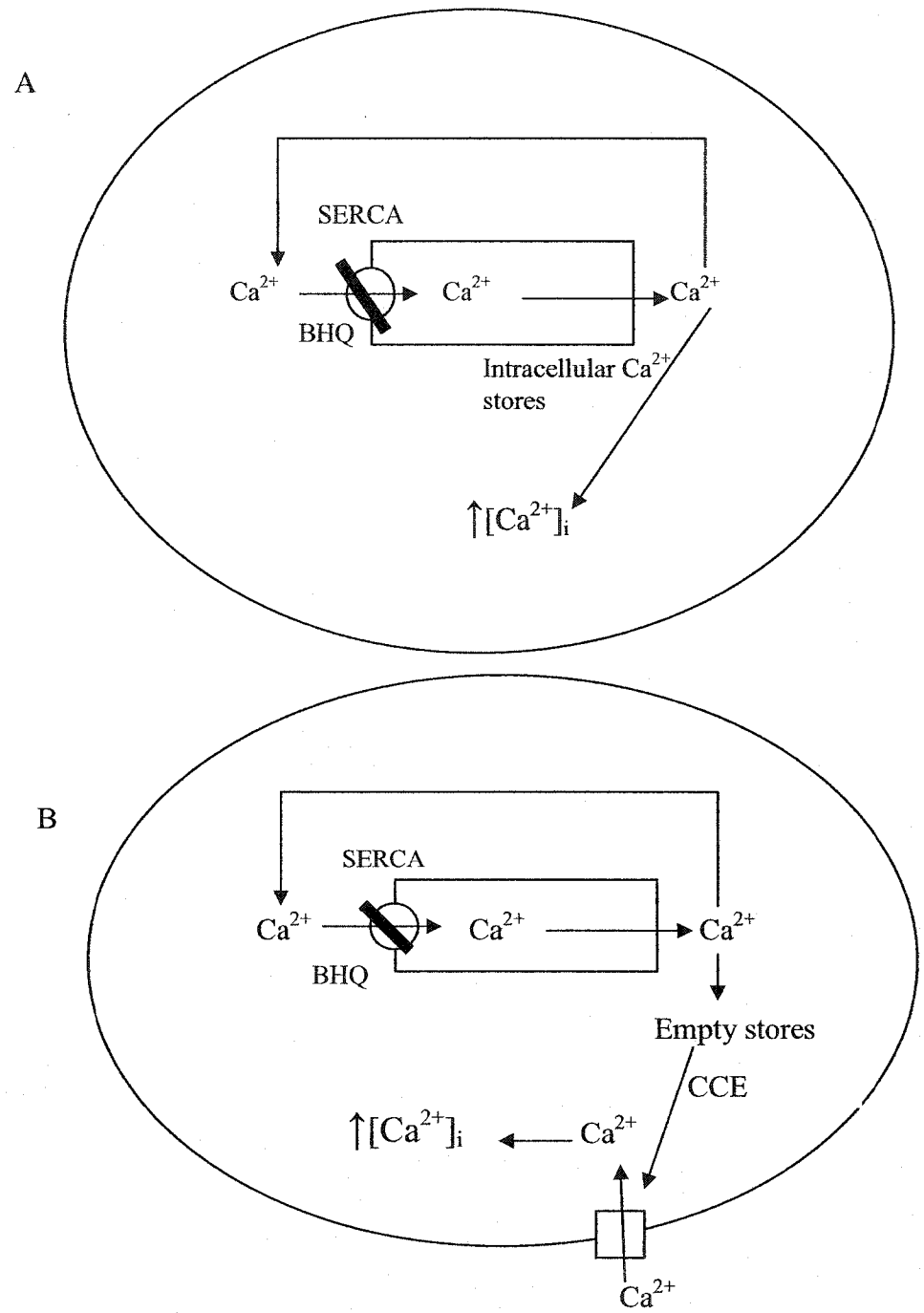

Figure 4.12: Two potential sources of BHQ mediated $[Ca^{2+}]_i$ increase.
The two potential sources for the BHQ mediated increase in $[Ca^{2+}]_i$ (A) intracellular Ca^{2+} stores and (B) extracellular Ca^{2+} entry. (See text for description)

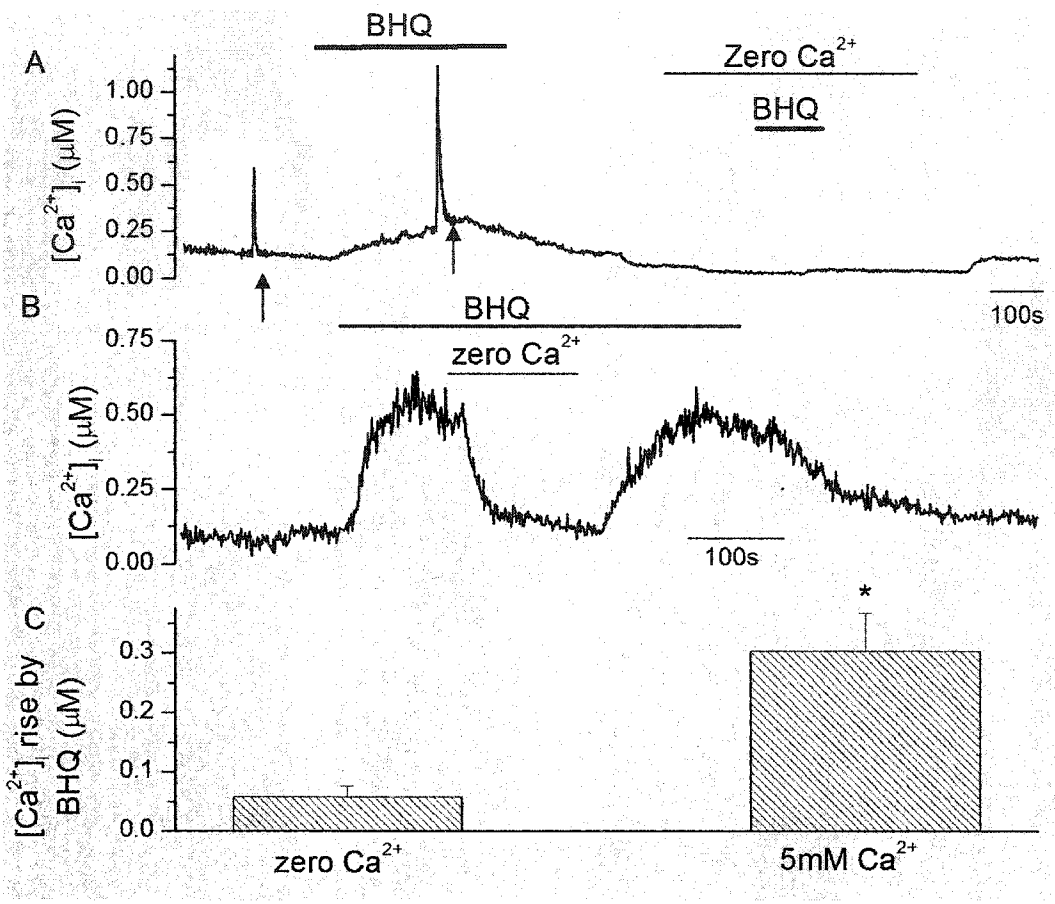

Figure 4.13: BHQ mediated increase in $[Ca^{2+}]_i$ required extracellular Ca^{2+}.
A. BHQ induced increase in $[Ca^{2+}]_i$ was suppressed in zero Ca^{2+} solution. Each arrow represents a train of depolarizations being applied to the cell. B. Removal of extracellular Ca^{2+} reversed BHQ mediated increase in $[Ca^{2+}]_i$. (representative of 5 cells) C. Summary of the BHQ mediated $[Ca^{2+}]_i$ rise in zero and 5 mM Ca^{2+} extracellular solution (n = 12). *$p < 0.006$

the two mechanisms is the requirement for extracellular Ca^{2+}. In order to differentiate the two possibilities, the effect of BHQ in zero Ca^{2+} external solution was examined. To test the effect of BHQ in zero Ca^{2+} external solution (no added Ca^{2+} plus 1 mM EGTA), BHQ was first applied in the presence of 5 mM Ca^{2+}. The cell was then exposed for 2-3 minutes to the zero Ca^{2+} extracellular before challenged with BHQ again (in the absence of extracellular Ca^{2+}) (Figure 4.13A). The removal of extracellular Ca^{2+} caused a small decrease in $[Ca^{2+}]_i$ which was typical of the majority of cells tested (Figure 4.13A). In this example BHQ induced a rise in $[Ca^{2+}]_i$ of 0.17 μM and 0.03 μM in 5mM extracellular Ca^{2+} and 0 mM extracellular Ca^{2+} respectively (Figure 4.13A). On average, BHQ caused a 0.06 ± 0.02 μM rise in $[Ca^{2+}]_i$ in the absence of extracellular Ca^{2+} compared to 0.30 ± 0.06 μM in 5 mM Ca^{2+} ($p < 0.006$; $n = 12$) (Figure 4.13C). To further confirm the importance of extracellular Ca^{2+} for the BHQ-mediated increase in $[Ca^{2+}]_i$, extracellular Ca^{2+} was removed while in the continuous presence of BHQ (Figure 4.13B). When external Ca^{2+} was removed the BHQ induced $[Ca^{2+}]_i$ rise reversed and $[Ca^{2+}]_i$ returned to almost pre-BHQ $[Ca^{2+}]_i$ level. When external Ca^{2+} was reintroduced, the $[Ca^{2+}]_i$ rose again. This cell was a representative of what was seen in 5 cells.

The zero extracellular Ca^{2+} experiments strongly suggest that the BHQ mediated increase in $[Ca^{2+}]_i$ required extracellular Ca^{2+} indicating BHQ may activate a Ca^{2+} influx pathway. One way of measuring Ca^{2+} influx is the manganese quench method. The entry of Mn^{2+} via Ca^{2+} influx pathways will decrease the fluorescence of indo-1 at both 405 nm and 500 nm. Since the fluorescence at 405 (F405) is not affected by changes in $[Ca^{2+}]_i$ decreases in F405 can be used to monitor Mn^{2+} entry. On the other hand, the ratio of the indo-1 fluorescence can still be used to monitor $[Ca^{2+}]_i$. The details of this method have

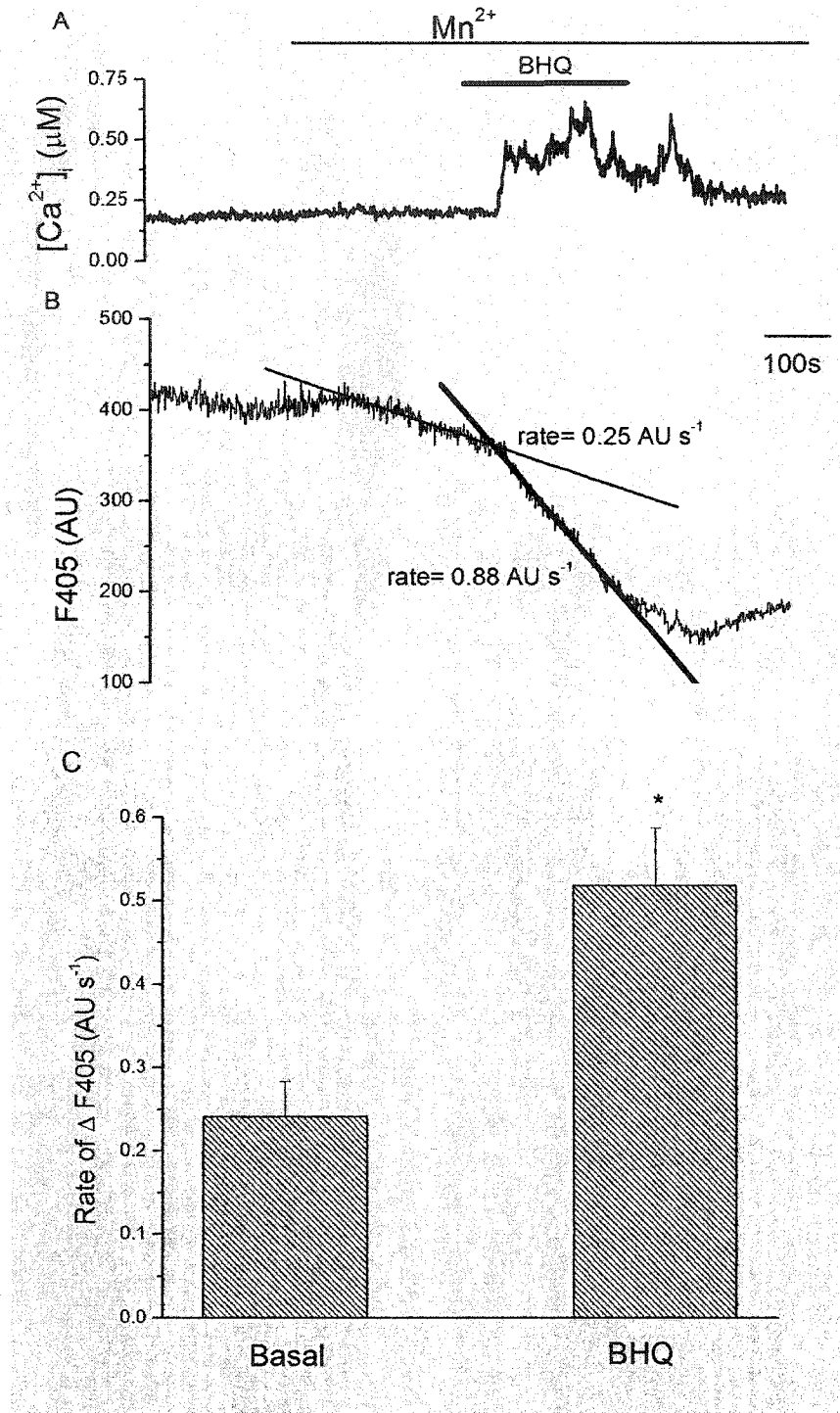

Figure 4.14: BHQ increased extracellular Ca^{2+} influx.
A. BHQ increased $[Ca^{2+}]_i$ in the presence of 0.2 mM Mn^{2+}. B. In the presence of Mn^{2+} there was a slow decrease in the fluorescence measured at 405nm (F405) at a rate of 0.25 AU s^{-1} reflecting a basal Ca^{2+}influx. When BHQ was applied, this rate increased to 0.88 AU s^{-1} reflecting an increase in extracellular Ca^{2+} influx. The lines show the slope of the decrease. C. Summary of the rates Δ F405 under basal conditions and in the presence of BHQ (n = 21). *p < 0.002

been described in Chapter 2. An example of one such experiment is shown in Figure 4.14A. In this un-patched, indo-1-AM loaded cell, application of 0.2 mM $MnCl_2$ caused a decrease in F405 at a rate of 0.25 AU s^{-1} indicating that there was a basal influx of Ca^{2+}. When BHQ was applied the rate of F405 decrease increased to 0.88 AU s^{-1}. Note that at the same time BHQ increased $[Ca^{2+}]_i$. On average, the rate of F405 decrease went from 0.24 ± 0.04 AU s^{-1} to 0.52 ± 0.07 AU s^{-1} ($p < 0.002$; $n = 21$) following BHQ application (Figure 4.14B). This indicates that BHQ induced an increase in extracellular Ca^{2+} influx into the cell.

The zero extracellular Ca^{2+} and Mn^{2+} quench data strongly suggest that BHQ causes the activation of a Ca^{2+} permeable channel resulting in a large increase in $[Ca^{2+}]_i$. One obvious candidate is the CCE channel as it has been well documented, in other cell types, that SERCA pump inhibitors can activate CCE (Parekh, 2003; Putney, Jr. & McKay, 1999). To test this, the CCE inhibitor 2-APB was used. 2-APB reportedly is a "selective" inhibitor of CCE with a K_i of 30 μM (Bootman *et al.*, 2002; Putney, Jr., 2001). Because of reports that it may inhibit VGCC at 100 μM (Dyachok & Gylfe, 2001), the concentration of 50 μM was initially tested. In the cell shown in Figure 4.15A, BHQ increased $[Ca^{2+}]_i$ by 0.450 μM and when 2-APB was applied $[Ca^{2+}]_i$ returns to pre-BHQ levels. In this particular cell, it was quite clear that 2-APB reversed the BHQ mediated Ca^{2+} increase. However, in other cells the effect of 2-APB was more puzzling. In the cell shown in Figure 4.15B, application of 2-APB in the presence of BHQ caused a transient $[Ca^{2+}]_i$ rise. When 2-APB was applied alone to this cell, it increased $[Ca^{2+}]_i$ transiently on its own (Figure 4.15B). When all cells in which 2-APB caused a $[Ca^{2+}]_i$ increase on its own were excluded, 2-APB reversed or partially reversed the BHQ

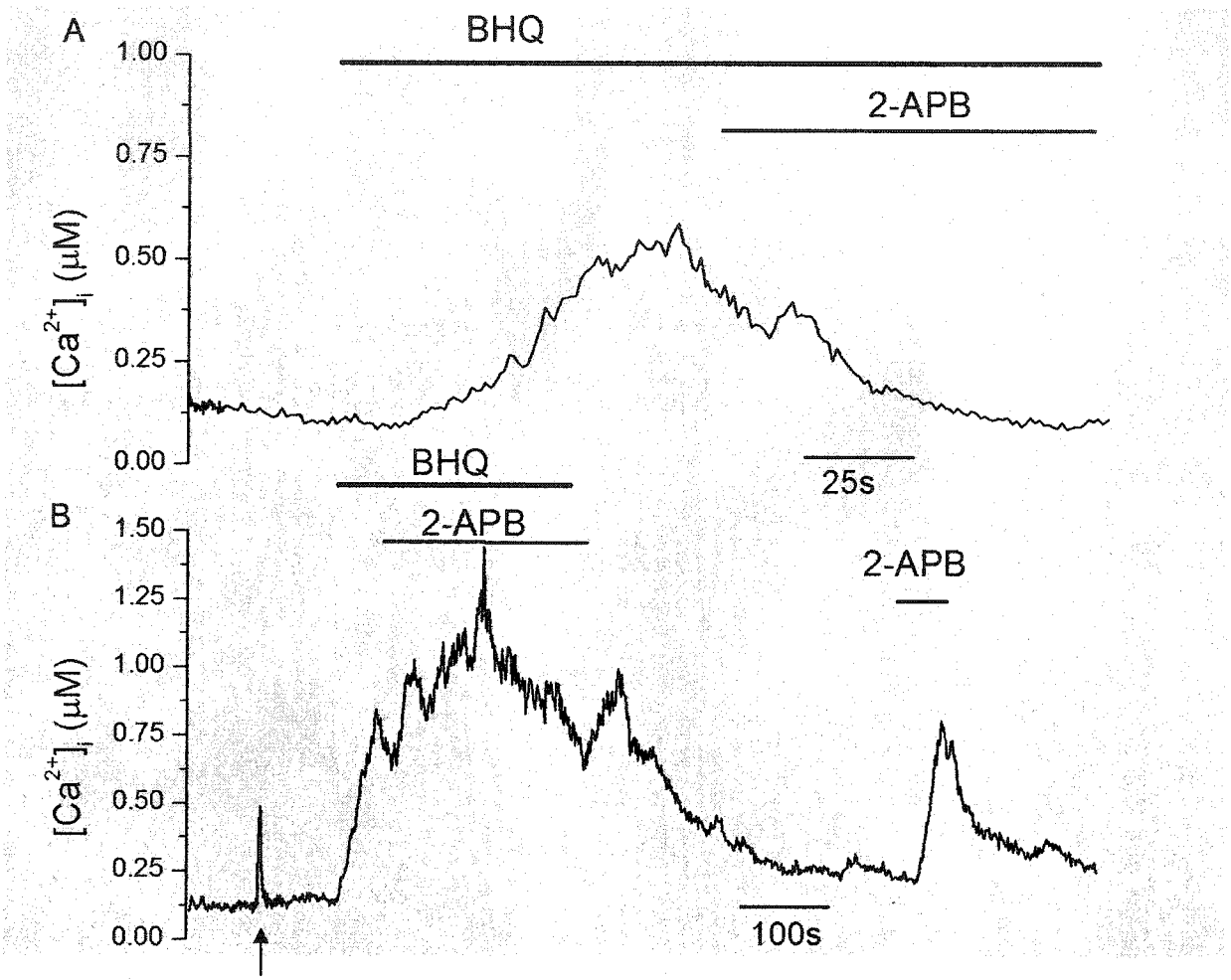

Figure 4.15: The CCE inhibitor, 2-APB produced mixed results on $[Ca^{2+}]_i$. 2-APB (50 μM) (A) inhibited BHQ mediated $[Ca^{2+}]_i$ increase in some cells while in other cells (B) it increased $[Ca^{2+}]_i$ on its own. The arrow represents a train of depolarizations being applied to the cell.

mediated $[Ca^{2+}]_i$ increase in 7 out of 9 cells (78 %). Potential causes of the incomplete inhibition by 2-APB and the increase in Ca^{2+} will be discussed in Chapter 5 (the discussion).

Because of the complicated effects of 2-APB on $[Ca^{2+}]_i$, the effects of 2-APB on Ca^{2+} influx was also examined. An example of this is shown in Figure 4.16A. In this cell, the application of BHQ increased the rate of Mn^{2+} quench of F405 from 0.04 AU s^{-1} to 0.89 AU s^{-1}. When 2-APB was applied the rate decreases to 0.38 AU s^{-1} (Figure 4.16A). In all 9 cells tested, 2-APB decreased the rate of Mn^{2+}quenching. On average, the rate of Mn^{2+}quenching went from 0.16 ± 0.05 AU s^{-1} to 0.53 ± 0.1 AU s^{-1} ($p < 0.02$; $n = 9$) with BHQ to 0.26 ± 0.4 AU s^{-1} ($p < 0.02$; $n = 9$) with BHQ and 2-APB (Figure 4.16B). These results indicate that the increase in Ca^{2+} influx mediated by BHQ can be at least partially inhibited by 2-APB.

All of the data from the zero Ca^{2+}, Mn^{2+} quench, and 2-APB experiments suggest that BHQ empties intracellular Ca^{2+} stores, which activates a CCE channel, allowing Ca^{2+} influx into the cell resulting in an increase in $[Ca^{2+}]_i$.

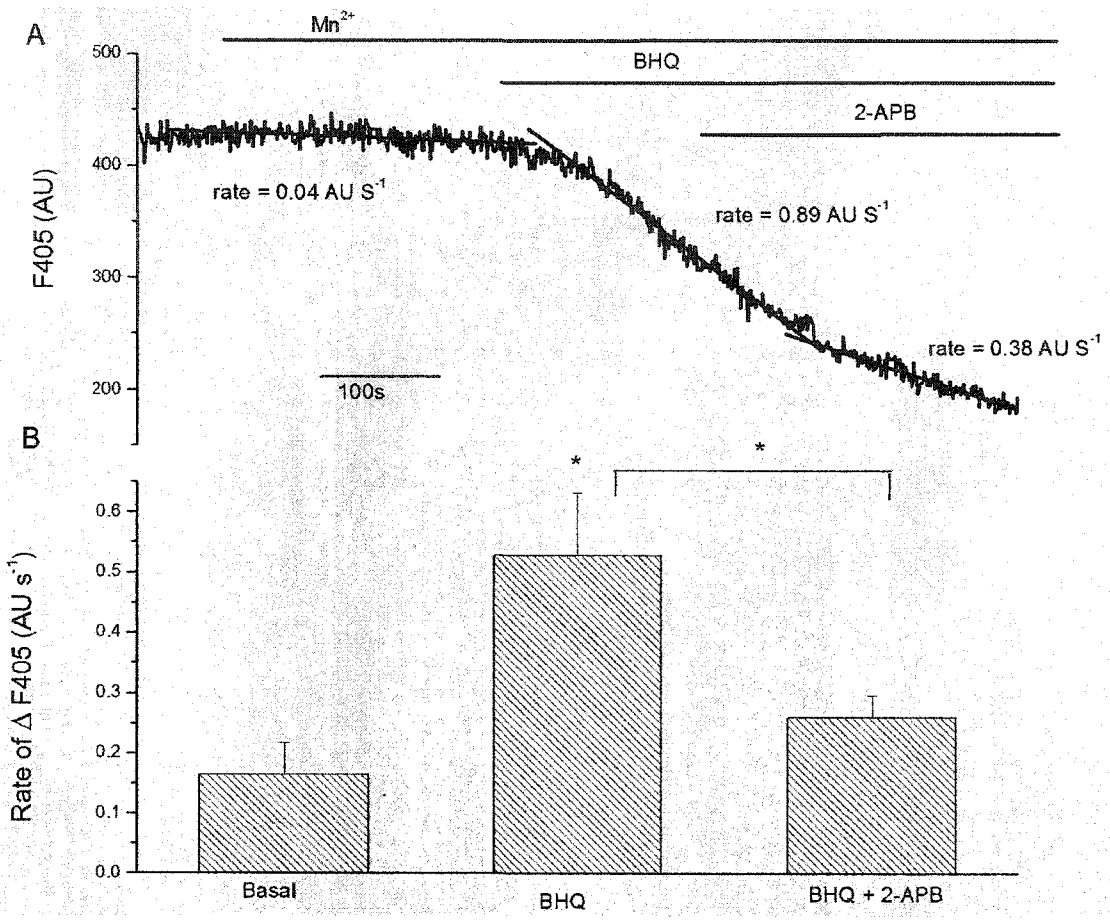

Figure 4.16: 2-APB decreased BHQ mediated increase in Ca^{2+} influx.
(A) An example of 2-APB decreasing the BHQ mediated increase in the F405 change. The lines are the slopes of the decrease. (B) Summary of the rate of F405 decrease under basal conditions and in the presence of BHQ and BHQ plus2-APB. (n = 9) *p < 0.02

Chapter 5: Discussion

A. Calcium and exocytosis

The results presented in Chapter three show a couple of different phenomena. First, the amount of Ca^{2+} entering the cell is an important factor in determining the rate and/or amount of secretion. Second, in rat β cells exocytosis is strongly dependent on temperature.

I. Exocytosis is highly temperature dependent

As shown is Chapter 3 there are several major differences in exocytosis between 22 °C and 30 °C. First, at 30 °C a single depolarization was sufficient to trigger exocytosis in most cells while at 22 °C the same depolarization (with comparable Ca^{2+} entry) was rarely enough to trigger exocytosis (Figure 3.2). Second, when compared at a higher $[Ca^{2+}]_i$ elevation (e.g. ~1.5 μM), the rate of exocytosis measured over the first five depolarization at 30 °C was ~10 fold faster than at 22 °C (Figure 3.3). Third, the rate of exocytosis increased dramatically with $[Ca^{2+}]_i$ increases at 30 °C, but only slightly at 22 °C (Figure 3.3). Finally, despite similarities in the amplitude of the depolarization triggered Ca^{2+} transient, the total amount of exocytosis at 30 °C was 1.8 to 4 fold higher than at 22 °C (Figure 3.4). The Q_8 for the ΔC_m after 1 and 5 depolarizations as well as the rate of ΔC_m was ~5 to 5.5. This value is very similar to the Q_{10} of exocytosis previously found in mouse β cells of >5 (Renstrom *et al.*, 1996).

There are several possible explanations for these differences, but before they can be explained, further information on exocytosis must be provided. In endocrine and

neuroendocrine cells, there are several pools of vesicles. These include: the immediately releasable pool (IRP), the readily releasable pool (RRP), and the reserve pool.The IRP consists of vesicles that are primed and are co-localized with VGCC while the RRP vesicles consists of both the co-localized vesicles (IRP) and primed vesicles located farther from the VGCC. In rat chromaffin cells, Horrigan and Bookman (Horrigan & Bookman, 1994) found that only 10 % of RRP vesicles are immediately releasable. However, in mouse β cells it has been reported that 50 % of the RRP are a part of the IRP (Barg *et al.*, 2002a). When the RRP is depleted, vesicles from the reserve pool replenish the RRP. Typically, this replenishment is mediated via mobilization or translocation of non-docked vesicles to the membrane followed by vesicle priming (Burgoyne & Morgan, 2003). However, in β cells a large pool of docked non-primed vesicles is suggested to be present and initial replenishment of vesicles is thought to involve chemical modification or priming of vesicles that are already docked instead of the physical movement of vesicles (Barg *et al.*, 2002a; Rorsman & Renstrom, 2003; Barg *et al.*, 2002b). The refilling of the RRP is known to be dependent on ATP, Ca^{2+}, and temperature (Eliasson *et al.*, 1997; Gromada *et al.*, 1999; Renstrom *et al.*, 1996).

There are several potential reasons for changes in exocytosis at different temperatures. First, it has been reported, in chromaffin cells, that the size of the RRP of vesicles is ~2.4 fold larger at 32 °C compared to 22 °C (Dinkelacker *et al.*, 2000). If more vesicles are available for release at 30 °C in rat β cells, this can explain the faster rate of exocytosis as well as the larger amount of exocytosis. However, studies in mouse β cells (Renstrom *et al.*, 1996), melanotrophs (Thomas *et al.*, 1993), and hippocampal neurons (Pyott & Rosenmund, 2002) did not find any change in the size of the RRP with

temperature. Another potential reason is the acceleration of vesicle replenishment at higher temperatures (Renstrom *et al.*, 1996; Dinkelacker *et al.*, 2000). This would enable the cell to continue to exocytose even after the depletion of the RRP. A study in mouse β cells suggested that the size of the RRP at 24 °C and 34 °C was similar, but the ability of vesicles to mobilize and replenish the RRP was reduced at room temperature (Renstrom *et al.*, 1996). Thus, it is possible that for rat β cells at 22 °C there is no vesicle replenishment after depletion of the RRP and thus a smaller exocytotic response. On the other hand, at 30 °C, the depletion of the RRP is followed by mobilization of additional vesicles and thus more exocytosis. An additional explanation is that the kinetics of exocytosis are temperature dependent. In rat melanotrophs, the RRP size was not altered by temperature, but it took 3 times as long for the vesicles to undergo exocytosis at room temperature compared to at 30 °C (Thomas *et al.*, 1993). A lower temperature has also been found to increase the time necessary for completion of exocytosis in rat mast cells (Pihel *et al.*, 1996). Finally, another potential reason for the temperature dependence is a difference in the coupling or co-localization of vesicles and VGCC at the different temperatures. In mouse β cells, it was suggested that 50 % of RRP vesicles were located in close proximity (within 10 nm (Barg *et al.*, 2002a)) to L-type VGCC such that these granules were exposed to local high [Ca^{2+}] following VGCC activation (Satin, 2000; Barg *et al.*, 2002a; Rorsman & Renstrom, 2003; Barg *et al.*, 2001b; Bokvist *et al.*, 1995). However, it is not clear whether the coupling of vesicles to VGCC can be affected by temperature as vesicle coupling to VGCC has been found at room temperature in chromaffin cells (Horrigan & Bookman, 1994). However, if at 30 °C there were better coupling between vesicles and VGCC, this would result in faster exocytosis. In the

following section, I shall examine whether some of these mechanisms may explain my observation in the temperature dependence of the exocytosis in rat β cells.

Figure 3.2 shows that a single 150 ms depolarization could stimulate some exocytosis at both temperatures. However, at a similar influx of Ca^{2+} more exocytosis was triggered at 30 °C. The possibility that the RRP was larger at 30 °C and the depolarization releases a similar percentage of the RRP at both temperatures was unlikely to underlie this difference as it would require the RRP at 22 °C to almost be non-existent. In addition, a change in RRP size could not adequately explain why increases in Ca^{2+} entry did not increase exocytosis at 22 °C. On the same line, it is unlikely that a change in rate of mobilization or vesicle replenishment would affect the ΔC_m after one depolarization, as the maximum ΔC_m after a single step is less than the RRP and vesicle replenishment would not be necessary. Another possibility is that there is better coupling between vesicles and L-type VGCC at higher temperatures. That is, the IRP makes up a larger percentage of the RRP. Studies examining vesicle co-localization with vesicles in mouse β cells were performed at 31-33 °C (Barg *et al.*, 2001b; Bokvist *et al.*, 1995), and the size of the IRP has not been examined at room temperature. However, co-localization has been found in chromaffin cells at room temperature (Horrigan & Bookman, 1994). If at 22 °C, the vesicles were located further from L-type VGCC, a localized region of high $[Ca^{2+}]_i$ near VGCC might not reach many vesicles and thus less exocytosis. While at higher temperatures, the localized region of high $[Ca^{2+}]_i$ will stimulate the exocytosis of more vesicles near L-type VGCC. This would result in more exocytosis, after one depolarization, at higher temperatures. Therefore, changes in vesicle co-localization (and IRP size) could result in the changes in exocytosis presented here, although there is no

precedent for temperature affecting vesicle co-localization with VGCC. One other possibility is that a change in the kinetics of exocytosis may result in more exocytosis following one depolarization. Since the process of exocytosis involves fusion of membranes and opening up of fusion pores, it is likely that many of these steps are sensitive to temperature. However, in contrast to what was observe in melanotrophs and chromaffin cells (Thomas *et al.*, 1993; Gil *et al.*, 2001; Pihel *et al.*, 1996) the kinetics of exocytosis in mouse β cells was suggested to have little dependence of temperature (Renstrom *et al.*, 1996). Nevertheless, my results suggest that a change either in the kinetics of exocytosis or in the co-localization of vesicles to VGCC may be responsible for difference in the exocytosis response triggered by a single depolarization at the two temperatures.

The second aspect examined here was the rate and amount of exocytosis over the first five steps. This was dependent on cumulative integral of I_{Ca} or the average $[Ca^{2+}]_i$ over the five steps. At 30 °C, increases in the cumulative I_{Ca} integral or average $[Ca^{2+}]_i$ were accompanied by an increase in the rate and amount of C_m increase (Figure 3.3). At 22 °C, increases in either average $[Ca^{2+}]_i$ or cumulative I_{Ca} integral only caused a very small increase in the rate or amount of exocytosis (Figures 3.3 and 3.4). In addition, the rate and total ΔC_m increase was larger at the higher temperature (Figures 3.3 and 3.4). Note that the total ΔC_m after 5 depolarizations at 30 °C was ~100 to 120 fF (Figure 3.4). This was less than the estimates of the RRP size at room temperature (199 ± 14 fF; n = 4 unpublished observations of A Tse). Thus, it is unlikely that the size of the RRP or the replenishment of the RRP contribute to the differences in the rate or amount of exocytosis after the first 5 depolarizations. Again, it is also possible that changes in

exocytosis kinetics occur with temperature change. Faster kinetics would result in faster and more exocytosis. One way of determining if the kinetics of exocytosis is changed with temperature would be to release (photolyse) a caged Ca^{2+} compound (e.g.: NP-EGTA) and thus bypassing VGCC to trigger exocytosis. Renström *et al.* (Renström *et al.*, 1996) did this experiment in mouse β cells and found no difference in the rate of exocytosis between 24 and 34 °C. In rat melanotrophs a similar experiment found that the rate of C_m increase was strongly dependent on temperature (Thomas *et al.*, 1993). Because of this uncertainty, more experiments are necessary to determine if the kinetics of exocytosis in rat β cells are temperature sensitive.

Finally, a difference in vesicle coupling to VGCC at different temperatures needs to be considered. It has been demonstrated that changes in the coupling can cause changes in exocytosis. Barg *et al.* (Barg *et al.*, 2002a; Barg *et al.*, 2001b) disrupted the coupling of vesicles to L-type VGCC in mouse β cells by over supplying a peptide containing the portion of the L-type VGCC responsible for vesicle coupling. This resulted in the first few depolarizations of a train not being able to trigger any C_m increase, while the control cell exocytose in response to one depolarization (Barg *et al.*, 2002a; Barg *et al.*, 2001b). The subsequent depolarizations could trigger exocytosis in the treated cell but, the total C_m increase was less than controls (Barg *et al.*, 2002a; Barg *et al.*, 2001b). Disrupting the L-type VGCC and vesicle coupling was also done by selectively knocking-out L-type VGCC in mouse β cells (Schulla *et al.*, 2003). This resulted in the failure of the first depolarization in a train to stimulate exocytosis, but later depolarizations were not affected (Schulla *et al.*, 2003). The selective loss of early exocytosis was due to the loss of the IRP and subsequent depolarizations triggered

exocytosis was due to the accumulation of Ca^{2+} and thus release from the RRP. In view of this, it is unlikely that the small rate and amount of exocytosis during the first 5 depolarizations was due to a small IRP at room temperature as the Ca^{2+} accumulation in the first 5 depolarizations should have triggered release from the RRP. Thus an increase in the kinetics of exocytosis at 30 °C may be a better explanation for the more robust exocytosis observed at 30 °C.

On the other hand, the total C_m increase triggered by the train of depolarizations (15 depolarizations) might involve depletion of RRP and RRP replenishment. The total C_m increase (~190 fF) at room temperature approached the size of the RRP and at 30 °C the C_m increase exceeded the RRP at room temperature (Figure 3.5). Assuming that, the size of the RRP did not increase at 30 °C additional vesicles must be mobilized and released. Since the rate of mobilization is known to be temperature dependent (Renstrom *et al.*, 1996), it is likely that an increase in the rate of mobilization at 30 °C contributes to the larger C_m increase triggered by the train of depolarization.

In summary, there is a clear enhancement of exocytosis with temperature in rat β cells. A temperature dependent increase in the kinetics of exocytosis, the rate of the RRP replenishment, and possibly vesicle co-localization with VGGC may contribute to this enhancement.

II. Comparison of the Ca^{2+} dependence of exocytosis between mouse and rat β cells

As mentioned previously the relationship between $[Ca^{2+}]_i$, I_{Ca}, and exocytosis has been studied extensively in mouse β cells. However, very little is known in rat β cells.

Although the data presented here is not a complete investigation, it can provide some insight into this relationship and possible differences between rat and mouse.

In mouse β cells, the number of vesicles in the RRP has been estimated to be between 50 and 100 vesicles (Barg *et al.*, 2002a; Rorsman *et al.*, 2000; Barg *et al.*, 2001b; Eliasson *et al.*, 1997), however estimates of 20 to 35 vesicles have also been published (Renstrom *et al.*, 1997; Olsen *et al.*, 2003; Eliasson *et al.*, 2003). Using the data from Figure 3.5 it is possible to estimate of the size of the RRP in rat β cells. This estimate is based on one assumption. That, mobilization of vesicles only contributes marginally to the total ΔC_m at 22 °C. Thus, the total ΔC_m at 22 °C mostly represents exocytosis of RRP vesicles. The maximum total change in ΔC_m at 22 °C was ~192 fF, however from Figure 3.4 it appeared that this value might not have reached a plateau. That is if a larger increase in $[Ca^{2+}]_i$ occurred it might be possible to get a larger total ΔC_m. However, this value was similar to the 199 ± 14 fF estimated using photolysis of caged Ca^{2+} at room temperature (A Tse unpublished observations). Therefore, it is likely that a train of depolarizations at 22°C can almost deplete the RRP. Using the conversion of 1.7 fF/vesicle (Ammäla *et al.*, 1993b) the 192 fF is equivalent to ~112 vesicles. The size of the RRP at room temperature in rat β cells is slightly larger than that reported in mouse β cells (50-100 vesicles) at 30 °C. Such a difference in RRP size may underlie the differences in the first phase of insulin secretion between rat and mouse that have been reported (Ma *et al.*, 1995).

The rates of the ΔC_m over the first five depolarizations (Figure 3.3) at 30 °C can be compared to rates calculated at similar $[Ca^{2+}]_i$ in mouse β cells. The rates of exocytosis in mouse β cells were calculated by dialysis of a known $[Ca^{2+}]$ into the cells

and measuring the rate of ΔC_m. This method has the advantage that $[Ca^{2+}]_i$ is elevated uniformly over the entire cell. However, depletion of the RRP might occur while Ca^{2+} is diffusing into the cells from the recording pipette. Thus, the Ca^{2+}-dependent rate of exocytosis might be underestimated in these studies. On the other hand, $[Ca^{2+}]_i$ in my experiment will be underestimated as the depolarization might trigger local $[Ca^{2+}]_i$ gradient near the vesicles. Nevertheless, such comparisons should provide some insights to whether there is any dramatic differences in the Ca^{2+} dependence of exocytosis between the two species.

In mouse β cells it has been published that 1.5 μM $[Ca^{2+}]_i$ can stimulate exocytosis at a rate of 30 fF s^{-1} (Renstrom *et al.*, 1997). This value is slightly slower than the 50 fF s^{-1} at 1.4 μM seen in rat (Figure 3.4). However, in mouse β cells ~25 fF s^{-1} of exocytosis could be detected at 0.34 μM $[Ca^{2+}]_i$ (Renstrom *et al.*, 1997). In comparison, at 0.49 μM $[Ca^{2+}]_i$ the rate of exocytosis in rat β cells was only 7 fF s^{-1} (Figure 3.4). In the mid range $[Ca^{2+}]_i$ (~0.8 μM) the rate of exocytosis in mouse β cells was 21 fF s^{-1} (Hoy *et al.*, 2003), similar to the 15 fF s^{-1} observed in rat β cells (Figure 3.4). Hoy *et al.* (Hoy *et al.*, 2003), compared exocytosis in both rat and mouse β cells and found that at 2 μM $[Ca^{2+}]_i$, exocytosis occurred at a slightly slower rate in rat β cells than mouse β cells. However, in this study, the rate of exocytosis for both rat and mouse was considerably slower (11 and 14 fF s^{-1} respectively) than those reported elsewhere at lower $[Ca^{2+}]_i$ (Figure 3.4 and Renstrom *et al.*, 1997). The differences in the rate of exocytosis observed in rat β cells compared to mouse (Renstrom *et al.*, 1997; Hoy *et al.*, 2003) may be due to procedural difference (dialysis of a Ca^{2+} buffered internal vs. train of depolarization) as dialysis does not cause localized high $[Ca^{2+}]_i$ and the rate of ΔC_m is measured over a

longer period of time. However, some of the differences, especially at low $[Ca^{2+}]_i$, may be related to species differences. In mouse β cells the ability to exocytosis in response to $[Ca^{2+}]_i$ lower than 0.2 μM has been attributed to the presence of a Ca^{2+} sensor (synaptotagmin) with high affinity for Ca^{2+} (Rorsman & Renstrom, 2003). The exact isoform of synaptotagmin that serves as the Ca^{2+} sensor in β cells is still a matter of debate (Rorsman & Renstrom, 2003) and it is not known if the same Ca^{2+} sensor are present in both species. In addition, in the dialysis experiments $[Ca^{2+}]_i$ is not measured. Thus it is possible that the $[Ca^{2+}]_i$ was underestimated. Nevertheless, my results suggest that there is no drastic difference in Ca^{2+} dependence of exocytosis between mouse and rat β cells at physiological range of $[Ca^{2+}]_i$ (< 2 μM).

B. Regulation of calcium homeostasis in rat β cells

The results of Chapter 4 show that the inhibition of the SERCA pump by BHQ dramatically increased basal $[Ca^{2+}]_i$, the amplitude of depolarization induced Ca^{2+} transient, and slowed down Ca^{2+} removal. In contrast, inhibition of the PMCA, NCX, or mitochondria had only small affects on Ca^{2+} homeostasis (summarized in Table 1 and Figure 5.1).

The average τ of Ca^{2+} removal of 1.51 ± 0.06 s in rat β cells observed here at 22 °C is in agreement with the 1.7 s (intact cells; Chen *et al.*, 2003), 1.8 to 2.0 s (perforated patch; Gall *et al.*, 1999), and 1.0 s (whole-cell patched cells; Chen *et al.*, 2003) that have been reported in mouse β cells at 35 °C . In contrast, the time constant of Ca^{2+} removal has been reported to be 4.6 s in corticotrophs (Lee & Tse, 2004), 3.85 s in

Table 1: Summary of the effects of inhibition of a specific Ca^{2+} removal mechanisms on Ca^{2+} homeostasis.

Ca^{2+} removal mechanism	τ	$[Ca^{2+}]_i$	Amplitude of $[Ca^{2+}]_i$ transient
Mitochondria	increase (60 %)	increase	increase
PMCA	increase (35 %)	no change	no change
NCX (with SEA0400)	increase (35 %)	increase	no change
SERCA	increase (420 %)	increase	increase

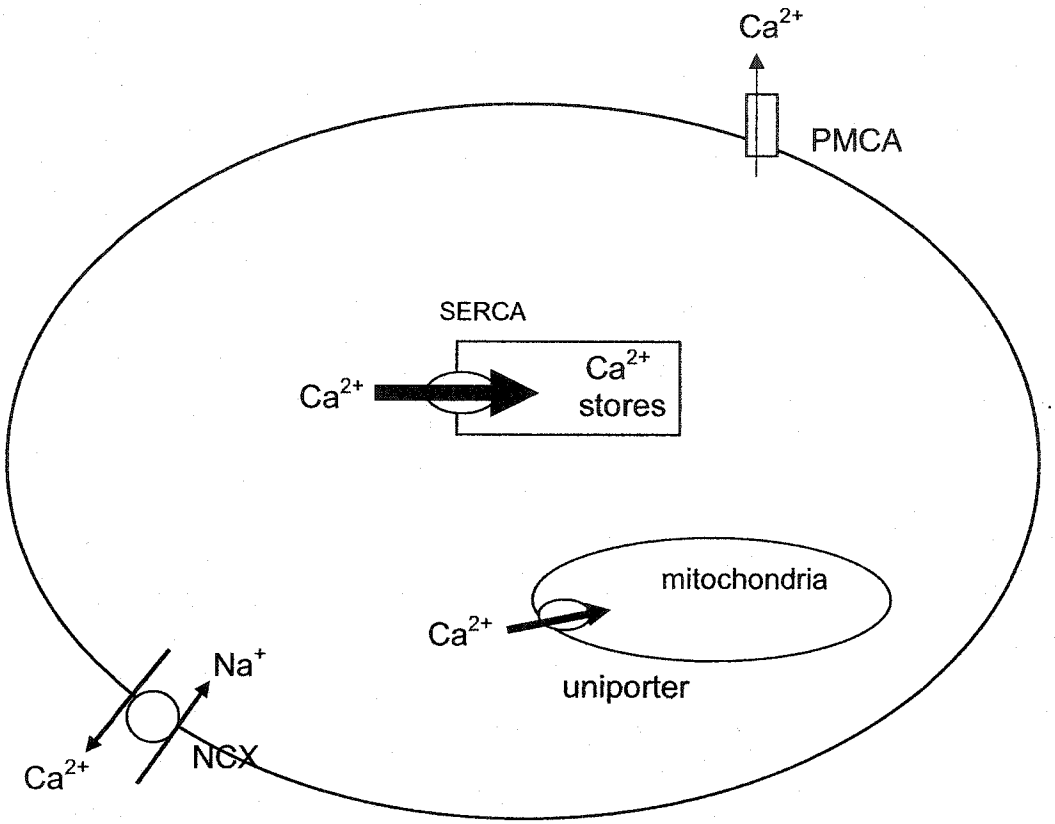

Figure 5.1: Summary of the Ca^{2+} removal mechanisms in rat β cells.
The thickness of the arrow reflect relative importance of different Ca^{2+} removal mechanisms in removing Ca^{2+} from the β cell following depolarization induced Ca^{2+} entry.

gonadotrophs (Tse *et al.*, 1994), 4.4 s in melanotrophs (Thomas *et al.*, 1990), and 3 to 4 s in chromaffin cells (Dinkelacker *et al.*, 2000; Herrington *et al.*, 1996). Better or faster Ca^{2+} removal mechanisms in β cells in comparison to other endocrine and neuroendocrine cells may be related to the tight coupling between $[Ca^{2+}]_i$ and insulin secretion in β cells.

I. Role of the SERCA pump in Ca^{2+} homeostasis.

The inhibition of SERCA pumps by BHQ affects several parameters of Ca^{2+} homeostasis. BHQ slowed the time course of Ca^{2+} clearance by over 400 % (Figure 4.11A), increased the amplitude of the Ca^{2+} transit by 180 % (Figure 4.11C), and increased the basal $[Ca^{2+}]_i$ by an average of 0.57 μM (Figure 4.11B). These findings indicate SERCA pumps play multiple important roles in Ca^{2+} regulation of β cells. The dramatic effect of BHQ on Ca^{2+} removal and the small effect of inhibitors of other Ca^{2+} removal mechanisms indicate that SERCAs are the primary mechanism of Ca^{2+}removal in rat β cells. This is again, in agreement with what was observed in mouse β cells where thapsigargin (a SERCA inhibitor) increased the time constant of Ca^{2+} removal 4.4 fold in patched cells (Chen *et al.*, 2003). The increase in the amplitude of the Ca^{2+} transient in the presence of BHQ indicates that SERCA pumps normally pump Ca^{2+} into intracellular stores during the depolarization and help to limit the increase in $[Ca^{2+}]_i$. SERCA inhibition increasing the Ca^{2+} transient amplitude has also been reported in mouse β cells in response to depolarizations mediated by KCl (Chen *et al.*, 2003; Gilon *et al.*, 1999) and glucose (Gilon *et al.*, 1999; Arredouani *et al.*, 2002b).

Under basal conditions, the basal efflux (or leak) from intracellular Ca^{2+} stores is balanced by the reuptake of Ca^{2+} into stores by SERCA pumps (Camello *et al.*, 2002). When BHQ inhibits SERCA pumps the increase in basal $[Ca^{2+}]_i$ may be due to unbalanced Ca^{2+} leak from intracellular stores (Camello *et al.*, 2002; Dyachok *et al.*, 2004; Gilon *et al.*, 1999). However, several pieces of evidence suggest the effect of BHQ on basal $[Ca^{2+}]_i$ is mostly due to extracellular Ca^{2+} entry. First, in the presence of zero extracellular Ca^{2+} (and 1 mM EGTA), BHQ increases $[Ca^{2+}]_i$ by only 0.06 μM. This is ~20 % of the BHQ mediated increase in basal $[Ca^{2+}]_i$ in the presence of 5 mM Ca^{2+} (0.30 μM) (Figure 4.13C). Second, the removal of extracellular Ca^{2+} in the continuous presence of BHQ restored $[Ca^{2+}]_i$ to basal levels (Figure 4.13B). These results support the notion that extracellular Ca^{2+} was required for the BHQ mediated $[Ca^{2+}]_i$ increase. One possible explanation for this is that the Ca^{2+} stores are small such that it is rapidly depleted in the presence of BHQ. The emptying of the stores in turn triggers extracellular Ca^{2+} entry via activation of capacitative Ca^{2+} entry (CCE) channels. This possibility was tested here using the CCE inhibitor 2-APB. 2-APB was reported to be a "selective" inhibitor of CCE with a K_i of 30 μM (Bootman *et al.*, 2002; Putney, Jr., 2001). When all the cells that 2-APB was found to increase $[Ca^{2+}]_i$ on its own were excluded 2-APB inhibited or partially inhibited the BHQ mediated $[Ca^{2+}]_i$ rise in 7 of 9 cells (Figure 4.15). There are a couple of reasons why 2-APB alone may increase basal $[Ca^{2+}]_i$. It has been reported that in lymphocytes (Ma *et al.*, 2002; Prakriya & Lewis, 2001), T cells (Prakriya & Lewis, 2001), and basophilic leukemia cells (Prakriya & Lewis, 2001) 2-APB at concentrations of 1-10 μM can activate CCE. 2-APB has also been reported to activate a Ca^{2+} permeable channel in basophilic leukemia cells at 100

μM (Braun *et al.*, 2003a). It is possible that at 50 μM 2-APB will activate some Ca^{2+} permeable channels in β cells. As well, the ability of 2-APB to increase $[Ca^{2+}]_i$ on its own in some cells may be caused by a weak inhibitory effect on SERCA pumps (Bootman *et al.*, 2002; Missiaen *et al.*, 2001). Nevertheless, in 78 % of the cells (7/9) where 2-APB did not cause an increase in $[Ca^{2+}]_i$, 2-APB inhibited or partially inhibited the BHQ mediated $[Ca^{2+}]_i$ increase. This suggests that 2-APB partially inhibits the channel BHQ activates, providing support that the BHQ-mediated increase in basal $[Ca^{2+}]_i$ is due to activation of CCE. The activation of CCE by BHQ was further supported by the Mn^{2+} quench experiments. As shown in Figures 4.14 and 4.16, BHQ increased extracellular Ca^{2+} entry and this Ca^{2+} entry was partially inhibited by 2-APB.

CCE has also been reported in mouse β cells when intracellular Ca^{2+} stores were emptied with carbachol (Dyachok & Gylfe, 2001; Liu & Gylfe, 1997), thapsigargin (Liu & Gylfe, 1997; Miura *et al.*, 1997), or cyclopiazonic acid (CPA) (Dyachok & Gylfe, 2001). The carbachol and CPA induced extracellular Ca^{2+} entry was also inhibited by 2-APB (Dyachok & Gylfe, 2001). However, in mouse β cells inhibition of SERCA pumps caused only small basal $[Ca^{2+}]_i$ increases. Thapsigargin was reported to increase basal $[Ca^{2+}]_i$ by 79 nM (Miura *et al.*, 1997) and 12 % (tens of nanomolar) (Chen *et al.*, 2003) in mouse, while others groups report "small" increases in $[Ca^{2+}]_i$ by thapsigargin (Liu & Gylfe, 1997) and CPA (Dyachok & Gylfe, 2001) in ob/ob mice. These values are all considerably smaller then the average increase of 570 nM reported here for rat β cells. Some of this difference may be due to methodological differences between the studies. The work presented here was performed on patch-clamped cells that were voltage clamped -70 mV. In contrast, the studies on mouse β cells were performed on intact

(non-patched) cells where the cells were held at negative resting potentials with the K_{ATP} channel opener diazoxide. So it is possible that cells in the mouse experiments were not sitting at as negative membrane potentials resulting in a smaller driving force for Ca^{2+} entry. In addition, the mouse experiments were performed in 1.28-2.5 mM Ca^{2+} compared to 5 mM here. This would result in less Ca^{2+} entry. As well, the mouse experiments were performed when the intracellular Ca^{2+}stores had been filled by exposure to 15 to 20 mM glucose. The difference in filled state of the Ca^{2+} stores may make emptying the intracellular stores, and therefore activating capacitative Ca^{2+} entry, more difficult. The one study that tested thapsigargin in un-patched rat β cells also only report a small rise in $[Ca^{2+}]_i$ (Aizawa *et al.*, 1995).

Besides activating CCE, BHQ also empties intracellular Ca^{2+} stores. This effect is visible in the absence of extracellular Ca^{2+}. In INS-1 cells (Maechler *et al.*, 1999) and ob/ob mice cells (Tengholm *et al.*, 1998), it has been reported that SERCA inhibition almost completely empties intracellular Ca^{2+} stores. However, in my work with rat β cells in the absence of extracellular Ca^{2+} only a small increase (0.06 μM) in $[Ca^{2+}]_i$ occurs. This may indicate that Ca^{2+} stores are small in rat β cells. In addition, the rat β cells in my study were exposed to zero Ca^{2+} extracellular solution prior to the BHQ challenge. The absence of extracellular Ca^{2+} might cause a partial depletion of the store.

II. Role of the other calcium removal mechanisms

As previously mentioned SERCA pumps are the major mediator of Ca^{2+} removal in rat β cells. However, other mechanisms do play a role in Ca^{2+} removal. Other than the SERCA pumps, mitochondria plays the largest role in Ca^{2+} homeostasis.

Mitochondrial Ca^{2+} uptake has been reported to be an important mechanism of Ca^{2+} removal in chromaffin cells (Herrington *et al.*, 1996; Park *et al.*, 1996), gonadotrophs (Hehl *et al.*, 1996), and corticotrophs (Lee & Tse, 2004). In comparison, the results presented in Chapter 4II indicate that in rat β cells the role of the mitochondria is smaller compared to other endocrine and neuro-endocrine cells. When mitochondrial function was disrupted in rat β cells by either cyanide and oligomycin or CCCP, the time course of Ca^{2+} removal was slowed by ~60 % (Figure 4.4 and 4.5). This effect was unlikely to be caused by slowing of other Ca^{2+} removal mechanisms (e.g. PMCA, SERCA) due to the disruption of ATP production in the mitochondria as all the cells were supplied with 5 mM ATP via the recording pipette. In mouse β cells, it has been reported that mitochondrial inhibition had no effect on Ca^{2+} removal (Chen *et al.*, 2003). This difference could be due to species differences, or differences in methods used (see above). However, in both patched and un-patched mouse cells mitochondrial inhibition was reported to have little effect on Ca^{2+} removal (Chen *et al.*, 2003). This suggests that the mitochondria may play a more important role in Ca^{2+} removal in rat β cells than in mouse. An enhanced role of the mitochondria in rat Ca^{2+} removal can potentially result in larger increases in mitochondrial $[Ca^{2+}]$ ($[Ca^{2+}]_m$) in rat β cells following glucose stimulation. As some enzymes in the Krebs cycle are activated by Ca^{2+} (Duchen, 1999), increases in $[Ca^{2+}]_m$ may enhance the production of metabolites involved in either the K_{ATP} dependent and independent pathways of glucose stimulated insulin secretion (Maechler & Wollheim, 2000). If rat β cells have a larger increase in $[Ca^{2+}]_m$ following glucose stimulation this may result in larger production of mediators stimulating insulin secretion and thus could underlie the enhanced second phase of insulin secretion in rat.

In addition to slowing Ca^{2+} removal, mitochondrial inhibition also caused a small increase in basal $[Ca^{2+}]_i$ and increased the amplitude of the depolarization triggered Ca^{2+} transient in rat β cells. The effect on the Ca^{2+} transient amplitude indicates that the mitochondria may help to limit the increase in $[Ca^{2+}]_i$ following a stimulation. An increase in basal $[Ca^{2+}]_i$ following mitochondria inhibition has also been reported in mouse β cells (Chen *et al.*, 2003; Dufer *et al.*, 2002) and other cell types (Lee & Tse, 2004; Bergmann & Keller, 2004; Hehl *et al.*, 1996). The $[Ca^{2+}]_i$ increase may be due to efflux of Ca^{2+} from the mitochondria (Bergmann & Keller, 2004; Tengholm *et al.*, 1998; Dufer *et al.*, 2002).

The role of the PMCA in rat β cells was examined by decreasing its activity with a pH 8.8 external solution (Xu *et al.*, 2000). The pH 8.8 solution increased the time constant of Ca^{2+} removal by 35 % (Figure 4.7A), but has no effect on basal $[Ca^{2+}]_i$ (Figure 4.7B), or the amplitude of the Ca^{2+} transient (Figure 4.73). These results indicate that the PMCA plays a minor role in Ca^{2+} removal, regulation of basal $[Ca^{2+}]_i$, and limiting the increase in $[Ca^{2+}]_i$ following a stimulus. This is in general agreement with what as been reported in mouse β cells (Chen *et al.*, 2003).

Two approaches were used to determine the NCX's role in Ca^{2+} homeostasis. The traditional approach of removing Na^+ and replacing it with NMG was used, along with the newer pharmacological approach of using the NCX inhibitor SEA0400. SEA0400 increased the time constant of Ca^{2+} removal by approximately 35 % (Figure 4.9A). In addition, SEA0400 caused a small, but statistically significant, increase in basal $[Ca^{2+}]_i$ (Figure 4.9B), but had no effect on the amplitude of the Ca^{2+} transient (Figure 4.9C). The results indicate that NCX plays a small role in Ca^{2+} removal and possibly in regulating

basal $[Ca^{2+}]_i$, but does not appear to regulate the increase in $[Ca^{2+}]_i$ following a stimulation. To further examine the role of the NCX in Ca^{2+} removal, the time constant of Ca^{2+} removal was examined in a Na^+ free external solution. In Na^+ free solution Ca^{2+} removal slowed by 20 % (Figure 4.9D), a change which was statistically significant, but was smaller than basal changes (22 %) (Figure 4.2A). Na^+ removal had no effect on basal $[Ca^{2+}]_i$ or the amplitude of the Ca^{2+} transient. The lack of effect of Na^+ removal on Ca^{2+} homeostasis raises the possibility that the effect of SEA0400 might be due to some non-specific effects of the drug. Thus, the NCX probably does not play a role in Ca^{2+} homeostasis in rat β cells.

This finding is in agreement with what was reported in mouse β cells (Chen *et al.*, 2003; Gall *et al.*, 1999). However, it is opposite to a study by Van Eylen *et al.* (Van Eylen *et al.*, 1998) that suggest that the NCX is responsible for up to 70 % of Ca^{2+} removal in rat β cells. The same study also suggests that the NCX in reverse mode contributes to $[Ca^{2+}]_i$ increases during a depolarization (Van Eylen *et al.*, 1998). There are a couple of reasons for this discrepancy. Firstly, the time course of Ca^{2+} removal was very different in the two studies. To cause an increase in $[Ca^{2+}]_i$, Van Eylen *et al* (1998) applied a high (50 mM) K^+ solution to the cell for approximately 10 minutes. This resulted in a prolonged elevation of $[Ca^{2+}]_i$ (500 nM for 10 minutes). Secondly, in my study the cells were constantly supplied with ATP but in Van Eylen's study the cells were not supplied with ATP. A prolonged $[Ca^{2+}]_i$ elevation (minutes) could result in cell damage and ATP depletion. This may explain why Ca^{2+} removal took minutes in Van Eylen's study and not seconds seen in my study. It is possible when the ATP dependent SERCA, PMCA, and mitochondria activity is reduced, the NCX becomes an important

Ca^{2+}removal mechanism. If the NCX, working in the reverse mode, was involved in Ca^{2+} influx during a depolarization, then its inhibition should decrease the amplitude of the Ca^{2+} transient. However, this was not found in my study (Figure 4.9C). This indicates that the NCX in reverse mode does not contribute to the increase in $[Ca^{2+}]_i$ following a depolarization.

As mentioned in the introduction the effects of glucose on $[Ca^{2+}]_i$ differ between rat and mouse β cells. In mouse, the typical response is $[Ca^{2+}]_i$ oscillations (Antunes *et al.*, 2000; Miura *et al.*, 1997; Liu *et al.*, 1995). While in rat β cells the response is more variable, in general glucose causes a sustained increase in $[Ca^{2+}]_i$ with slow Ca^{2+} oscillations in some cells (Antunes *et al.*, 2000; Theler *et al.*, 1992). It has been suggested that the increased expression of the NCX in rat β cells is the cause of the differences in the pattern of glucose stimulated $[Ca^{2+}]_i$ increase (Herchuelz *et al.*, 2002). However, the data presented here suggest that the NCX plays a minor role in Ca^{2+} homeostasis in both mouse and rat β cells, therefore it is unlikely the NCX contributes to the different pattern of glucose stimulated $[Ca^{2+}]_i$ signal in the two species of β cells.

III. Physiological relevance of capacitative calcium entry

The data presented here clearly demonstrates that inhibition of SERCA pumps has a dramatic effect on Ca^{2+} homeostasis in rat β cells by both limiting Ca^{2+} uptake into intracellular stores and by activation of CCE. This raises the question as to what physiological role CCE may play.

In β cells, ACh stimulates Ca^{2+} release from IP_3 stores (Gilon & Henquin, 2001). Emptying of intracellular Ca^{2+} stores by cholinergic agonists has been shown to activate

CCE (Gilon & Henquin, 2001; Miura *et al.*, 1997; Liu & Gylfe, 1997; Dyachok & Gylfe, 2001). However, there are doubts as to whether CCE contributes to cholinergic mediated increases in $[Ca^{2+}]_i$ physiologically (Gilon & Henquin, 2001). This is because the Ca^{2+} entry via CCE is reported to be small (Gilon & Henquin, 2001; Miura *et al.*, 1997; Liu & Gylfe, 1997; Dyachok & Gylfe, 2001). This is also complicated by the possibility that ACh may also depolarize β cells (Gilon & Henquin, 2001; Miura *et al.*, 1997; Rolland *et al.*, 2002; Olsen *et al.*, 2003) which reduces capacitative calcium entry (Gilon & Henquin, 2001; Miura *et al.*, 1997). The magnitude of this depolarization depends on glucose concentration with more depolarization in higher concentrations of glucose. As discussed earlier, CCE may be larger in the presence of low glucose so it is possible that CCE contributes to the ACh mediated increase in $[Ca^{2+}]_i$ more in the presence of low glucose levels. Nevertheless, Ca^{2+}entry through CCE is likely to contribute to the increase in $[Ca^{2+}]_i$ following ACh stimulation.

As mentioned in the introduction, glucose may stimulate the release of Ca^{2+} from intracellular stores. If glucose empties intracellular Ca^{2+} stores, glucose may also activate CCE leading to a further rise in $[Ca^{2+}]_i$. Glucose emptying of the intracellular Ca^{2+} stores has been reported to activate a non-selective cation channel (Roe *et al.*, 1998; Worley, *et al.*, 1994), however, it is not clear if this channel is the same channel BHQ activates.

In addition to cholinergic and glucose mediated activation of CCE, another potential activator may be insulin. One group has proposed that insulin exerts its positive autocrine feedback through inhibition of SERCA pumps (Borge *et al.*, 2002). If this is true then insulin inhibiting SERCA pumps can cause two effects. It will help empty intracellular stores, which will in turn activate CCE. As well, it will slow down Ca^{2+}

removal and thus prolonging and increasing glucose mediated $[Ca^{2+}]_i$ rise. However, whether insulin acts on SERCA pumps is not clear as some studies indicate that the insulin mediated effects on Ca^{2+} stores is due to Ca^{2+} release from NAADP sensitive Ca^{2+} stores (Patel, 2003).

C. Regulating calcium and exocytosis.

The first part of this thesis examines the relationship between $[Ca^{2+}]_i$ and exocytosis, while, the second part examines regulation of Ca^{2+} homeostasis. These two concepts may appear to be two separate things, however, they are closely coupled. From the first part of this thesis it should be apparent that $[Ca^{2+}]_i$ is important in regulating the amount and rate of exocytosis from rat β cells. While, the second part of this thesis shows the importance of different Ca^{2+} removal mechanisms in regulating $[Ca^{2+}]_i$. If one Ca^{2+} removal mechanism has its activity changed, this can change the amplitude and recovery of a Ca^{2+} transient. This change in $[Ca^{2+}]_i$ would result in changes in exocytosis. In other words, what regulates Ca^{2+} homeostasis also indirectly regulates exocytosis.

The importance of $[Ca^{2+}]_i$ regulation in modulating insulin secretion has been shown in several studies. Inhibition of SERCA pumps using either thapsigargin (Aizawa *et al.*, 1995), CPA (Chen *et al.*, 2003), or by knock-out of SERCA 3 (Arredouani *et al.*, 2002a) increases insulin secretion in response to either glucose (Arredouani *et al.*, 2002a; Aizawa *et al.*, 1995) or KCl (Chen *et al.*, 2003). In addition, Kang and Holtz (Kang & Holz, 2003) found that the increase in $[Ca^{2+}]_i$ following thapsigargin application stimulated exocytosis in INS-1 cells. Although, inhibition of mitochondrial function does change $[Ca^{2+}]_i$ regulation, the enhancing effects of $[Ca^{2+}]_i$ on insulin secretion may

be counter balanced by other effects of mitochondria inhibition. Inhibition of mitochondria will result in a decrease in ATP production, resulting in the opening of K_{ATP} channels and the hyper-polarization of the cell. As well, inhibition of mitochondrial function would disrupt production of the mediator of the K_{ATP} independent pathway of glucose. In addition, lowering ATP levels will affect processes such as vesicle mobilization and priming. Therefore, inhibition of mitochondrial function is likely to decrease insulin secretion.

In summary, insulin secretion is dependent on $[Ca^{2+}]_i$ elevation. Mechanisms underlying Ca^{2+} homeostasis are important regulators of insulin secretion. Therefore, it would be interesting to see in rodent models of diabetes if there are changes in Ca^{2+} removal.

Chapter 6: Conclusions and Further Directions

I. Conclusions

The work of this thesis looks at two related processes in rat β cells. One, the relationship between I_{Ca}, $[Ca^{2+}]_i$, and exocytosis at both room temperature and elevated temperatures was examined. Secondly, the roles of different Ca^{2+} removal mechanisms in Ca^{2+} homeostasis was also determined.

When examining the relationship between I_{Ca}, $[Ca^{2+}]_i$, and exocytosis, a couple of things were determined. One, the amount of Ca^{2+} entering the cell and the increase in $[Ca^{2+}]_i$ regulate the amount and rate of exocytosis in rat β cells. In addition, exocytosis in rat β cells is highly temperature dependent. At comparable $[Ca^{2+}]_i$ both the rate and amount of exocytosis was greatly increased at 30 °C. Potential causes for the temperature dependence include changes in the kinetics of exocytosis or vesicle co-localization with VGCC and enhanced vesicle replenishment. Finally, the relationship between $[Ca^{2+}]_i$ and exocytosis in rat β cells shares both similarities (amount of exocytosis at moderate $[Ca^{2+}]_i$) and differences (ability to exocytose at low $[Ca^{2+}]_i$) with mouse β cells. In addition, it appears that the RRP size is larger in rat β cells, which may underlie the differences in size of the first phase of insulin secretion between the two species.

While examining the role of different Ca^{2+} removal mechanisms it is clear that the most important removal mechanism in rat β cells is the SERCA pump. Inhibition of the SERCA pump changes basal $[Ca^{2+}]_i$, the amplitude of Ca^{2+} transients, and the time course of Ca^{2+} removal. In addition, inhibition of SERCA pumps causes the activation of a CCE channel which results in the influx of extracellular Ca^{2+}. Other Ca^{2+} removal

mechanisms also play a role, but they appear not to be as important. My findings rule out the possibility that NCX is the cause for the differences in glucose mediated $[Ca^{2+}]_i$ signaling between rats and mice. However, differences in the role of the mitochondria in Ca^{2+} removal may be partially responsible for the differences in the second phase of insulin secretion between rat and mouse. The order of importance of the different Ca^{2+} removal mechanisms in rat β cells appears to be SERCA>>>mitochondria>NCX>PMCA.

II Future directions

The current method of a train of depolarizations to cause an increase in $[Ca^{2+}]_i$ and stimulate exocytosis has some limitations. For example, the $[Ca^{2+}]_i$ rise was limited by the VGCC density, it was not possible to differentiate between release from the RRP and mobilization of vesicles. Because of these limitations, it is impossible to completely determine the reason for the temperature dependence. As well, it is impossible to get a more exact estimate of RRP size and see how it differs to mouse. For those reasons, one future study in rat β cells should be to determine the RRP size by measuring exocytosis following a rapid increase in $[Ca^{2+}]_i$ after the photolysis of a caged calcium compound at both 22 °C and 30 °C. This would allow the kinetics of exocytosis to be measured as well as the RRP size. This would help to resolve if the kinetics of exocytosis are temperature dependent in β cells as well as to confirm that temperature does not affect RRP size.

One problem in conclusively determining whether BHQ's increase in $[Ca^{2+}]_i$ is mediated by CCE, is the lack of specific inhibitors for CCE. 2-APB has been considered a relatively selective inhibitor of CCE (Putney, Jr., 2001); however, the data presented

here and elsewhere (Braun *et al.*, 2003b; Missiaen *et al.*, 2001) raise doubts about that. To confirm further the role of CCE, another CCE inhibitor can be tested. One potential inhibitor could be SF&K96365, which has been reported to inhibit CCE, although it may also block VGCC (Putney, Jr., 2001). In my study the $[Ca^{2+}]_i$ rise by BHQ is considerably larger than the values presented elsewhere for mouse β cells. It would be interesting to determine if CCE is larger in rat or if this difference was caused by methodological differences.

Another interesting idea would be to examine $[Ca^{2+}]_m$ in both rat and mouse β cells. A larger role for the mitochondria in Ca^{2+} removal in rat β cells should result in a larger increase in $[Ca^{2+}]_m$ following a stimulus. This would support the possibility that differences in mitochondrial Ca^{2+} uptake may be partially responsible for differences in Ca^{2+} homeostasis and the size of the second phase of insulin secretion between mouse and rat β cells.

References

Ahren, B. (2000). Autonomic regulation of islet hormone secretion--implications for health and disease. *Diabetologia* 43, 393-410.

Aizawa, T., Komatsu, M., Asanuma, N., Sato, Y., & Sharp, G. W. (1998). Glucose action 'beyond ionic events' in the pancreatic beta cell. *Trends Pharmacol.Sci.* 19, 496-499.

Aizawa, T., Yada, T., Asanuma, N., Sato, Y., Ishihara, F., Hamakawa, N., Yaekura, K., & Hashizume, K. (1995). Effects of thapsigargin, an intracellular Ca^{2+} pump inhibitor, on insulin release by rat pancreatic B-cell. *Life Sci.* 57, 1375-1381.

Ammäla, C., Ashcroft, F. M., & Rorsman, P. (1993a). Calcium-independent potentiation of insulin release by cyclic AMP in single beta-cells. *Nature* 363, 356-358.

Ammäla, C., Eliasson, L., Bokvist, K., Berggren, P. O., Honkanen, R. E., Sjoholm, A., & Rorsman, P. (1994a). Activation of protein kinases and inhibition of protein phosphatases play a central role in the regulation of exocytosis in mouse pancreatic beta cells. *Proc.Natl.Acad.Sci.U.S.A* 91, 4343-4347.

Ammäla, C., Eliasson, L., Bokvist, K., Berggren, P. O., Honkanen, R. E., Sjoholm, A., & Rorsman, P. (1994b). Activation of protein kinases and inhibition of protein phosphatases play a central role in the regulation of exocytosis in mouse pancreatic beta cells. *Proc.Natl.Acad.Sci.U.S.A* 91, 4343-4347.

Ammäla, C., Eliasson, L., Bokvist, K., Larsson, O., Ashcroft, F. M., & Rorsman, P. (1993b). Exocytosis elicited by action potentials and voltage-clamp calcium currents in individual mouse pancreatic B-cells. *J.Physiol* 472, 665-688.

Ammäla, C., Eliasson, L., Bokvist, K., Larsson, O., Ashcroft, F. M., & Rorsman, P. (1993c). Exocytosis elicited by action potentials and voltage-clamp calcium currents in individual mouse pancreatic B-cells. *J.Physiol* 472, 665-688.

Ammäla, C., Larsson, O., Berggren, P. O., Bokvist, K., Juntti-Berggren, L., Kindmark, H., & Rorsman, P. (1991b). Inositol trisphosphate-dependent periodic activation of a Ca^{2+}-activated K^+ conductance in glucose-stimulated pancreatic beta-cells. *Nature* 353, 849-852.

Ammäla, C., Larsson, O., Berggren, P. O., Bokvist, K., Juntti-Berggren, L., Kindmark, H., & Rorsman, P. (1991a). Inositol trisphosphate-dependent periodic activation of a Ca^{2+}-activated K^+ conductance in glucose-stimulated pancreatic beta-cells. *Nature* 353, 849-852.

Antunes, C. M., Salgado, A. P., Rosario, L. M., & Santos, R. M. (2000). Differential patterns of glucose-induced electrical activity and intracellular calcium responses in single mouse and rat pancreatic islets. *Diabetes* 49, 2028-2038.

Arredouani, A., Guiot, Y., Jonas, J. C., Liu, L. H., Nenquin, M., Pertusa, J. A., Rahier, J., Rolland, J. F., Shull, G. E., Stevens, M., Wuytack, F., Henquin, J. C., & Gilon, P. (2002a). SERCA3 ablation does not impair insulin secretion but suggests distinct roles of different sarcoendoplasmic reticulum Ca^{2+} pumps for Ca^{2+} homeostasis in pancreatic beta-cells. *Diabetes* 51, 3245-3253.

Arredouani, A., Henquin, J. C., & Gilon, P. (2002b). Contribution of the endoplasmic reticulum to the glucose-induced $[Ca^{2+}]_c$ response in mouse pancreatic islets. *Am.J.Physiol Endocrinol.Metab* 282, E982-E991.

Ashcroft, S. J. (2000). The beta-cell K_{ATP} channel. *J Membr.Biol.* 176, 187-206.

Barg, S., Eliasson, L., Renstrom, E., & Rorsman, P. (2002a). A subset of 50 secretory granules in close contact with L-type Ca^{2+} channels accounts for first-phase insulin secretion in mouse beta-cells. *Diabetes* 51 Suppl 1, S74-S82.

Barg, S., Huang, P., Eliasson, L., Nelson, D. J., Obermuller, S., Rorsman, P., Thevenod, F., & Renstrom, E. (2001a). Priming of insulin granules for exocytosis by granular Cl^- uptake and acidification. *J.Cell Sci.* 114, 2145-2154.

Barg, S., Ma, X., Eliasson, L., Galvanovskis, J., Gopel, S. O., Obermuller, S., Platzer, J., Renstrom, E., Trus, M., Atlas, D., Striessnig, J., & Rorsman, P. (2001b). Fast exocytosis with few Ca^{2+} channels in insulin-secreting mouse pancreatic B cells. *Biophys.J.* 81, 3308-3323.

Barg, S., Olofsson, C. S., Schriever-Abeln, J., Wendt, A., Gebre-Medhin, S., Renstrom, E., & Rorsman, P. (2002b). Delay between fusion pore opening and peptide release from large dense-core vesicles in neuroendocrine cells. *Neuron* 33, 287-299.

Barg, S., Renstrom, E., Berggren, P. O., Bertorello, A., Bokvist, K., Braun, M., Eliasson, L., Holmes, W. E., Kohler, M., Rorsman, P., & Thevenod, F. (1999). The stimulatory

action of tolbutamide on Ca^{2+}-dependent exocytosis in pancreatic beta cells is mediated by a 65-kDa mdr-like P-glycoprotein. *Proc.Natl.Acad.Sci.U.S.A* 96, 5539-5544.

Barnett, D. W. & Misler, S. (1995). Coupling of exocytosis to depolarization in rat pancreatic islet beta-cells: effects of Ca^{2+}, Sr^{2+} and Ba^{2+} containing extracellular solutions. *Pflugers Arch.* 430, 593-595.

Bergmann, F. & Keller, B. U. (2004). Impact of mitochondrial inhibition on excitability and cytosolic Ca^{2+} levels in brainstem motoneurones from mouse. *J.Physiol* 555, 45-59.

Bernardi, P. (1999). Mitochondrial transport of cations: channels, exchangers, and permeability transition. *Physiol Rev.* 79, 1127-1155.

Berridge, M. J., Bootman, M. D., & Roderick, H. L. (2003). Calcium signalling: dynamics, homeostasis and remodelling. *Nat.Rev.Mol.Cell Biol.* 4, 517-529.

Berridge, M. J., Lipp, P., & Bootman, M. D. (2000). The versatility and universality of calcium signalling. *Nat.Rev.Mol.Cell Biol.* 1, 11-21.

Bertrand, G., Ishiyama, N., Nenquin, M., Ravier, M. A., & Henquin, J. C. (2002). The elevation of glutamate content and the amplification of insulin secretion in glucose-stimulated pancreatic islets are not causally related. *J.Biol.Chem.* 277, 32883-32891.

Bokvist, K., Eliasson, L., Ammäla, C., Renstrom, E., & Rorsman, P. (1995). Co-localization of L-type Ca^{2+} channels and insulin-containing secretory granules and its significance for the initiation of exocytosis in mouse pancreatic B-cells. *EMBO J.* 14, 50-57.

Bootman, M. D., Collins, T. J., Mackenzie, L., Roderick, H. L., Berridge, M. J., & Peppiatt, C. M. (2002). 2-aminoethoxydiphenyl borate (2-APB) is a reliable blocker of store-operated Ca^{2+} entry but an inconsistent inhibitor of $InsP_3$ induced Ca^{2+} release. *FASEB J.* 16, 1145-1150.

Borge, P. D., Moibi, J., Greene, S. R., Trucco, M., Young, R. A., Gao, Z., & Wolf, B. A. (2002). Insulin receptor signaling and sarco/endoplasmic reticulum calcium ATPase in beta-cells. *Diabetes* 51 Suppl 3, S427-S433.

Braun, F. J., Aziz, O., & Putney, J. W., Jr. (2003a). 2-aminoethoxydiphenyl borane activates a novel calcium-permeable cation channel. *Mol.Pharmacol.* 63, 1304-1311.

Braun, F. J., Aziz, O., & Putney, J. W., Jr. (2003b). 2-aminoethoxydiphenyl borane activates a novel calcium-permeable cation channel. *Mol.Pharmacol.* 63, 1304-1311.

Burgoyne, R. D. & Morgan, A. (2003). Secretory granule exocytosis. *Physiol Rev.* 83, 581-632.

Camello, C., Lomax, R., Petersen, O. H., & Tepikin, A. V. (2002). Calcium leak from intracellular stores--the enigma of calcium signalling. *Cell Calcium* 32, 355-361.

Chen, L., Koh, D. S., & Hille, B. (2003). Dynamics of calcium clearance in mouse pancreatic beta-cells. *Diabetes* 52, 1723-1731.

Dinkelacker, V., Voets, T., Neher, E., & Moser, T. (2000). The readily releasable pool of vesicles in chromaffin cells is replenished in a temperature-dependent manner and transiently overfills at 37 degrees C. *J.Neurosci.* 20, 8377-8383.

Duchen, M. R. (1999). Contributions of mitochondria to animal physiology: from homeostatic sensor to calcium signalling and cell death. *J Physiol* 516 (Pt 1), 1-17.

Dufer, M., Krippeit-Drews, P., & Drews, G. (2002). Inhibition of mitochondrial function affects cellular Ca^{2+} handling in pancreatic B-cells. *Pflugers Arch.* 444, 236-243.

Dyachok, O. & Gylfe, E. (2001). Store-operated influx of Ca^{2+} in pancreatic beta-cells exhibits graded dependence on the filling of the endoplasmic reticulum. *J.Cell Sci.* 114, 2179-2186.

Dyachok, O., Tufveson, G., & Gylfe, E. (2004). Ca^{2+}-induced Ca^{2+} release by activation of inositol 1,4,5-trisphosphate receptors in primary pancreatic [beta]-cells. *Cell Calcium* 36, 1-9.

Eliasson, L., Ma, X., Renstrom, E., Barg, S., Berggren, P. O., Galvanovskis, J., Gromada, J., Jing, X., Lundquist, I., Salehi, A., Sewing, S., & Rorsman, P. (2003). SUR1 regulates PKA-independent cAMP-induced granule priming in mouse pancreatic B-cells. *J.Gen.Physiol* 121, 181-197.

Eliasson, L., Proks, P., Ammäla, C., Ashcroft, F. M., Bokvist, K., Renstrom, E., Rorsman, P., & Smith, P. A. (1996). Endocytosis of secretory granules in mouse pancreatic beta-cells evoked by transient elevation of cytosolic calcium. *J.Physiol* 493 (Pt 3), 755-767.

Eliasson, L., Renstrom, E., Ding, W. G., Proks, P., & Rorsman, P. (1997). Rapid ATP-dependent priming of secretory granules precedes Ca^{2+}-induced exocytosis in mouse pancreatic B-cells. *J.Physiol* 503 (Pt 2), 399-412.

Gall, D., Gromada, J., Susa, I., Rorsman, P., Herchuelz, A., & Bokvist, K. (1999). Significance of Na/Ca exchange for Ca^{2+} buffering and electrical activity in mouse pancreatic beta-cells. *Biophys.J.* 76, 2018-2028.

Garcia-Barrado, M. J., Jonas, J. C., Gilon, P., & Henquin, J. C. (1996). Sulphonylureas do not increase insulin secretion by a mechanism other than a rise in cytoplasmic Ca^{2+} in pancreatic B-cells. *Eur.J.Pharmacol.* 298, 279-286.

Gil, A., Viniegra, S., & Gutierrez, L. M. (2001). Temperature and PMA affect different phases of exocytosis in bovine chromaffin cells. *Eur J Neurosci.* 13, 1380-1386.

Gillis, K. D. (1995). Techniques for membrane capacitance measurments. In *Single-channel recording*, eds. Sakmann, B. & Neher, E., pp. 155-198. Plenum press.

Gillis, K. D. & Misler, S. (1992). Single cell assay of exocytosis from pancreatic islet B cells. *Pflugers Arch.* 420, 121-123.

Gillis, K. D. & Misler, S. (1993). Enhancers of cytosolic cAMP augment depolarization-induced exocytosis from pancreatic B-cells: evidence for effects distal to Ca^{2+} entry. *Pflugers Arch.* 424, 195-197.

Gilon, P., Arredouani, A., Gailly, P., Gromada, J., & Henquin, J. C. (1999). Uptake and release of Ca^{2+} by the endoplasmic reticulum contribute to the oscillations of the cytosolic Ca^{2+} concentration triggered by Ca^{2+} influx in the electrically excitable pancreatic B-cell. *J.Biol.Chem.* 274, 20197-20205.

Gilon, P. & Henquin, J. C. (2001). Mechanisms and physiological significance of the cholinergic control of pancreatic beta-cell function. *Endocr.Rev.* 22, 565-604.

Gromada, J., Frokjaer-Jensen, J., & Dissing, S. (1996). Glucose stimulates voltage- and calcium-dependent inositol trisphosphate production and intracellular calcium mobilization in insulin-secreting beta TC3 cells. *Biochem.J* 314 (Pt 1), 339-345.

Gromada, J., Holst, J. J., & Rorsman, P. (1998). Cellular regulation of islet hormone secretion by the incretin hormone glucagon-like peptide 1. *Pflugers Arch.* 435, 583-594.

Gromada, J., Hoy, M., Renstrom, E., Bokvist, K., Eliasson, L., Gopel, S., & Rorsman, P. (1999). CaM kinase II-dependent mobilization of secretory granules underlies acetylcholine-induced stimulation of exocytosis in mouse pancreatic B-cells. *J.Physiol* 518 (Pt 3), 745-759.

Grynkiewicz, G., Poenie, M., & Tsien, R. Y. (1985). A new generation of Ca^{2+} indicators with greatly improved fluorescence properties. *J.Biol.Chem.* 260, 3440-3450.

Hamill, O. P., Marty, A., Neher, E., Sakmann, B., & Sigworth, F. J. (1981). Improved patch-clamp techniques for high-resolution current recording from cells and cell-free membrane patches. *Pflugers Arch.* 391, 85-100.

Hehl, S., Golard, A., & Hille, B. (1996). Involvement of mitochondria in intracellular calcium sequestration by rat gonadotropes. *Cell Calcium* 20, 515-524.

Hellman, B., Dansk, H., & Grapengiesser, E. (2004). Pancreatic beta-cells communicate via intermittent release of ATP. *Am.J Physiol Endocrinol.Metab* 286, E759-E765.

Henquin, J. C. (2000). Triggering and amplifying pathways of regulation of insulin secretion by glucose. *Diabetes* 49, 1751-1760.

Henquin, J. C., Ravier, M. A., Nenquin, M., Jonas, J. C., & Gilon, P. (2003). Hierarchy of the beta-cell signals controlling insulin secretion. *Eur.J.Clin.Invest* 33, 742-750.

Herchuelz, A., Diaz-Horta, O., & Van Eylen, F. (2002). Na/Ca exchanger in function, growth, and demise of beta-cells. *Ann.N.Y.Acad.Sci.* 976, 315-324.

Herrington J., Newton K.R., & and Bookman R.J. (1995). *Pulse Control V4.6: Igor XOPs for patch clamp data acquisitin and capacitance measurments* University of Miaimi Press, Miami FL.

Herrington, J., Park, Y. B., Babcock, D. F., & Hille, B. (1996). Dominant role of mitochondria in clearance of large Ca^{2+} loads from rat adrenal chromaffin cells. *Neuron* 16, 219-228.

Holz, G. G. (2004). Epac: a new cAMP-binding protein in support of glucagon-like peptide-1 receptor-mediated signal transductio in the pancreatic β-cell. *Diabetes* 53, 5-13.

Holz, G. G., Leech, C. A., Heller, R. S., Castonguay, M., & Habener, J. F. (1999). cAMP-dependent mobilization of intracellular Ca^{2+} stores by activation of ryanodine receptors in pancreatic beta-cells. A Ca^{2+} signaling system stimulated by the insulinotropic hormone glucagon-like peptide-1-(7-37). *J Biol.Chem.* 274, 14147-14156.

Horrigan, F. T. & Bookman, R. J. (1994). Releasable pools and the kinetics of exocytosis in adrenal chromaffin cells. *Neuron* 13, 1119-1129.

Hoy, M., Berggren, P. O., & Gromada, J. (2003). Involvement of protein kinase C-epsilon in inositol hexakisphosphate-induced exocytosis in mouse pancreatic beta-cells. *J Biol.Chem.* 278, 35168-35171.

Hoy, M., Maechler, P., Efanov, A. M., Wollheim, C. B., Berggren, P. O., & Gromada, J. (2002). Increase in cellular glutamate levels stimulates exocytosis in pancreatic beta-cells. *FEBS Lett.* 531, 199-203.

Islam, M. S. & Berggren, P. O. (1997). Cyclic ADP-ribose and the pancreatic beta cell: where do we stand? *Diabetologia* 40, 1480-1484.

Josefsen, K., Stenvang, J. P., Kindmark, H., Berggren, P. O., Horn, T., Kjaer, T., & Buschard, K. (1996). Fluorescence-activated cell sorted rat islet cells and studies of the insulin secretory process. *J.Endocrinol.* 149, 145-154.

Kadenbach, B. (2003). Intrinsic and extrinsic uncoupling of oxidative phosphorylation. *Biochim.Biophys.Acta* 1604, 77-94.

Kang, G. & Holz, G. G. (2003). Amplification of exocytosis by Ca^{2+}-induced Ca^{2+} release in INS-1 pancreatic beta cells. *J Physiol* 546, 175-189.

Kim, S. J., Sung, J. J., & Park, Y. S. (1998). L-type and dihydropyridine-resistant calcium channel trigger exocytosis with similar efficacy in single rat pancreatic beta cells. *Biochem.Biophys.Res.Commun.* 243, 878-884.

Lacy, P. E. & Kostianovsky, M. (1967). Method for the isolation of intact islets of Langerhans from the rat pancreas. *Diabetes* 16, 35-39.

Lee, A. K. & Tse, A. Tyrosine kinases regulate mitochondria calcium transport in rat pituitary corticotrophs. 2004.
Ref Type: Unpublished Work

Li, G. D., Milani, D., Dunne, M. J., Pralong, W. F., Theler, J. M., Petersen, O. H., & Wollheim, C. B. (1991). Extracellular ATP causes Ca^{2+}-dependent and -independent insulin secretion in RINm5F cells. Phospholipase C mediates Ca^{2+} mobilization but not Ca^{2+} influx and membrane depolarization. *J Biol.Chem.* 266, 3449-3457.

Light, P. E. (2002). The ABCs of Sulfonylurea Receptors, Islet K_{ATP} channels and the control of insulin secretion. *Can.J.Diabetes* 26, 223-231.

Light, P. E., Manning Fox, J. E., Riedel, M. J., & Wheeler, M. B. (2002). Glucagon-like peptide-1 inhibits pancreatic ATP-sensitive potassium channels via a protein kinase A- and ADP-dependent mechanism. *Mol.Endocrinol.* 16, 2135-2144.

Liu, Y. J., Grapengiesser, E., Gylfe, E., & Hellman, B. (1995). Glucose induces oscillations of cytoplasmic Ca^{2+}, Sr^{2+} and Ba^{2+} in pancreatic beta-cells without participation of the thapsigargin-sensitive store. *Cell Calcium* 18, 165-173.

Liu, Y. J. & Gylfe, E. (1997). Store-operated Ca^{2+} entry in insulin-releasing pancreatic beta-cells. *Cell Calcium* 22, 277-286.

Luzi, L. & DeFronzo, R. A. (1989). Effect of loss of first-phase insulin secretion on hepatic glucose production and tissue glucose disposal in humans. *Am.J Physiol* 257, E241-E246.

Ma, H. T., Venkatachalam, K., Parys, J. B., & Gill, D. L. (2002). Modification of store-operated channel coupling and inositol trisphosphate receptor function by 2-aminoethoxydiphenyl borate in DT40 lymphocytes. *J.Biol.Chem.* 277, 6915-6922.

Ma, Y. H., Wang, J., Rodd, G. G., Bolaffi, J. L., & Grodsky, G. M. (1995). Differences in insulin secretion between the rat and mouse: role of cAMP. *Eur J Endocrinol.* 132, 370-376.

Maechler, P. (2003). Novel regulation of insulin secretion: the role of mitochondria. *Curr.Opin.Investig.Drugs* 4, 1166-1172.

Maechler, P., Gjinovci, A., & Wollheim, C. B. (2002). Implication of glutamate in the kinetics of insulin secretion in rat and mouse perfused pancreas. *Diabetes* 51 Suppl 1, S99-102.

Maechler, P., Kennedy, E. D., Sebo, E., Valeva, A., Pozzan, T., & Wollheim, C. B. (1999). Secretagogues modulate the calcium concentration in the endoplasmic reticulum of insulin-secreting cells. Studies in aequorin-expressing intact and permeabilized ins-1 cells. *J.Biol.Chem.* 274, 12583-12592.

Maechler, P. & Wollheim, C. B. (2000). Mitochondrial signals in glucose-stimulated insulin secretion in the beta cell. *J Physiol* 529 Pt 1, 49-56.

Mariot, P., Gilon, P., Nenquin, M., & Henquin, J. C. (1998). Tolbutamide and diazoxide influence insulin secretion by changing the concentration but not the action of cytoplasmic Ca^{2+} in beta-cells. *Diabetes* 47, 365-373.

Martin, F. & Soria, B. (1996). Glucose-induced [Ca2+]i oscillations in single human pancreatic islets. *Cell Calcium* 20, 409-414.

Matsuda, T., Arakawa, N., Takuma, K., Kishida, Y., Kawasaki, Y., Sakaue, M., Takahashi, K., Takahashi, T., Suzuki, T., Ota, T., Hamano-Takahashi, A., Onishi, M., Tanaka, Y., Kameo, K., & Baba, A. (2001). SEA0400, a novel and selective inhibitor of the Na^{+}-Ca^{2+} exchanger, attenuates reperfusion injury in the in vitro and in vivo cerebral ischemic models. *J.Pharmacol.Exp.Ther.* 298, 249-256.

Misler, S., Barnett, D. W., Gillis, K. D., & Pressel, D. M. (1992a). Electrophysiology of stimulus-secretion coupling in human beta-cells. *Diabetes* 41, 1221-1228.

Misler, S., Barnett, D. W., Pressel, D. M., Gillis, K. D., Scharp, D. W., & Falke, L. C. (1992b). Stimulus-secretion coupling in beta-cells of transplantable human islets of Langerhans. Evidence for a critical role for Ca^{2+} entry. *Diabetes* 41, 662-670.

Missiaen, L., Callewaert, G., De Smedt, H., & Parys, J. B. (2001). 2-Aminoethoxydiphenyl borate affects the inositol 1,4,5-trisphosphate receptor, the intracellular Ca^{2+} pump and the non-specific Ca^{2+} leak from the non-mitochondrial Ca^{2+} stores in permeabilized A7r5 cells. *Cell Calcium* 29, 111-116.

Miura, Y., Henquin, J. C., & Gilon, P. (1997). Emptying of intracellular Ca^{2+} stores stimulates Ca^{2+} entry in mouse pancreatic beta-cells by both direct and indirect mechanisms. *J.Physiol* 503 (Pt 2), 387-398.

Neher, E. (1998). Vesicle pools and Ca^{2+} microdomains: new tools for understanding their roles in neurotransmitter release. *Neuron* 20, 389-399.

Okamoto, H., Takasawa, S., & Nata, K. (1997). The CD38-cyclic ADP-ribose signalling system in insulin secretion: molecular basis and clinical implications. *Diabetologia* 40, 1485-1491.

Olsen, H. L., Hoy, M., Zhang, W., Bertorello, A. M., Bokvist, K., Capito, K., Efanov, A. M., Meister, B., Thams, P., Yang, S. N., Rorsman, P., Berggren, P. O., & Gromada, J. (2003). Phosphatidylinositol 4-kinase serves as a metabolic sensor and regulates priming of secretory granules in pancreatic beta cells. *Proc.Natl.Acad.Sci.U.S.A* 100, 5187-5192.

Parekh, A. B. (2003). Store-operated Ca^{2+} entry: dynamic interplay between endoplasmic reticulum, mitochondria and plasma membrane. *J.Physiol* 547, 333-348.

Park, Y. B., Herrington, J., Babcock, D. F., & Hille, B. (1996). Ca^{2+} clearance mechanisms in isolated rat adrenal chromaffin cells. *J.Physiol* 492 (Pt 2), 329-346.

Patel, S. (2003). NAADP on the up in pancreatic beta cells-a sweet message? *Bioessays* 25, 430-433.

Pihel, K., Travis, E. R., Borges, R., & Wightman, R. M. (1996). Exocytotic release from individual granules exhibits similar properties at mast and chromaffin cells. *Biophys.J* 71, 1633-1640.

Pozzan, T., Rizzuto, R., Volpe, P., & Meldolesi, J. (1994). Molecular and cellular physiology of intracellular calcium stores. *Physiol Rev.* 74, 595-636.

Prakriya, M. & Lewis, R. S. (2001). Potentiation and inhibition of Ca^{2+} release-activated Ca^{2+} channels by 2-aminoethyldiphenyl borate (2-APB) occurs independently of IP(3) receptors. *J.Physiol* 536, 3-19.

Putney, J. W., Jr. (2001). Pharmacology of capacitative calcium entry. *Mol.Interv.* 1, 84-94.

Putney, J. W., Jr. & McKay, R. R. (1999). Capacitative calcium entry channels. *Bioessays* 21, 38-46.

Pyott, S. J. & Rosenmund, C. (2002). The effects of temperature on vesicular supply and release in autaptic cultures of rat and mouse hippocampal neurons. *J Physiol* 539, 523-535.

Renstrom, E., Barg, S., Thevenod, F., & Rorsman, P. (2002). Sulfonylurea-mediated stimulation of insulin exocytosis via an ATP-sensitive K^+ channel-independent action. *Diabetes* 51 Suppl 1, S33-S36.

Renstrom, E., Eliasson, L., Bokvist, K., & Rorsman, P. (1996). Cooling inhibits exocytosis in single mouse pancreatic B-cells by suppression of granule mobilization. *J.Physiol* 494 (Pt 1), 41-52.

Renstrom, E., Eliasson, L., & Rorsman, P. (1997). Protein kinase A-dependent and -independent stimulation of exocytosis by cAMP in mouse pancreatic B-cells. *J.Physiol* 502 (Pt 1), 105-118.

Ricordi, C., Lacy, P. E., Finke, E. H., Olack, B. J., & Scharp, D. W. (1988). Automated method for isolation of human pancreatic islets. *Diabetes* 37, 413-420.

Rizzuto, R., Bernardi, P., & Pozzan, T. (2000). Mitochondria as all-round players of the calcium game. *J.Physiol* 529 Pt 1, 37-47.

Roe, M. W., Lancaster, M. E., Mertz, R. J., Worley, J. F., III, & Dukes, I. D. (1993). Voltage-dependent intracellular calcium release from mouse islets stimulated by glucose. *J Biol.Chem.* 268, 9953-9956.

Roe, M. W., Worley, J. F., III, Qian, F., Tamarina, N., Mittal, A. A., Dralyuk, F., Blair, N. T., Mertz, R. J., Philipson, L. H., & Dukes, I. D. (1998). Characterization of a Ca^{2+} release-activated nonselective cation current regulating membrane potential and $[Ca^{2+}]_i$ oscillations in transgenically derived beta-cel_{ls}. *J Biol.Chem.* 273, 10402-10410.

Rolland, J. F., Henquin, J. C., & Gilon, P. (2002). G protein-independent activation of an inward Na^+ current by muscarinic receptors in mouse pancreatic beta-cells. *J.Biol.Chem.* 277, 38373-38380.

Rorsman, P. (1997). The pancreatic beta-cell as a fuel sensor: an electrophysiologist's viewpoint. *Diabetologia* 40, 487-495.

Rorsman, P., Eliasson, L., Renstrom, E., Gromada, J., Barg, S., & Gopel, S. (2000). The Cell Physiology of Biphasic Insulin Secretion. *News Physiol Sci.* 15, 72-77.

Rorsman, P. & Renstrom, E. (2003). Insulin granule dynamics in pancreatic beta cells. *Diabetologia* 46, 1029-1045.

Satin, L. S. (2000). Localized calcium influx in pancreatic beta-cells: its significance for Ca^{2+}-dependent insulin secretion from the islets of Langerhans. *Endocrine.* 13, 251-262.

Schulla, V., Renstrom, E., Feil, R., Feil, S., Franklin, I., Gjinovci, A., Jing, X. J., Laux, D., Lundquist, I., Magnuson, M. A., Obermuller, S., Olofsson, C. S., Salehi, A., Wendt, A., Klugbauer, N., Wollheim, C. B., Rorsman, P., & Hofmann, F. (2003). Impaired insulin secretion and glucose tolerance in beta cell-selective Ca(v)1.2 Ca^{2+} channel null mice. *EMBO J.* 22, 3844-3854.

Shapiro, A. M., Hao, E., Rajotte, R. V., & Kneteman, N. M. (1996). High yield of rodent islets with intraductal collagenase and stationary digestion--a comparison with standard technique. *Cell Transplant.* 5, 631-638.

Speier, S. & Rupnik, M. (2003). A novel approach to in situ characterization of pancreatic beta-cells. *Pflugers Arch.* 446, 553-558.

Straub, S. G. & Sharp, G. W. (2002). Glucose-stimulated signaling pathways in biphasic insulin secretion. *Diabetes Metab Res.Rev.* 18, 451-463.

Takahashi, N., Kadowaki, T., Yazaki, Y., Ellis-Davies, G. C., Miyashita, Y., & Kasai, H. (1999). Post-priming actions of ATP on Ca^{2+}-dependent exocytosis in pancreatic beta cells. *Proc.Natl.Acad.Sci.U.S.A* 96, 760-765.

Takasawa, S., Nata, K., Yonekura, H., & Okamoto, H. (1993). Cyclic ADP-ribose in insulin secretion from pancreatic beta cells. *Science* 259, 370-373.

Tanaka, H., Nishimaru, K., Aikawa, T., Hirayama, W., Tanaka, Y., & Shigenobu, K. (2002). Effect of SEA0400, a novel inhibitor of sodium-calcium exchanger, on myocardial ionic currents. *Br.J.Pharmacol.* 135, 1096-1100.

Tengholm, A., Hagman, C., Gylfe, E., & Hellman, B. (1998). In situ characterization of nonmitochondrial Ca^{2+} stores in individual pancreatic beta-cells. *Diabetes* 47, 1224-1230.

Theler, J. M., Mollard, P., Guerineau, N., Vacher, P., Pralong, W. F., Schlegel, W., & Wollheim, C. B. (1992). Video imaging of cytosolic Ca^{2+} in pancreatic beta-cells stimulated by glucose, carbachol, and ATP. *J Biol.Chem.* 267, 18110-18117.

Thomas, P., Surprenant, A., & Almers, W. (1990). Cytosolic Ca^{2+}, exocytosis, and endocytosis in single melanotrophs of the rat pituitary. *Neuron* 5, 723-733.

Thomas, P., Wong, J. G., Lee, A. K., & Almers, W. (1993). A low affinity Ca^{2+} receptor controls the final steps in peptide secretion from pituitary melanotrophs. *Neuron* 11, 93-104.

Tse, A., Tse, F. W., & Hille, B. (1994). Calcium homeostasis in identified rat gonadotrophs. *J.Physiol* 477 (Pt 3), 511-525.

Van Eylen, F., Lebeau, C., Albuquerque-Silva, J., & Herchuelz, A. (1998). Contribution of Na/Ca exchange to Ca^{2+} outflow and entry in the rat pancreatic beta-cell: studies with antisense oligonucleotides. *Diabetes* 47, 1873-1880.

Wollheim, C. B. & Sharp, G. W. (1981). Regulation of insulin release by calcium. *Physiol Rev.* 61, 914-973.

Worley, J. F., III, McIntyre, M. S., Spencer, B., & Dukes, I. D. (1994). Depletion of intracellular Ca^{2+} stores activates a maitotoxin-sensitive nonselective cationic current in beta-cells. *J Biol.Chem.* 269, 32055-32058.

Xu, W., Wilson, B. J., Huang, L., Parkinson, E. L., Hill, B. J., & Milanick, M. A. (2000). Probing the extracellular release site of the plasma membrane calcium pump. *Am.J.Physiol Cell Physiol* 278, C965-C972.

Yamasaki, M., Masgrau, R., Morgan, A. J., Churchill, G. C., Patel, S., Ashcroft, S. J., & Galione, A. (2004). Organelle selection determines agonist-specific Ca^{2+} signals in pancreatic acinar and beta cells. *J Biol.Chem.* 279, 7234-7240.

Zawalich, W. S., Zawalich, K. C., Tesz, G. J., Sterpka, J. A., & Philbrick, W. M. (2001). Insulin secretion and IP levels in two distant lineages of the genus Mus: comparisons with rat islets. *Am.J Physiol Endocrinol.Metab* 280, E720-E728.